12-2015

Mobilization of Adipose Stromal Cells in Obesity and Cancer by SPARC and its Proteolytic Isoforms

Chieh Tseng

MOBILIZATION OF ADIPOSE STROMAL CELLS IN OBESITY AND CANCER BY SPARC AND ITS PROTEOLYTIC ISOFORMS

By

Chieh Tseng, B.S.

APPROVED:

_____
Mikhail G Kolonin, Ph.D
Advisory Professor

_____
Gary E. Gallick, Ph.D

_____
Jan A. Burger, MD, Ph.D

_____
Pamela L. Wenzel, Ph.D

_____
Qing Ma, Ph.D

_____
Rick A. Wetsel, Ph.D

APPROVED:

_____
Dean, The University of Texas
Graduate School of Biomedical Science at Houston

MOBILIZATION OF ADIPOSE STROMAL CELLS IN OBESITY AND CANCER BY SPARC AND ITS PROTEOLYTIC ISOFORMS

A
Dissertation

Presented to the Faculty of
The University of Texas
Health Science Center at Houston
and
The University of Texas
MD Anderson Cancer Center
Graduate School of Biomedical Sciences
in Partial Fulfillment

of the Requirements

for the Degree of

Doctor of Philosophy

By

Chieh Tseng, B.S.
Houston, Texas

December 2015

MOBILIZATION OF ADIPOSE STROMAL CELLS IN OBESITY AND CANCER BY SPARC AND ITS PROTEOLYTIC ISOFORMS

Chieh Tseng, Ph.D.

Advisory Professor: Mikhail G.Kolonin, Ph.D.

Obesity increases cancer risk and progression as shown by epidemiologic studies. However, the underlying pathophysiology remained unclear. Adipose stromal cells (ASC) are adipose tissue-derived mesenchymal progenitors, abundant in white adipose tissue (WAT). In this study, we show that the ASC pool is expanded in obesity and is associated with promoted tumor growth. Next, by using a chimeric GFP-RFP bone marrow transplant model, we observed higher tumor infiltrating cells with ASC phenotype in obese mice compared to lean. Consistently, systemic circulating ASC frequency is six fold higher in tumor-bearing obese mice compared to lean. The tumor infiltrating cells with ASC phenotype are found to be perivascular, suggesting them being incorporated into vessels as pericytes to support tumor vasculature. We obtained evidence that ASC is mobilized in response to obesity and cancer, however, the mechanisms regulating ASC trafficking are poorly defined. We previously reported that the binding of the matricellular protein SPARC to β1 integrin on ASC surface induces their motility. Here, we demonstrate that absence of SPARC diminishes ASC capacity to mobilize. As adiposity correlates with circulating SPARC and is the major producer of it, we evaluate

SPARC level in distinct adipose depots and identify two SPARC proteolytic isoforms: C-SPARC (lacking the N-terminus) and N-SPARC (lacking the C-terminus), generated in the mesenteric white adipose tissue of obese mice. Both isoforms exhibit distinct β1 integrin binding capacity. C-SPARC binds to β1 integrin on ASC, while N-SPARC fails to, but shows to be a potent extracellular matrix (ECM) / integrin interaction blocker and these events are associated with integrin-dependent FAK-ERK signaling and integrin-independent ILK-Akt signaling. We show that both isoforms induce ASC de-adhesion and, acting through different mechanisms, have additive effect in promoting ASC migration.

Table of Contents

Abstract …….. iii

Table of contents……..… v

List of Tables……vi

List of Figures……...vi

Chapter 1: Introduction……. 1

Chapter 2: Literature Review…… 4

Chapter 3: Methods and Material…….. 37

Chapter 4: Results…….. 47

Chapter 5: Discussion and Conclusion…….. 88

Chapter 6: Future direction…… 95

Bibliography…….. 100

Vita…… 123

List of Tables

Table 1: ASC and MSC immunophenotype……12

List of Figures

Figure 1-1. Cellular components of white adipose tissue…… 9

Figure1-2. Proposed functions of ASC in adipose tissue remodeling and tumor progression …….. 16

Figure1-3. Functional domains of SPARC …….. 22

Figure 4-1. ASC expansion promotes tumor growth …….. 52

Figure 4-2. Pericyte recruitment in obesity and tumor vascularization…… 56

Figure 4-3. SPARC promotes ASC mobilization and migration…….. 60

Figure 4-4. SPARC induce ASC deadhesion is linked with β1 integrin signaling... 64

Figure 4-5. Obesity-induced SPARC isoforms in MS WAT…… 70

Figure 4-6. C-SPARC but not N-SPARC binds to ASC…….. 75

Figure 4-7. N-SPARC is a potent extracellular matrix (ECM) binder and integrin... 78
interaction blocker

Figure 4-8. Both C-SPARC and N-SPARC modulate β1 integrin signaling…… 81

Figure 4-9. Both C-SPARC and N-SPARC induce ASC deadhesion and cooperate in triggering ASC migration…….. 84

Figure 4-9. Proposed model…….. 86

Figure 6-1. Absence of host SPARC is associated with tumor growth deficiency.. 98

Figure 6-2. Decreased vasculature in tumors grown in SPARC$^{-/-}$ mice…… 99

Chapter 1

Introduction

OBESITY

Obesity, a term to describe excessive accumulation of white adipose tissue (WAT) is defined as body mass index (BMI=weight/height^2) of ≥30 kg/m^2 (Renehan et al., 2008). The association of obesity and disease has been long recognized, as Greek physician Hippocrates wrote "Corpulence is not only a disease itself, but the harbinger of others" (Haslam and James, 2005). Indeed, subsequent epidemiological studies demonstrated that obesity increases the risk and mortality rate and is associated with multiple diseases including metabolic disorders, cardiovascular diseases and several cancers (colorectal, esophageal, kidney and pancreatic cancer) (Basen-Engquist and Chang, 2011; Renehan et al., 2008).

Report by World Health Organization (WHO) showed that the worldwide obesity rate has doubled since 1980 and it is estimated that at least 6 million adults worldwide were obese in 2014. Unfortunately, the obesity problem extends to children as well. It is reported that at least 42 million children below the age of five are overweight. This predisposes the child to obesity in adulthood and causes them to be more susceptible to metabolic disorders. The alarming rise in obesity incidence accompany its negative health impact is appalling and has highlighted the importance of understanding obesity pathophysiology.

The causes of obesity are multifactorial and have been associated with complex interaction between genetic and environmental components (Renehan et al., 2015). The genetic influence on obesity is observed in twin studies showing a stronger concordance for fat mass among identical twins (70–90%) compared to fraternal twins (35–45%) (Gibbons, 2008; Silventoinen et al., 2010). In addition, genetic aberrations including single gene mutations in melanocortin-4 receptor (MC4R), pro-opiomelanocortin (POMC), leptin and

leptin receptor or single-nucleotide polymorphisms also attribute individuals to higher obesity susceptibility (Barsh et al., 2000). These studies have provided compelling evidence on the importance of genetic heritability on obesity (Stunkard et al., 1986). The other major attributors to obesity includes changes in human behavior of adapting to a more sedentary lifestyle, aging, increased accessibility to and intake of high caloric foods parallel the rising prevalence of obesity worldwide (Kopelman, 2000). In sum, obesity results from a chronic surplus in energy which tips over the immune balance of adipose tissue. This drives the adipose tissue microenvironment to become pro-inflammatory and remain in the state of chronic inflammation (Cinti, 2005; Kopelman, 2000). To elucidate the pathophysiology of obesity and its clinical manifestations, it is fundamental to have a comprehensive understanding in the role of adipose tissue and its link in pathology.

Chapter 2

Literature Review

Obesity and Inflammation

Obesity, characterized by a prolonged state of low-grade inflammation, has been linked by mounting evidence to increase cancer risks and is involved in the development of metabolic disorders including type II diabetes, dyslipidemia and cardiovascular diseases (Muoio and Newgard, 2008; Ouchi et al., 2011).

Inflammation is a biological response triggered by pathological events such as tissue injuries, infection and toxic stimuli (Medzhitov, 2008). Short-term (acute) inflammation is largely believed to be beneficial that facilitates tissue repair and protects against infection. However, when inflammation is prolonged as observed in obesity, detrimental effects result as chemical mediators and structural dynamics of adipose tissue changes (Sun et al., 2011).

Generally, the adipose tissue (AT) of a healthy individual predominantly resides with regulatory immune cells such as type 2 lymphocytes and eosinophils (Sun et al., 2011). The cytokines secreted by regulatory immune cells include interleukin (IL)-10, IL-4 and IL-13, which promote adipose tissue-residing macrophages (ATM) to retain their anti-inflammatory M2 state (Makki et al., 2013). However, in obesity, the rapid expansion of adipose tissue associated with elevated expression of stress makers on the adipocyte cell surface, increased cellular turnover rate and upregulation of chemotactic factors that have been shown to increase pro-inflammatory M1 macrophages (Wellen and Hotamisligil, 2003). The heightened production of IFN-γ by pro-inflammatory immune cells (e.g. NK cells and $CD8^+$ T cells), drives ATM to polarize and switch to pro-inflammatory M1 state. In addition, elevated cell death and increased expression levels of monocyte chemotactic

protein (MCP)-1, -1α, -2, -3 and RANTES in adipose tissue also increase macrophage infiltration. Previous studies reported an increase from 10-15% of ATM in lean visceral adipose tissue to 50% ATMs in obese mice (Schipper et al., 2012; Sun et al., 2011). These pro-inflammatory macrophages increase collagen deposition and induce adipose tissue fibrosis, which leads to further exacerbation of adipose tissue inflammation as it limits proper adipose tissue expansion and deregulates adipocyte function. Macrophages infiltrating WAT in obesity are the major secretors of IL -6 and tumor necrosis factor-α (TNF-α), which lead to insulin resistance by blocking insulin signaling (Hotamisligil et al., 1994) and reduce glucose transporter GLUT4 expression in adipocytes (Lumeng et al., 2007). Aside from macrophages, adipokines from adipocytes and other adipose-residing cells are also associated with poor clinical manifestations of obesity.

Insulin resistance and glucose intolerance have been associated with aberrations in adipokines: leptin and TNF-α that regulate inflammatory responses and glucose metabolism through modulating activities of JNK-1 and IKKβ pathway (de Luca and Olefsky, 2008), while resistin promotes insulin resistance by modulating the activity of the insulin signaling inhibitor: suppressor of cytokine signalling 3 (SOCS3) (Ouchi et al., 2011). Adipokines with trophic effects including insulin-like growth factors (IGFs), epidermal growth factor (EGF), and transforming growth factor-beta (TGF-β) confer malignant cells with advantages in survival and proliferation. Upregulated TGF-β and IL-6 in obesity promote tumor angiogenesis by stimulating growth factors activity such as hepatocyte growth factor (HGF), vascular endothelial growth factor (VEGF), and fibroblast growth factors (FGF-1 and FGF-2) (Calle and Kaaks, 2004; Renehan et al., 2008).

Adipose Tissue Function and Composition

The AT consists of two different type of adipose tissue, namely the energy-storing WAT and energy-dissipating brown adipose tissue (BAT). WAT and BAT exhibit distinct functionality. BAT is characterized by high level of mitochondria uncoupling protein 1 (UCP1), best known to produce heat by non-shivering thermogenesis through uncoupling the oxidative respiration from adenosine triphosphate production (Cinti, 2011; Virtanen et al., 2009). During cold acclimation, the activation of β-adrenergic receptor in brown adipocyte cell membranes leads to free fatty acid (FFA) production (Ouellet et al., 2012). The high level of FFA activates UCP-1 to increase proton leakage and heat dissipation. Morphologically, brown adipocyte contains smaller, multilocular lipid droplets whereas WAT is characterized by large unilocular lipid droplets (Cinti, 2011; Hassan et al., 2012).

Structurally, the WAT takes the form of loose connective tissue that is commonly found attached to other organs. WAT is present in multiple discrete sites in the body. The best-defined WAT depots in human are subcutaneous (SC) WAT and intra-abdominal WAT. The intra-abdominal WAT is also known as visceral or intraperitoneal (i.p.). The visceral adipose depots include omental WAT (associated with stomach), mesenteric WAT (associated with intestine) and peripheric (surrounding the kidney). Adipocytes can be found embedded in with other tissues such as skeletal muscles and lymph nodes) (Bjorndal et al., 2011; Lee et al., 2013). Given its organization and distribution, WAT has been recognized as a thermal insulator (providing heat and protecting organ against mechanical stress) and energy storing depot of the body (Cinti, 2012). The unique feature of WAT to uptake and store excessive energy as triacylglycerols and release of the lipids in times of

need, helps an animal survival when food is scarce. A more comprehensive evaluation of WAT function in recent years has found WAT to be an active endocrine organ that regulates metabolism, inflammation and reproduction (Trayhurn and Wood, 2005).

The lipid-laden adipocyte is the major component of AT that constitutes about 50% of the AT cellular contents while the other half are immune cells, fibroblast, endothelial cells and progenitor cells (adipose stromal cells) (Fig. 1-1) (Tsuji et al., 2014). To study the highly heterogeneous cellular content of AT, physical dissociation (mincing) along with enzymatic collagenase digestion, followed by a defined immunophenotype of the cell surface markers can be employed to isolate specific cell population of interest.

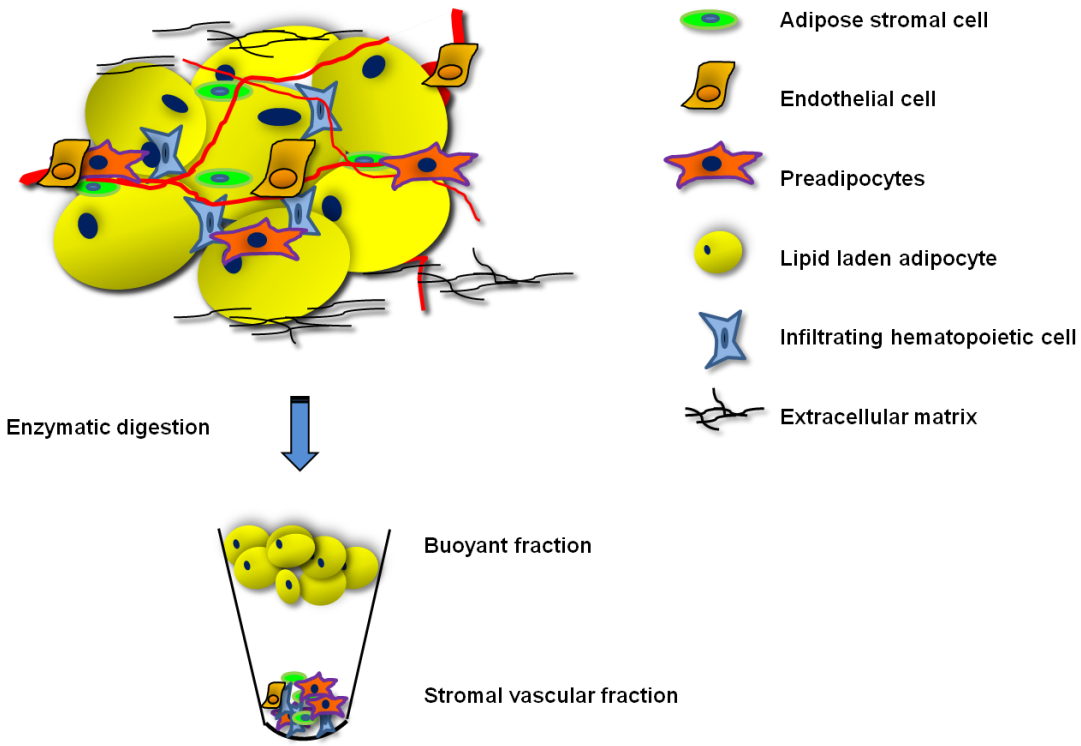

Figure1-1 Cellular components of white adipose tissue. The white adipose tissue composed of mainly the lipid-laden adipocyte (50%) and stromal vascular fraction (cell pellet) containing haematopiotic cells, preadipocyte, endothelial cells and progenitor cells (adipose stromal cells). The cellular components within WAT can be separated by enzymatic collagenase digestion.

Figure obtained with permission of Springer from book chapter "Tseng C & Kolonin MG. Adipose Tissue-Derived Progenitor Cells and Cancer. In: Angiogenesis in Adipose Tissue. Springer, New York, 2013, pp321-337

Adipose stromal cells

The adipose stromal cells (ASC) are a multipotent cell population residing in the perivascular niche of AT (Kolonin et al., 2012). ASC share traits previously reported in bone marrow-derived mesenchymal stem cell (MSC), documented as plastic-adhering fibroblastoid colony-forming units (CFU-F). ASC display high proliferative capacity and are able to differentiate into cells of mesodermal lineages: fat, bone, cartilage, muscle and non-mesodermal origin: neuron-like cells (Gimble et al., 2011). Previous studies revealed activation of ASC under ischemic conditions, as well as them participating in tissue repair by supporting angiogenesis and modulating immune response (Bagno et al., 2012; Puissant et al., 2005). Given the ease of isolation and abundance of ASC in adipose tissue, ASC has emerged as a promising source of progenitor cells for regenerative medicine (Gimble et al., 2007). ASC can be isolated from resected AT by enzymatic collagenase digestion to obtain the non-lipid-laden cell pellet named the stromal vascular fraction (SVF).

Similar to progenitor cells from different sources, the heterogeneity and sensitivity of surface marker expression to manipulation (cell isolation protocol and culture conditions) of ASC have rendered it a challenge to accurately assign a specific immunophenotypic signature to ASC. Thus, at present, no definitive surface markers are given to the ASC cell population. To characterize ASC, the International Society for Cellular Therapy (ISCT) and International Federation for Adipose Therapeutics and Science (IFATS) have recommended basing the definition of ASC on their multilineage potential, plastic adherent properties and immunophenotype (Bourin et al., 2013).

The surface marker expression on ASC has been characterized by several groups (Bourin et al., 2013; Maumus et al., 2011; Zimmerlin et al., 2010) using flow cytometry. As ASC and MSC have overlapping traits and functions, initially, it was postulated that the two cell populations may be identical. However, more recent studies showed a different propensity of ASC and MSC to differentiate into distinct cell lineages (Huang et al., 2005; Im et al., 2005) and differences in cell surface marker profile (described in Table 1). It is shown that CD36 and CD34 are expressed on ASC but not on MSC (Pachon-Pena et al., 2011; Sengenes et al., 2005).

Our group and others have isolated plastic-adhering fibroblastoid cells that are negative for leukocyte and endothelial cell surface markers: CD45 and CD31, respectively and positive for the progenitor cell marker CD34 (Traktuev et al., 2008; Zhang et al., 2009). This CD45 negative CD31 negative CD34 positive (CD45-CD31- CD34+) immunophenotype has been faithful for isolation of cells validated to be capable of differentiating into chondrocytes, adipocytes and osteoblasts in vitro. Recently, by combinatorial phage display approaches, our group has identified $\alpha 5\beta 1$ integrin and a new decorin derivative to be expressed on ASC with progenitor capacity (Nie et al., 2008) (Daquinag et al., 2011).

	Adipose stromal cells (ASC)	Bone marrow mesenchymal cells (MSC)
Positive	CD13 CD29 CD34 CD36 CD44 CD73 CD90 CD105 CD166 MHC class I HLA-ABC	CD13 CD29 CD44 CD73 CD90 CD105 CD166 MHC class I HLA-ABC
Negative	CD11b/14 CD31 CD38 CD40 CD45 CD80 CD86 HLA-DR MHC class II	CD34 CD36 CD38 CD40 CD45 CD80 CD86 HLA-DR MHC class II

Table 1: ASC and MSC immunophenotype. The cell surface markers expression on freshly isolated ASC or MSC, determined by flow cytometry analysis.
(Adapted from Minteer, D.M., Marra, K.G., and Rubin, J.P. (2015). Adipose stem cells: biology, safety, regulation, and regenerative potential. Clin Plast Surg 43,169-179 and Bourin, P., Bunnell, B.A., Casteilla, L., Dominici, M., Katz, A.J., March, K.L., Redl, H., Rubin, J.P., Yoshimura, K., and Gimble, J.M. (2013). Stromal cells from the adipose tissue-derived stromal vascular fraction and culture expanded adipose tissue-derived stromal/stem cells: a joint statement of the International Federation for Adipose Therapeutics and Science (IFATS) and the International Society for Cellular Therapy (ISCT). Cytotherapy 15, 641-648.)

Multiple studies demonstrated beneficial effects of ASC, participating in tissue repair by increasing angiogenesis, immunosuppression (Puissant et al., 2005), resolving scar tissue formation and secretion of growth factors. Transplantation of ASC in hindlimb ischemic mice showed an increase in angiogenesis associated with elevated angiogenic growth factor production. Human and rat ASC engraftment in myocardial infarction models have shown to significantly improve cardiac function and diminish scar area in the injured region (Bagno et al., 2012; Cai et al., 2009). Similar to MSC, ASC do not express major

histocompatibility complex (MHC) class II (Tse et al., 2003), are immunoprivileged and inhibit lymphocyte activation and proliferation in response to mitogens (Puissant et al., 2005). In additional, ASC also modulate immune response by attenuating macrophage infiltration (Lin et al., 2013). Importantly, as the major component of SVF, the ASC are crucial in adipose tissue expansion serving as adipocytes precursor and to support blood vessel development (Fig.1-2). Angiogenesis relies on coordinated assembly of perivascular matrix, endothelial cells (EC) and pericytes (Song et al., 2005; von Tell et al., 2006). The formation of mature blood vessel requires close association of pericytes to EC (Gerhardt and Semb, 2008). The absence of pericyte coverage in pericytes-depleted mouse models (Song et al., 2005) or impaired pericytes recruitment by antagonist results in increased vessel permeabilization and leakage (Cooke et al., 2012). The perivascular location of ASC and association with EC suggested them as pericytes/adventitial cells (Tang et al., 2008; Traktuev et al., 2008). It is believed that the pro-angiogenic capacity of ASC is acted upon through its paracrine effect, by secretion of angiogenic factors that modulate EC growth, survival and differentiation (Gerhardt and Semb, 2008; von Tell et al., 2006)

Adipose stromal progenitor cells and their potential pathological functions

The inherent properties of ASC have drawn great clinical interest, recognizing the potential of these cells in tissue repair coupled with immunosuppressive ability, therefore ASC, offer great therapeutic promise for a large number of immune and degenerative diseases. However, like a double-edge sword, the pro-angiogenic, cell death evading and immunomodulatory properties of ASC are implicated in pathological processes as well. Tumors may exploit these features to facilitate cancer progression, raising significant safety concerns for clinical applications (Bertolini et al., 2015; Zhang et al., 2009).

Similar to tissue growth, tumor progression relies on establishment of functional microenvironment and recruitment of cells to form new vasculatures, to support its expansion. Tumor vasculatures are distinct from normal tissues, as they are characterized by a chaotic mixture of irregular vessels that are often tortuous, functional flawed and leaky. The abnormalities in cellular arrangement and perivascular matrix result in compromised perfusion with inefficient nutrient delivery and waste clearance (Nagy and Dvorak, 2012). Multiple studies showed that ASC promote neovascularization, and that circulating ASC numbers increase in cancer (Bellows et al., 2011) (Kidd et al., 2012; Klopp et al., 2012; Zhang et al., 2009) In tumors, ASC are found located in the perivascular region, contributing to tumor vasculature integrity. It has been proposed that the secretomes from ASC contain growth factors such as HGF, VEGF and fibroblast growth factor that enhance EC survival, growth and sprouting in tumors.

In addition to their vasculogenic role, ASC contribute to ECM remodeling and enhance ECM stiffness (Chandler et al., 2012). ASC along with adipocytes and other SVF cells modulate the production of ECM structural proteins including collagens and fibronectin (Kolonin et al., 2012; Mariman and Wang, 2010). In obesity, the ASC pool is expanded. Concomitantly, changes in ECM structural components and upregulation of inflammatory genes (Henegar et al., 2008; Mariman and Wang, 2010) increase ECM rigidity. The ECM stiffness is crucial in dictating cell behavior (Mariman and Wang, 2010), showing increased proliferation and invasiveness of malignant cells on rigid ECM (Alexander et al., 2008; Ulrich et al., 2009).

ASC have been proposed to serve as cancer-associated fibroblasts (CAF) (Kidd et al., 2012; Klopp et al., 2012; Kolonin et al., 2012; Zhang et al., 2009). CAF are fibroblast-like cells that facilitate tumor progression through conferring oncogenic signals and structural support to malignant cells (Karnoub et al., 2007; Olumi et al., 1999). Furthermore, CAF increase malignant cell survival through activating nuclear factor-κB (NF-κB)-regulated anti-apoptotic signaling, and enhance tumor resistance to chemotherapy by reducing drug uptake (Loeffler et al., 2006) (Fig. 1-2).

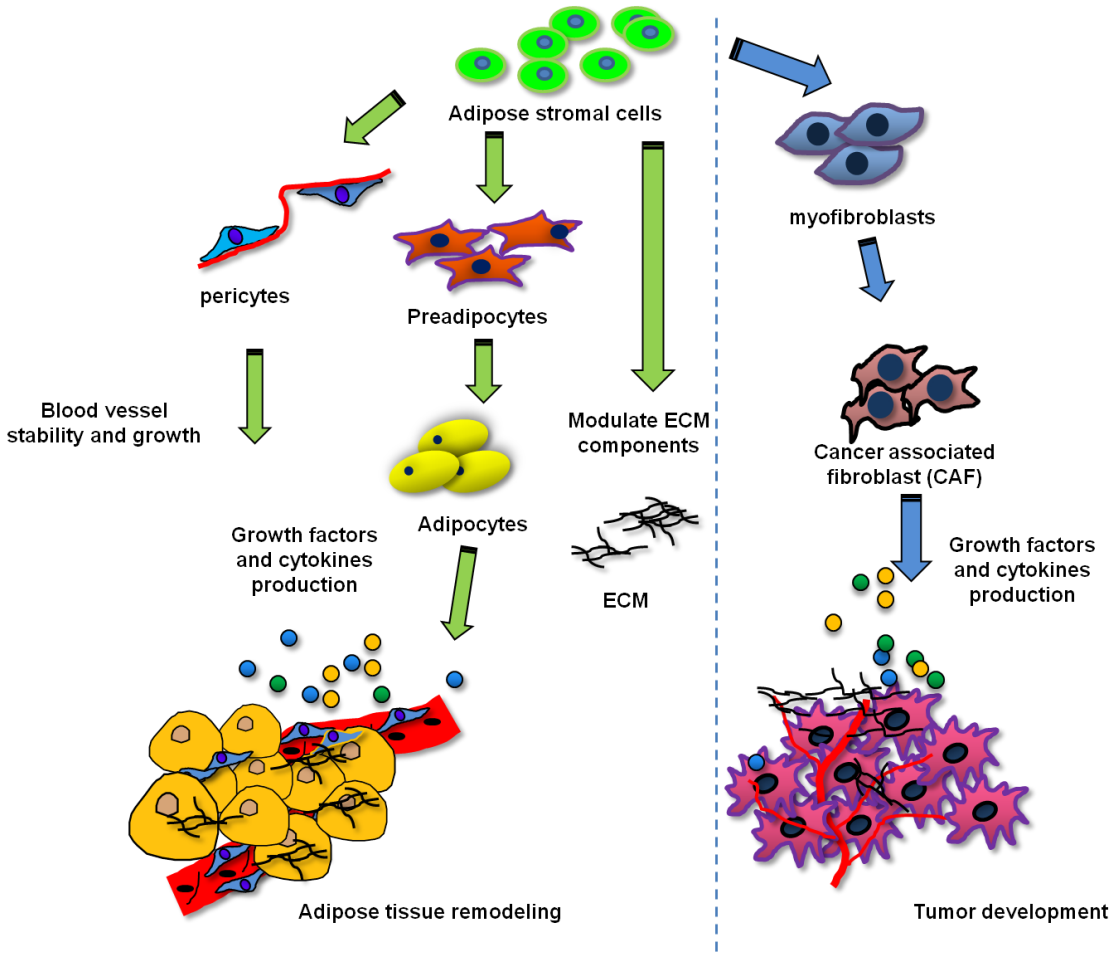

Figure 1-2. Proposed functions of ASC in adipose tissue remodeling and tumor progression. The hypothetical mechanisms through which ASC promote adipose tissue expansion, by contributing to preadipocyte pool to differentiate into mature adipocytes and support adipose tissue vasculatures functioning as pericytes and provide growth factors (shown in green arrows). ASC modulate extracellular matrix (ECM) components and rigidity to support adipose tissue expansion and stimulate tumor growth. In cancer, ASC may serve as source for adipocytes and cancer associated fibroblast (CAF), secreting pro-inflammatory cytokines to promote tumor survival and growth. ASC support tumor vasculature by incorporation into tumor vessel lumen (shown in blue and green arrows).

Figure obtained with permission of Springer from book chapter "Tseng C & Kolonin MG. Adipose Tissue-Derived Progenitor Cells and Cancer. In: Angiogenesis in Adipose Tissue. Springer, New York, 2013, pp321-337

Adipose Tissue Expansion

Adipose tissue, the energy repository in mammals provides a long-term fuel reserve for future need. In the event of energy overload, surplus energy is stored as triacylglycerols in adipocytes (Cinti, 2005). In contrast, the high energy fuel triacylglycerols are readily mobilized when energy is deficient. To meet the demand of constant energy fluctuations, adipose tissue is highly plastic and possesses the unique capability to retract and expand in a non-transformed state (Sun et al., 2011). Adipose tissue expansion, like any other tissue expansion, requires angiogenesis and structural remodeling (Cao, 2010). The formation of new vasculature is key in supplying cells, oxygen, growth factors and cytokines to facilitate tissue growth, repair and expansion. In addition, it is also crucial for removal of metabolic wastes.

The healthy expansion of adipose tissue relies on controlled changes in ECM components parallel with orchestrated events coordinated by hypertrophy and hyperplasia of various cell types including adipose progenitor cells, endothelial progenitor cells, and infiltrating immune cells (Sun et al., 2011). Adipose progenitor cells are capable of differentiating into adipocytes while endothelial progenitor cells incorporate and facilitate neovascularization. Immune cells such as macrophages provide growth, survival and angiogenic factors. The interplay of these cells is crucial in development of functional adipose tissue (Wernstedt Asterholm et al., 2014).

However, pathological expansion of adipose tissue ensues when the aforementioned processes are disrupted; resulting in poorly perfused hypoxic adipose tissue. Hypoxic adipose tissue is associated with inflammation and increased fibrosis. Hypoxia-inducible

transcription factors increase proinflammatory cytokines expression and migratory ability in activated macrophages (Imtiyaz et al., 2010). Ectopic overexpression of degradation resistant HIF-1α in mouse adipocytes showed an upregulation of ECM components including collagens, lysyl oxidase (LOX) and elastin (Sun et al., 2011). Abnormal deposition of these matrix components leads to hypoxia-induced fibrosis in AT.

Toward mechanisms controlling ASC mobilization

Cell mobilization is a term describing recruitment of a cell from its original niche into the circulation. This cascade of events involves multiple steps and interplays of different factors including adhesion molecules, proteases, cytokines and chemokines. For instance, upon granulocyte colony-stimulating factor (G-CSF) treatment, bone marrow residing cells respond by inducing proteases expression of matricellular factors that reduce hematopoietic stem cell (HSC) adhesion with its immediate surrounding matrix. In parallel, up-regulation of proteases and chemokines facilitate mobilized cells to traffic and extravasate into circulation (Petit et al., 2002). Homing of mobilized cells is dictated by a chemokine gradient. Although the molecular mechanisms governing ASC mobilization remained elusive, extensive clinical studies on haemapiotic stem cells led us to hypothesize that a similar mechanism underlies ASC mobilization.

Pathological expansion of tissues such as WAT in obesity or tumor growth in cancer progression, lead to inadequate oxygenation, creating hypoxic microenvironment within the organ (Bertolini et al., 2012). Hypoxia is a robust inducer of inflammatory and chemotactic factors, which promotes macrophage infiltration by upregulation of monocyte chemotactic proteins (MCP)-1, -1α, -2, -3, and RANTES expression in adipose tissue (Ota, 2013; Surmi and Hasty, 2008). In tumors, hypoxia induces upregulation of stromal cell-derived factor (SDF-1) in tumor-associated fibroblasts and promotes recruitment of CXCR4 expressing macrophages (Murdoch et al., 2004). Similarly, augmented CXCR4 expression in ASC is observed in ischemic conditions (Thangarajah et al., 2009). A recent study showed microperfusion of mouse fat pad with a CXCR4 antagonist increased ASC release, suggesting the involvement of the CXCL12/CXCR4 axis in regulating ASC

retention/migration *in vivo* (Gil-Ortega et al., 2013). Furthermore, glucagon-like peptide-1 receptor agonist stimulates ASC migration by upregulation the SDF-1/CXCR4 signaling cascade and p-Akt activity (Zhou et al., 2015). Interestingly, the CXCL12/CXCR4 signaling axis is also shown to be involved in HSC and endothelial progenitor cell mobilization and blockade of this signaling axis partially disrupts the recruitment of progenitor cells to the ischemic heart tissue (Abbott et al., 2004; Liu and Velazquez, 2008). Consistent with ASC displaying tropism to inflammatory cues, activation and increased mobilization of ASC are reported in both obesity and cancer. Our group and others reported expression of chemokine receptors: CCR1, CCR4, CCR7, CXCR1, CXCR2 and CXCR5 on ASC in response to inflammation stimuli (Klopp et al., 2012; Ponte et al., 2007; Von Luttichau et al., 2005). An increased in expression of chemokine (C-C motif) ligand (CCL)-2, -3, -5, -7, -8, -11 and chemokine receptors (CCR)-1, -2, -3, and -5 are observed in both subcutaneous and visceral AT of obese patient (Huber et al., 2008). However, the role of theses chemokines in modulating ASC migration remained to be determined. Similarly, the concomitant upregulation of CXCR1 and CXCR2 on ASC may be responsible for directing their migration in response to CXCL1 and IL-8 secreted by endometrial cancer cells (Klopp et al., 2012). The complex signaling networks of ASC migration in cancer remained unclear.

In cell mobilization, in addition to chemokine/chemokine receptor-directed ASC trafficking, the modulation of cell contacts with its microenvironment is key in regulating cell motility. Strong adhesion of cells to its niche prevents cell migration. Tissue expansion induces factors involved in ECM remodeling. One of such matricellular molecules is SPARC (secreted protein acidic rich in cysteine) (Kos and Wilding, 2010). SPARC is

known to control cell-cell interaction and cell adhesion. Previously, our group showed that binding of the SPARC to β1 integrin on ASC surface promotes cell migration, implicating the role of SPARC in cell mobilization (Nie et al., 2008). Indeed, SPARC has been shown to activate fibroblast migration in myocardial infarction models (Takahashi et al., 2001). Clinical data on elevated SPARC concentration in plasma of obese individual is consistent with the possibility that SPARC induces ASC deadhesion and migration, facilitating its incorporation into new WAT vessel during tissue expansion. Likewise, a similar mechanism maybe involved in tumor vascularization supported by elevated SPARC level in serum of cancer patients (Ikuta et al., 2005).

SPARC PROTEIN STRUCTURE

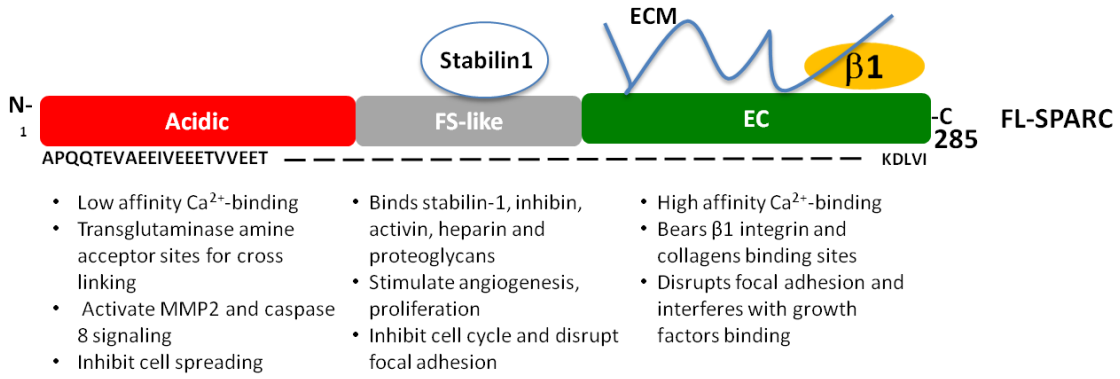

Figure 1-3. Functional domains of SPARC. SPARC consists of three distinct domains: acidic domain (red), the follistatin-like domain (grey) and extracellular calcium binding domain (green). The functional properties of distinctive domain and its interacting proteins are shown.

SPARC, also named as osteonectin when initially found in bone (Bolander et al., 1988), and BM-40 when discovered in the basement-membranes (Dziadek et al., 1986) , is a non-structural matricellular protein that is highly conserved across different species. The positions of cysteine residues within SPARC are found to be highly homologous among species, suggesting the importance of the 3D structure to its function.

SPARC has a molecular weight of 34kDa and migrates to 43kDa on sodium dodecyl sulfate polyacrylamide gel electrophoresis due to glycosylation. The signaling peptide of SPARC (17 amino acids) is removed during processing generating the mature SPARC. Mature SPARC consists of three domains, namely the N-terminal acidic domain (Ala1-Glu52), follistatin-like (FS) domain (amino acid Asn53-Pro137) and extracellular calcium (EC) -binding domain (Cys138-Ile286) (Chlenski and Cohn, 2010). Each domain has been reported to exhibit distinct functions (Figure 1-3). The N-terminus of SPARC has low

calcium ion binding affinity (Kd 10mM), bears the transglutaminase cross linking amine acceptor sites and was recently found to have a chemosensitizing role through activating caspase 8 signaling (Rahman et al., 2011). Synthetic peptides spanning regions of the SPARC N-terminus possess cells spreading inhibition ability (Lane and Sage, 1990) and also activates MMP2 (Gilles et al., 1998).

The structural morphology of the cysteine-rich FS domain of SPARC bears resemblance to the epidermal growth factor, supported by conserved distribution of the disulfide bonds (Chlenski et al., 2004). This region of SPARC binds multiple factors including inhibin, activin, heparin and proteoglycans. FS domain is a potent antagonist of angiogenesis and cell migration. Interestingly, it also bears the pro-angiogenic copper binding sequence KGHK (Bradshaw and Sage, 2001). The synthetic peptide spanning EGF module of the FS domain promotes fibroblast proliferation, disrupts endothelial cell focal adhesion, and inhibits its entry into S phase of the cell cycle (Chlenski et al., 2004).

The C-terminal EC-domain consists of two EF-hand motifs that bind calcium ions with high affinity Kd (0.08-0.6μM). Point mutations and deletion studies of this region identified the critical collagen binding sites consisting of residues R149, N156, L242, M245 and E246 (Sasaki et al., 1998). Single-bond peptide cleavage by an unknown protease or metalloproteinases within the EC-domain of SPARC increases its collagen binding affinity (Hohenester et al., 2008; Sasaki et al., 1998). The function of the synthetic peptide spanning the second EF-hand domain interferes with growth factors such as VEGF, PDGF and bFGF signaling, inhibits endothelial cell growth and disrupts focal adhesions (Chlenski and Cohn, 2010).

SPARC FUNCTION

SPARC is a multifunctional glycoprotein that is found to be ubiquitously expressed in various tissues. Upregulation of SPARC is commonly reported in tissues undergoing active tissue remodeling such as tissue renewal, tissue repair, mineralization, angiogenesis, embryonic development and tumorigenesis (Chlenski et al., 2004). Only limited basal expression is found in non-remodeling adult tissues. Elevated SPARC expression promotes fibroblastoid cells migration in myocardial infarction and also facilitates adipose tissue expansion (secreted protein acidic rich in cysteine) (Wu et al., 2006). Among the multifunctional roles of SPARC, it is best recognized as a modulator of cell-extracellular matrix (ECM) contact, cell-cell interactions, ECM deposition and migration (Naimi and Van Obberghen, 2009). SPARC disengages and induces rounding of bovine aortic endothelial cells (Sage et al., 1989) and enhances ASC migration (Nie et al., 2008). Further evidence links the counter-adhesive characteristic of SPARC to its ability to disrupt focal adhesion assembly and promote rearrangement of stress actin fiber in endothelial cells (Murphy-Ullrich et al., 1995). The multifaceted SPARC activities are mediated by interacting with the ECM proteins and several cellular surface receptors, including VCAM1, stabilin-1, and integrins.

SPARC in Extracellular Matrix (ECM) Remodeling

ECM comprises of two major types of macromolecules, namely the fibrous proteins and the proteoglycans. The fibrous proteins composed of collagens, fibronectin, laminins and elastins (Frantz et al., 2010). In the ECM, SPARC binds to multiple components including collagens (type I, II, III, IV and V), thrombospondin 1, entactin and vitronectin (Chlenski et al., 2004). Among these ECM components, the interaction of SPARC with collagens is best characterized. Collagens, the most abundant structural protein in vertebrate tissues provide mechanical support for protein anchorage or cell attachment. The proper formation of collagen fibers is critical to maintain tensile strength of tissue and retains its normal morphology. SPARC serves as a chaperone in modulating collagen fibril formation and incorporation of it into the ECM (Rentz et al., 2007). As SPARC is present in the secretary pathway, it is proposed to interact with collagen I and affect collagen I assembly and trafficking (Martinek et al., 2007). A study utilizing a SPARC mutant (Val196-Phe 203 deletion) which mimics activation by proteolysis, showed a drastic inhibition of collagen fibrillogenesis (Giudici et al., 2008).

Additional factors that have been shown to affect SPARC association with collagens include calcium concentration, proteases processing and glycosylation. SPARC derived from bone consists of high mannose and biantennary glycans, thereby shows a differential binding affinity to collagen I and V compared to platelet-derived SPARC that are decorated with bi and triantennary glycans (Chlenski et al., 2004). Furthermore, a previous study showed that absence of N-glycosylation at residue 99 significantly increases the capacity of SPARC binding to collagen V. This disparity in binding may be partly attributed to masking/unmasking of specific collagen binding sites on SPARC (Xie and

Long, 1995). EDTA chelation of calcium ions disrupts SPARC/ collagen binding. SPARC is a substrate for several extracellular proteases, producing bioactive proteolytic fragments. Single-bond peptide cleavage by an unknown protease or metalloproteinase within the EC-domain (Pro237-Leu238) of SPARC increases its collagen binding affinity without changing its α-helical conformation. Point mutation and deletion studies of this region identified the critical collagen binding sites consisting of residues R149, N156, L242, M245 and E246 (Sasaki et al., 1998).

To evaluate the physiological function of SPARC, SPARC-null mice in various transgenic backgrounds have been generated (Gilmour et al., 1998; Norose et al., 2000). Adult SPARC-deficient mice present with reduced collagen content in the dermis and harbor only approximately half the tensile strength compared to WT mice (Bradshaw et al., 2003b). Early onset of cataractogenesis results from irregular distribution of laminin and collagen IV in the lens capsule basement membrane is another prominent phenotypic abnormalities of SPARC-deficient mice (Bradshaw et al., 2003b; Norose et al., 2000). Proper matrix protein deposition in the lens capsule is critical for physiological permeability of the tissue (Norose et al., 2000). This impairment contributes to pathological changes in the ions and fluid balance across the basement membrane. SPARC- deficient mice also have reduced collagen deposition in bone and lower osteoblast and osteoclast numbers (Delany et al., 2000). This absence of SPARC in bone is proposed to result in impairment of linking organic and mineral phases of the bone tissue (Long, 2001; Mansergh et al., 2007). SPARC-deficient mice progress to severe osteopenia by 6 months of age. The early development of osteopenia is also partly attributed to the decreased synthesis of new bone by osteoblasts (Delany et al., 2000). Interestingly, the

reduced bone mass is accompanied by a higher adiposity in the SPARC-deficient mice (Bradshaw et al., 2003b). Overall, the absence of SPARC results in phenotypic abnormalities that is mostly associated with aberrations in ECM structure and assembly defect.

ECM assembly and deposition are greatly influenced by extracellular proteases. Matrix proteases degrade ECM components to facilitate tissue remodeling. An additional mechanism by which SPARC affects ECM remodeling is through modulating metalloproteinase expression by cells. SPARC promotes MMP1, MMP3, and MMP9 expression in fibroblasts; MMP1 and 9 in monocytes; and up-regulation of MMP2 activity in cancer cells (Chlenski and Cohn, 2010).

SPARC and Obesity

In obesity, the infiltration of pro-inflammatory cells into the tissue produces cytokines that change the dynamics of ECM deposition. These changes result in a more fibrotic tissue microenvironment characterized by increased ECM proteins expression such as integrins, type IV collagen, lumican and laminin β1 chain (Kos and Wilding, 2010). Excessive ECM deposition leads to increased rigidity of tissues and disrupts the normal tissue function and architecture. Previous studies identified SPARC as one of the key factors up-regulated in obesity (Tartare-Deckert et al., 2001). Elevated SPARC expression is observed in both obese human and mouse adipose tissue as compared to lean human and mouse. The serum levels of SPARC correlate with adiposity of human and fluctuate in accordance to the changes in BMI, suggesting adipose tissue to be the major source of SPARC in obesity. Given the capability of SPARC to modulate collagen deposition and its association with obesity, SPARC is proposed to be a pro-fibrotic factor. Consistent with such a role, a lower streptozoticin-induced renal fibrosis is detected in SPARC-deficient mice as compared to the wild-type mice (Taneda et al., 2003). In addition to directly affecting ECM deposition, SPARC induces pro-fibrotic protein Transforming Growth Factor-β (TGF-β) expression. TGF-β stimulates fibroblasts to contract ECM and synthesize matrix proteins such as collagen and fibronectin (Leask and Abraham, 2004).

The adipocytes are the predominant secretor of SPARC in obesity. Phenotypic characterization of adipose tissue in wild type or SPARC-deficient mice demonstrated significantly increased adiposity with increased adipocyte number and cell size in SPARC-deficient mice compared to wild-type mice (Nie and Sage, 2009). SPARC limits adipogensis by stimulation of the wnt/β-catenin signaling pathway and has been shown to

inhibit adipose stromal cell differentiation into adipocytes. Exogenous SPARC treatments decrease adipogenic transcription from genes. Consistently, SPARC-deficient marrow cells have higher adipsin and CCAAT/enhancer binding protein delta expression and display increased propensity towards adipocyte differentiation (Delany et al., 2003). SPARC expression during adipogenesis is biphasic, which spikes in preadipocytes during early stage of differentiation, followed by a drop as differentiation progresses. However, SPARC level eventually rises in mature adipocytes (Nie and Sage, 2009).

SPARC Proteolysis

The ECM is highly versatile and undergoes constant remodeling, i.e. assembly and degradation (Daley et al., 2008). Remodeling of ECM involves modification and degradation by proteases. This post-translational proteolytic protein processing is important in influencing the ECM microenvironment. ECM is crucial in providing structural and biochemical support to cells and dictates diverse biological events including cell growth, survival, differentiation and migration (Brekken and Sage, 2001). The matrix metalloproteinases (MMPs) are among the best-studied proteases involved in ECM degradation. In addition to cleaving the structural components of ECM, MMPs also target a wide range of non-structural ECM proteins.

Matricellular protein SPARC is a substrate for numerous extracellular proteases. Cleavage of SPARC produces bioactive fragments with distinct functions that are contextual. For example, limited proteolysis of recombinant SPARC by MMP3 generates 3 major fragments *in vi*tro. These truncated derivatives modulate cell growth, cell migration and angiogenesis distinctively (Sage et al., 2003). In addition, SPARC proteolysis occurring in chicken chorioallantoic membrane is associated with pro-angiogenic properties (Iruela-Arispe et al., 1995) and cathepsin K-cleaved SPARC promotes bone metastasis (Podgorski et al., 2009). Limited proteolysis of SPARC modulates collagen binding. Sasaki reported that cleavages of SPARC by unknown proteases or MMPS at in the EC domain residue L198, increases SPARC binding affinity for collagens. The proteolytic cleavage revealed masked epitope for collagen on SPARC, thereby increasing its affinity for collagen binding (Sasaki et al., 1997; Sasaki et al., 1998; Sasaki et al., 1999).

SPARC and ASC

Matricellular protein SPARC abundantly secreted by adipocytes is also secreted by adipose tissue-residing cells including fibroblasts, endothelial cells, pericytes and macrophages. SPARC has reported functions in influencing migration, mobilization and cellular structure. SPARC expression is transiently upregulated in injured myocardium and stimulates fibroblast migration, a process critical in wound healing (Wu et al., 2006). A counter adhesive role of SPARC induces endothelial cell rounding (Murphy-Ullrich et al., 1995) and increases endothelial permeability (Goldblum et al., 1994). SPARC regulates pericytes migration through interacting with TGF-β1 accesory receptor endoglin (Rivera and Brekken, 2011). The functional role of SPARC specifically in progenitor cell physiology remained unexplored. Our group identified SPARC as an ASC-interacting protein by characterizing ASC surface proteomic using phage display combinatorial random peptide library. These studies identified of the ASC surface SPARC receptor of to be α5β1 integrin (Nie et al., 2008; Weaver et al., 2008). The binding of SPARC to β1 integrin at focal adhesions on ASC is associated with changes in cellular structure resembling focal adhesion disassembly, mediating an intermediate cell adhesion state which favor cell migration (Nie et al., 2008).

In obesity, adipose tissue undergoes remodeling to accommodate energy surplus. The expansion of WAT relies on angiogenesis, differentiation of preadipocytes and ECM remodeling. Formation of new vasculature to support healthy WAT expansion involves mobilization and proliferation of progenitor cells. Elevated SPARC expression in obesity may contribute to ASC migration by binding to β1 integrin at focal adhesions, modulating ASC and ECM interactions. This event along with chemokine receptors CCR1, CCR4,

CCR7 and CXCR5 that are over expressed on ASC induced by inflammation stimuli (Klopp et al., 2012; Ponte et al., 2007; Von Luttichau et al., 2005), promotes ASC mobilization. Subsequent studies are required to elucidate the complex signaling networks involved in regulating ASC migration in response to obesity.

Integrin and Cell Adhesion

Integrins are transmembrane adhesion receptors expressed on cells as noncovalently-linked heterodimeric α and β subunits. In mammals, there are 18 α-integrin and 8 β-integrin subunits; heterodimerization of these subunits produces 24 distinct integrin heterodimers (Iwamoto and Calderwood, 2015). Integrin receptors are involved in cell adhesion to surrounding ECM proteins, generating signals critical for cellular processes that occur during development, immune response and progression of diseases (Hynes, 2002). Integrins bind a variety of matrix molecules ranging from ECM proteins, cell surface, or other soluble factors. The integrin repertoire expressed by a specific cell determines its ECM binding dynamic. Pertinent to our study, α5β1 integrin binds to fibronectin while α1β1 integrin binds to collagen. In addition to being an adhesion receptor, integrin directs intracellular signaling. The cytoplasmic domain of integrin associates with the intracellular focal adhesion (FA) complex proteins such as Focal adhesion kinase (FAK) and integrin-linked kinase (ILK) (Veevers-Lowe et al., 2011). Ligand binding results in integrin conformational changes and subsequently induces integrin clustering and formation of mature adhesion complex. More than 150 proteins have been identified within the adhesion complex including intracellular signaling components, adaptor proteins that interact with actin cytoskeletons. FAK is one of the major kinases involved in mediating signal from integrin to regulate focal adhesion, cell motility and shape. In general, integrin activation leads to FAK autophosphorylation at tyrosine 397 which allows recognition by SH2-containing proteins (SRC-family kinases) that subsequently bind and phosphorylate the adaptor protein paxillin as well as additional FAK sites. The FA signaling is highly complex and composition of FA varies according to its location. Molecular compositions

of FA at the cell edge are reported to be distinct from the core (Ivaska, 2012; Mitra et al., 2005).

Cell adhesion is central for cell motility. Strong adhesion of cells to extracellular substratum impedes the cell's ability to move, while low adhesion fails to provide sufficient traction to facilitate cell movement. Therefore, the maximum cell motility is observed in an intermediate adhesion regulated by the integrins and the concentrations of the ligands (Vicente-Manzanares et al., 2005).

FAs undergo assembly and dissociation during cell migration. As the cell migrates, it is polarized. Adhesion contacts are formed at the leading edge to provide traction force while disassembly and retraction of the rear involves disrupting integrin-ECM or integrin-cytoskeleton interaction (Lo, 2006; Nagano et al., 2012).

We and others have previously shown that SPARC associates with $\alpha 5\beta 1$ integrin (Nie et al., 2008; Weaver et al., 2008). This association on ASC is found to be localized to FAs. Given the counter-adhesive role of SPARC, it was proposed that SPARC interferes with $\alpha 5\beta 1$ binding to fibronectin which creates intermediate cell adhesion that facilitates cell mobility. Additional studies such as gain-of-function or loss-of-function of components involved in SPARC signalings are required to elucidate the precise mechanism involved in SPARC- induced cell rounding.

Focal Adhesion Kinase (FAK) and Integrin-linked kinase (ILK)

FAK, a non-receptor tyrosine kinase, first identified in 1992 (Parsons, 2003), is a major integrin- signaling protein localized to adhesion contact. FAK is expressed on most cells and serves as a central mediator of integrin signaling or other growth factors (Mitra et al., 2005; Parsons, 2003). FAK regulates a diverse array of biological functions including cell migration, cell survival, and cell cycle progression and growth factor signaling (Parsons, 2003; Zhao and Guan, 2011). FAK-null mutant mice are embryonic lethal characterized by profound mesodermal defects and FAK-deficient fibroblast form excessive focal contact and showed abnormality in their capacity to migrate. These phenotypes suggest that FAK is crucial in cell migration and modulating integrin-mediated adhesion disassembly (Mitra et al., 2005). Integrin engagement transduces outside-to-inside signals through activating FAK, characterized by increase in Tyr397 autophosphorylation. Following activation of FAK, SH2- and SH3-domain-containing proteins are recruited to the site, which mediate subsequent downstream signalings including the action of Rho family GTPases Rac and Cdc42, controlling cellular attachment, extension and retraction coordinated with actin-myosin cortex redistribution (Mitra et al., 2005; Parsons, 2003).

During cell migration, FA bindings to ECM provide traction force to pull the cell body forward. Subsequently, disruption of FA at the cell rear is essential to allow cell movement. The process of FA turnover is regulated by FAK. FAK phosphorylation at Tyr^{397} promotes recruitment of protein complex that are involved in integrin endocytosis. Dissociation of FA complexes and integrin endocytosis is associated with rapid dephosphorylation of FAK at Tyr^{397}(Nagano et al., 2012).

In addition to FAK, Integrin-linked kinase (ILK) is another well known integrin-interacting protein localized to FA (Widmaier et al., 2012). Both kinases constitute the FA signaling complex and are involved in mediating integrin signaling, thus may be partially interdependent (McDonald et al., 2008). ILK is an important mediator of integrin signaling regulating a wide array of processes such as cell growth, survival, differentiation and migration. Multiple studies in development and caner have demonstrated the role of ILK in modulating cell migration. Ligand binding to integrin leads to ILK activation which subsequently activates a diverse downstream effectors including glycogen synthase kinase 3 (GSK3) (McDonald et al., 2008).

Previous studies shown that FAK and ILK as proteins functionally engaged with SPARC modulating cell migration and survival (Nie et al., 2008; Shi et al., 2007; Weaver et al., 2008). However, their role in ASC migration remained unclear. Based on the role of ILK and FAK in cell migration, we hypothesized that SPARC/β1 signaling through these kinases is essential to induce ASC migration which leads to their mobilization.

Chapter 3

Methods and Materials

Part of this chapter is taken verbatim by permission from the Stem Cells: Chieh Tseng and Kolonin, Proteolytic Isoforms of SPARC Induce Adipose Stromal Cell Mobilization in Obesity, Stem Cells, Epub ahead of print.

3-1. Mice

All animal experimentations complied with protocols approved by UT Health Animal Care and Use Committee. Mouse strains C57BL/6, GFP-mice (UCP-GFP) and RFP-mice (ACTB-mRFP1)(Zhang et al., 2012) were purchased from Jackson. *SPARC*$^{-/-}$ mice were received from Dr. Helene Sage. For diet-induced obesity, mice were given fed high-fat (HFD) (60 kcal% fat) diet D12492, regular chow (13.1 kcal% fat) or low-fat diet (LFD) D12450B (10 kcal% fat) from Research Diets, New Brunswick, NJ. EchoMRI-100T (Echo Medical Systems) was used to measure adipose tissue mass and lean mass as described (Taicher et al., 2003). For tumor engraftment, 2.5x10^5 EO771 breast adenocarcinoma cells were subcutaneously injection into the mammary fat pat with 21-gauge needle. Tumor size was measured weekly with a caliper; tumor volume was calculated as (length X width^2 X 0.52). All mice were housed and care for in a standard 12 hours light/dark cycle, in accordance with institutional standards. Mice were carbon-dioxide-euthanatized prior to tissue extraction.

3-2. Cell isolation and culture

For isolation of stromal vascular fraction (SVF), adipose tissues from C57BL/6 *WT* and *SPARC*$^{-/-}$ mice were resected from various adipose depots (subcutaneous, intraperitoneal and epididymal), minced, and digested with collagenase (Worthington 250 U/ml in PBS) and dispase (Roche, 2.4U/ml in PBS) for an hour at room temperature with intermittent shaking. Preparations were passed through a 40 μm mesh and centrifuged at 400*g* for 8 min. The SVF pellets were washed and resuspended with alpha-MEM. The SVF pellets were subjected to immunostaining, flow cytometry analysis, Western blotting, or culture. ASC, enrichment for which was confirmed by flow cytometry using CD34,

CD31, and CD45 as markers, were cultured in alpha-MEM supplemented with 10% FBS and penicillin/streptomycin. To obtain peripheral blood mononucleated cells (PBMC), whole blood was collected from cardiac puncture of euthanized mice. The anticoagulant-treated blood was gently layered onto Ficoll-paque solution (GE) and centrifuged (Eppendorf centrifuge 5810R) at 2000rpm 20min, brake 0. The buffy coat layer enriched with mononuclear cells was collected and washed with alpha-MEM or fluorescence-activated cell sorting solution (2%BSA/1 mm EDTA) then subjected to flow analysis. 3T3-L1 and HEK 293 cells (purchased from American Type Tissue Collection) were cultured in Dulbecco's Modified Eagle's Media containing 10% fetal bovine serum (FBS) supplemented with 10% FBS and penicillin/streptomycin. Breast adenocarcinoma E0771 (from F.M.Sirotnak) was cultured in RPMI supplemented with 10% FBS supplemented with 10% FBS and penicillin/streptomycin.

3-3. Flow cytometry

For fluorescence-activated cell sorting (FACS) analysis, peripheral blood mononucleated cells (PBMCs) were obtained by Ficoll-sodium metrizoate centrifugation procedure (GE Health). PBMC or SVF cells (used as a gating control) were pretreated with red blood cell lysis buffer and stained with respective antibodies. Cells were prepared at a concentration of 1 million cells per milliliter and pregated to exclude non-viable cells, tissue debris, cell clumps, red blood cells based on 40,6-diamidino-2-phenylindole staining. Live PBMCs were sorted into populations as described with FACSAria/FACSDiva software based on the IgG clones: eFluor 660-conjugated rat anti-CD34 (RAM34, eBioscience, 1:100), PE conjugated rat anti-CD312 (MEC 13.3, BD Biosciences, 1:100),

and APC-cy7-conjugated rat anti-CD45 (30-F11, BD Biosciences,1:100). Gating was based on the corresponding isotype controls (BD Biosciences, San Jose, CA).

3-4. Transwell assay

Cell migration assays were conducted as described (Corning, USA). Cells were seeded (triplicate) in 200 μl of 0.1% FBS medium. Inserts were placed in wells containing 700 μl of 5% or 0.1% FBS medium supplemented with SPARC or indicated SPARC isoforms, 10% FBS was used as positive control. The cells were incubated for 16 hr. Non-migrated cells retaining in the insert were removed gently by swabbing with a cotton swab. The inserts were fixed with 4% paraformaldehyde for 10 min at room temperature and stained with crystal violet. Migrated cells attached on the other side of the insert were counted using a bright-field microscope.

3-4. Tissue processing and immunofluorescence microscopy

Tissues obtained were processed as previously described (Zhang et al., 2009), briefly, formalin-fixed and paraffin embedded 5 mm tissue sections were subjected to Novocastra antigen retrieval solution (Leica, Buffalo Grove, IL), washed with Phosphate Buffered Salt (PBS) containing 0.01% Triton-X, and blocked in serum-free protein block (DAKO, Carpinteria, CA). For preparation of WAT whole mounts, fragments of WAT were partly digested with collagenase/dispase for 15 minutes at room temperature and washed with PBS. Whole mounts or SVF cells, preincubated with SPARC proteins (100 nM) for 30 minutes where indicated, were prepared for immunofluorescence by washing with PBS and fixing with 4%

paraformaldehyde for 10 minutes at room temperature, rendered permeable with 0.3% Triton X-100 for 5 minutes, and blocking with Seablock (Thermo scientific, Waltham, MA) for 1 hour at 24 ^{o}C. Samples were incubated at 4 ^{o}C overnight with primary antibodies as follows: mouse anti-SPARC monoclonal antibody Mab303 (gift from Helene Sage, 1:100), goat anti-mouse SPARC (R&D Systems, Minneapolis, MN, 1:100), rabbit anti-perilipin (Cell Signaling Technology, Danvers, MA, 1:100), rat anti-mouse F4/80 (Abcam, Cambridge, MA1:100), rat anti-CD34 (Abcam, 1:100), rabbit anti-stabilin-1 (Santa Cruz, Santa Cruz, CA,1:100), rat anti active b1 integrin 9EG7 (BD Pharmingen, San Diego, CA,1:100), rabbit anti-paxillin Tyr118 (Cell Signaling Technology, Beverly, MA, 1:100), phalloidin (Invitrogen, Carlsbad, CA, 1:40), or biotinylated isolectin B4 (Vector Laboratories, Burlingame, CA,1:75). Following washing, the samples were incubated with secondary antibodies at room temperature for 1 hour in PBS/0.01% Triton-X. Secondary antibodies used were donkey Alexa 488-conjugated IgG (Invitrogen, 1:150) and Cy3-conjugated IgG (Jackson ImmunoResearch, West Grove, PA, 1:300). Nuclei were stained with Hoechst 33258 or DRAQ5 (Cell Signaling Technology, 1:1,000). Samples were mounted in ProLong Gold Antifade Mountant (Life Technologies, Austin, TX). Image acquisition was done using confocal Leica TCS SP5 microscope (images captured using Plan Apo 310/0.40CS, 340/0.75 U-V-I) and analyzed using LAS AF software or with Olympus IX70 (Center Valley, PA) inverted fluorescence microscope (images taken with 310/0.25, 320/0.40, or 340/0.60) using Olympus DP71 camera. Images were analyzed with cell-Sens software. Staining with secondary antibodies alone was used to set threshold and exclude nonspecific signal. All images were acquired at room temperature. Brightness and contrast of images were adjusted with Adobe Photoshop CS3.

3-5.Short-hairpin RNA (shRNA) lentiviral production and infection

β1 integrin, ILK, FAK silencing experiments were performed with lentiviral pLKO.1-puro vectors from Sigma-Aldrich (St. Louis, MO). The following oligonucleotides were used: TRCN0000066645 and TRCN0000066646 for b1integrin; TRCN0000023484 and TRCN0000023488 for FAK, TRCN0000022515 and TRCN0000022517 for ILK. Green fluorescent protein (GFP)-short-hairpin RNA (shRNA) PLKO.1 was used as untargeted shRNA control. 293T cells were co-transfected with indicated protein shRNA or control shRNA carrying GFP tag, packing plasmids (deltaVPR8.9) and envelope plasmid (VSV-G) using Lipofectamine 2000 reagent according to the manufacturer's instructions or calcium phosphate for 2 days, and virus particles containing indicated protein or control shRNAs were filtered through 0.45 μm pore cellulose acetate membranes and used to infect 3T3L1 cells. All the infected cells were cultured and puromycin (2 μg/ml) medium selection medium for 4 days. The knockdown efficiency was validated by western blotting.

3-6. ILK kinase assay

The ILK kinase assay was performed according to the manufacturer's protocol (Cell Signaling Technology, Nonradioactive Akt Kinase Assay Kit) with some modifications. 3T3-L1 cells (or immortalized mouse ASC (Zhang et al., 2009) used with the same result) transduced with indicated silencing constructs were serum-starved for 24 hr before incubation with SPARC or SPARC isoforms for 10 min. Cells were washed with PBS, harvested and lysed with cell lysis buffer. Lysate (500 μg) were immunoprecipitated with 2 μg of goat anti-ILK antibody (Santa Cruz) at 4^{o}C overnight. Protein A/G plus agarose

beads were used to pull down immune complexes (Thermo Scientific), followed by 3 washes with cell lysis buffer. The isolated immune complexes were then incubated with 1 μg GSK-3β fusion protein subtract in reaction buffer containing 200 μM ATP, for 30 min at 30°C. Western blotting with rabbit anti-phospho-GSK-3 α/β (Ser21/9) antibody (Cell Signaling Technology, 1:1000) was use to detect substrate phosphorylation.

3-7. Western blot analysis

Cells were lysed with radio-immuno-protein assay (RIPA) buffer (150 mM sodium chloride, 1.0% IGEPAL® CA-630, 0.5% sodium deoxycholate, 0.1% sodium dodecyl sulfate, and 50 mM Tris, pH 8.0, protease inhibitor cocktail (Roche). The protein concentration was determined with Bradford protein assay (Pierce, Appleton, WI). An equal amount of protein/lane was loaded onto 10% polyacrylamide SDS Tris–Glycine gels. After electrophoresis (20 mA/gel), proteins were electroblotted onto polyvinylidene fluoride (PVDF) membranes (Millipore, Billerica, MA). Membranes were blocked (5% nonfat dry milk) and then incubated with primary antibody overnight at 4^{o}C, followed by incubation with horseradish peroxidase (HRP)-conjugated secondary antibody at room temperature for 1 hr. The blots were developed by using enhanced chemiluminescence (Pierce). Mouse anti-β-actin antibody was from Sigma (1:5000). Goat anti-β1 integrin and anti-ILK antibodies were from Santa Cruz Biotechnology (1:1000). Goat anti-SPARC (R&D Systems), mab303, rabbit anti-FAK (Abcam) and rabbit anti-phospho-FAK (pY397) (Invitrogen) were used at 1:1000. Rabbit anti-Akt, anti-phospho-Akt (S473), anti-phospho-paxillin (Tyr118), anti-ERK, and anti-phospho-ERK1/2 (Thr202/Tyr204) antibodies were from Cell Signaling Technology (1:1000).

3-8. Expression and purification of recombinant proteins

The cDNA encoding SPARC and its truncated fragments were PCR-amplified using the SPARC cDNA as a template, cloned into vector pcDNA3.1 and sequence-verified. Human embryonic kidney 293 (HEK-293) cells were transiently transfected with the vectors by calcium phosphate precipitation. Empty vector for expression was used as a negative control. The recombinant His-tagged proteins were purified from conditioned culture media by Ni-NTA-Bind Resin (Novagen, Madison, WI) according to manufacturer's protocol with minor modifications. Briefly, the Ni-NTA-Bind resin slurry was pre-washed with 1X Ni-NTA bind buffer (50 mM NaH2PO4, pH 8.0; 300 mM NaCl; 10 mM imidazole) and mixed with conditioned medium for an hour at 4^{o}C. The protein-resin complex was packed into column for subsequent wash (1X Ni-NTA Wash Buffer: 50 mM NaH2PO4, pH 8.0; 300 mM NaCl; 20 mM imidazole) and elution (1X Ni-NTA Elute Buffer: 50 mM NaH2PO4, pH 8.0; 300 mM NaCl; 250 mM imidazole). The eluted His-tagged proteins were subjected to desalting and dialysis (Pierce). The purity of isolated proteins was examined by SDS-PAGE. The identity of the isolated recombinant proteins was confirmed by Western blot analyses using mouse anti-His (Sigma, 1:1000) and goat anti-SPARC (R&D Systems, 1:1000) antibodies.

3-9. ELISA Protein Binding Assays

For direct ELISA binding assays, 20 lg/ml of collagen I (Cultrex, Gaithersburg, MD), collagen IV (Cultrex), or fibronectin (BD Bioscience) was immobilized onto 96-well Maxisorb Immunoplates (NUNC) overnight at 4^{o}C, respectively, by absorption. The coated plates were washed with PBS/0.01% Triton-X (PBST), followed by blocking with 3% bovine serum albumin (BSA) at room temperature for 2 hours. Full length (FL)-SPARC,

C-SPARC, N-SPARC, and a control His6-tagged protein CLIC4 (Daquinag et al., 2011) were biotinylated (Thermo Scientific) and 100 nM of proteins was added and allowed to bind for 2 hours at room temperature (Fig. 4-7A). Similarly, direct ELISA binding assay was also performed with SPARC protein immobilized onto 96-well followed by washes, blocking, and treatment with biotinylated α5β1 integrin (R&D Systems, 1.25 μg/ml) (Fig. 4-5G). For competitive ELISA binding assays (Fig. 4-7B), the ECM-coated plates were washed with PBST, followed by blocking with 3% BSA. Biotinylated mouse α5β1 or α1β1 integrin (R&D Systems, 1.25 mg/ml) was pretreated with 100 nM of His6-tagged SPARC, C-SPARC, N-SPARC, or CLIC4 then allowed to bind to the ECM-coated wells. Bound biotinylated proteins were probed with streptavidin-HRP (R&D Systems, 1:200) after three washes with PBST. Ultra-TMB (Pierce) substrate was added, and absorbance was measured at 450 nm using a SpectraMax M2 (Molecular Devices, Sunnyvale, CA).

3-10. Cell adhesion and detachment assay

Cell adhesion assay was performed as described (Humphries, 2009) with minor modifications. Briefly, 96-well plates were coated with 20 μg/ml fibronectin (BD Bioscience) overnight at 48C and blocked with 10 mg/ml of heat-denatured BSA for 30 minutes at room temperature.Passage-1 $SPARC^{-/-}$ ASC were trypsinized and resuspended in warm DMEM/HEPES (gassed with 5% CO2) at a concentration of $5x10^5$ cells per milliliter followed by 10 minutes incubation at 37 ^oC. Fifty milliliters of cell suspension was mixed with FL-SPARC or SPARC isoforms (500 nM) and plated onto the fibronectin-coated plates in triplicates. Cells were incubated at 37 ^oC and at the 15 minutes time point, phase-contrast images were captured. After 1 hour incubation, wells were washed with

PBS, fixed with paraformaldehyde, and stained with crystal violet. For quantification, the percentage of cells with rounded morphology was scored by analyzing 10 representative x10 view fields. Cell detachment assay was performed with passage-1 SPARC$^{-/-}$ ASC or 3T3L1 transduced with non-targeted shRNA or shRNA silencing b1 integrin, ILK, or FAK that were plated onto fibronectin-coated 96-well plate. 500 nM of FLSPARC, C-SPARC, or N-SPARC was added to ASC (for indicated time interval) or 3T3L1 control knockdown or protein silenced clones (for 30 minutes). The dislodged cells were aspirated and wells were washed with PBS. Remaining cells were fixed with 10% paraformaldehyde for 10 minutes at room temperature followed by washing and crystal violet staining/microscopy. For quantification, cells in 10 x10 view fields were counted or crystal violet stain was dissolved with 10% acetic acid and cell number was read as absorbance (570 nm). The percentage of adherent cells was measured by normalizing to OD of untreated control wells.

Statistical Analyses

Microsoft Excel was used to graph data as mean ± SEM and to calculate P-values using homoscedastic Student's t-Test. $P < 0.05$ was considered significant. Data met assumptions of normality.

Chapter 4

Results

Figures 4-1 to 4-2 are obtained and modified by permission from the American Association for Cancer Research: Yan Zhang, Alexes C. Daquinag, Felipe Amaya-Manzanares, Olga Sirin, Chieh Tseng, and Mikhail G. Kolonin. Stromal Progenitor Cells from Endogenous Adipose Tissue Contribute to Pericytes and Adipocytes That Populate the Tumor Microenvironment. Cancer Research, 2012, 72(20), 5198-5208. And Figures 4-3 to 4-14 are obtained by permission from Stem Cells: Chieh Tseng and Kolonin, Proteolytic Isoforms of SPARC Induce Adipose Stromal Cell Mobilization in Obesity, Stem Cells, Epub ahead of print.

SUMMARY

Obesity increases cancer risk and progression as shown by epidemiologic studies. However, the underlying pathophysiology remains unclear. In this study, we show that the ASC pool is expanded in obesity and is associated with promoting of tumor growth. Next, by using a chimeric GFP-RFP bone marrow transplant model, we observed higher numbers of tumor-infiltrating cells with ASC phenotype in tumor grafted in obese mice compared to lean. Consistently, systemic circulating ASC frequency is six fold higher in tumor-bearing obese mice compared to lean. The tumor infiltrating cells with ASC phenotype are found to be perivascular, suggesting that there are being incorporated into vessels as pericytes to support tumor vasculature. We have obtained evidence that ASC are mobilized in response to obesity and cancer; however, the mechanisms regulating ASC trafficking are poorly defined. Previously, we reported the binding of the matricellular protein SPARC to β1 integrin on ASC surface induces their motility (Nie et al., 2008). However, the physiological significance of this SPARC effect has not been established. Here, for the first time, we report that SPARC is required for ASC mobilization in obesity and investigate the biochemical mechanism of its function. We show that SPARC is required for ASC mobilization into the systemic circulation in obesity. We also identified the mechanism of signal transduction induced by SPARC binding to its receptor, β1 integrin, on ASC surface. Our result demonstrates that this interaction induces ASC motility through integrin-dependent FAK-ERK signaling and integrin independent ILK-Akt signaling. We further identified two SPARC proteolytic isoforms, CSPARC (lacking the N-terminus) and N-SPARC (lacking the C-terminus), generated in visceral WAT in the context of obesity. We show that C-SPARC, but not N-SPARC, binds to β1 integrin on ASC, while N-SPARC

preferentially binds to the ECM and blocks ECM/integrin interaction. Our study demonstrates that that both C-SPARC and N-SPARC induce ASC de-adhesion from the ECM, which is associated with modulation of integrin-dependent FAK-MAPK signaling and integrin-independent ILK-Akt signaling. Importantly, we show that these SPARC isoforms, acting on ASC through distinct mechanisms, have an additive effect in inducing ASC migration.

RESULTS

Obesity-induced promoted tumor growth independent of diet

Obesity promotes tumor growth, which has been demonstrated by multiple groups (Allott and Hursting, 2015; Calle and Kaaks, 2004; Calle et al., 2003). In our study, we set up cohort of obese (body weight greater than 45 grams) and lean mice (body weight less than 30 grams) by placing them on high-fat diet or low-fat diet. To eliminate the difference in diet as confounding variables in cancer progression, diet normalization was initiated by subjecting both groups of mice to regular chow for 1 month before tumor engraftment. Consistent with previous studies, Lewis lung carcinoma (LLC) growth engrafted in obese mice exhibited accelerated growth kinetics as compared to the lean mice (Fig. 4-1A). A concomitant reduction in body weight was observed in obese mice as tumors grew in size; however, the lean mice weight remained relatively constant throughout (Fig. 4-1A). Our data suggest that the excessive WAT in obesity is a crucial component in obesity-induced tumor growth. In obese mice, a 7-fold increase in WAT mass was observed (data not shown). As WAT is characterized by abundance of ASC, we next evaluated the effect of increased adiposity on ASC frequency. ASC frequency was measured by enumerating CD34+CD31-CD45- expressing cells with flow cytometry (Zhang et al., 2009). Our result showed modest elevation in ASC frequency in obese mice intraperitoneal (i.p.) WAT measuring 32.6 % whereas in lean mice, a 30.4% was detected. Given the WAT mass was expanded in obesity, with a total of 1.0 ± 0.23 grams in lean and 6.19 ± 0.25 grams from obese mice i.p. WAT. The net number of ASC from obese mice was extrapolated to be 6 times higher in obese mice as compared to lean mice (Fig. 4-1C). Taking advantage of plastic-adhering properties of ASC, we subjected the WAT stromal/vascular cells fraction

to culture. We quantified and recovered a higher number of ASC from obese mice (Fig. 4-1E), characterized by defined nuclei and nucleoli (white arrow) distinct from Indian ink internalizing monocytic cells (black arrow) (Fig. 4-1D). Together, these data demonstrated that the expanded WAT mass in obesity act as additional ASC reserve. We next set out to test if the increased ASC reserve contributes to cancer progression by facilitating ASC trafficking into systemic circulation and recruitment to tumors. We analyzed circulating ASC frequency of tumor-bearing obese and lean mice, by comparing CD34+CD45- cell in PBMC. The result showed limited frequency of circulating CD34+CD45-cells (0.06%) in lean mice, while in obese mice, a 6-fold increase in frequency was registered (to 0.37%) (Fig. 4-1F). Morphologic analysis of FACS sorted-cell expressing CD34+CD31-CD45- from PBMC or WAT, revealed them to be similar and undistinguishable from one another (Fig. 4-1G). PBMC-derived CD34+CD31-CD45- cells from obese mice formed fibroblastoid colonies with adipogenic potential, characterized by lipid-containing adipocytes (Fig. 4-1H). Combined, our data showed increased obesity-associated egress of CD34+CD31-CD45- adipose tissue-derived progenitors in circulation with ASC phenotype.

Figure 4-1: ASC expansion promotes tumor growth

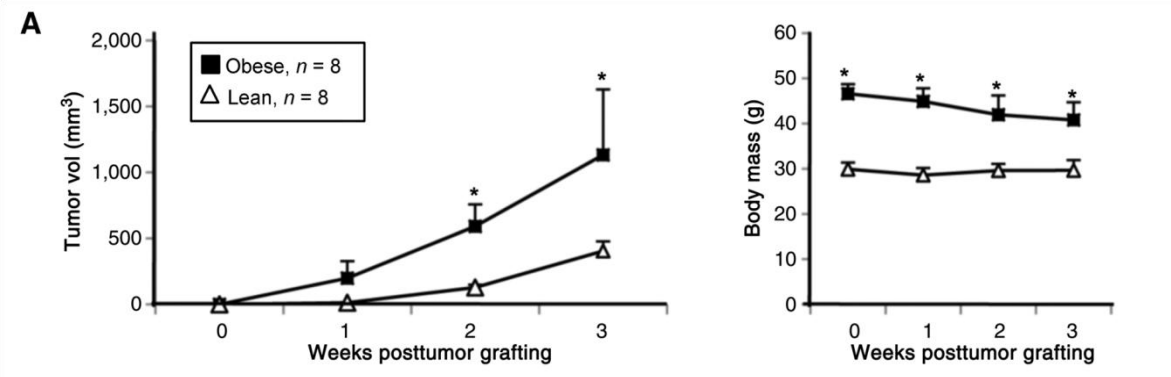

(**A**) LLC tumor growth kinetic in diet-induced lean and obese C57BL/6 mice. Following diet normalization (week 0), LLC were engrafted onto lean and obese C57BL/6 mice (left). Body mass of mice following tumor engraftment (right). Error bars, SEM. *, $P < 0.05$.

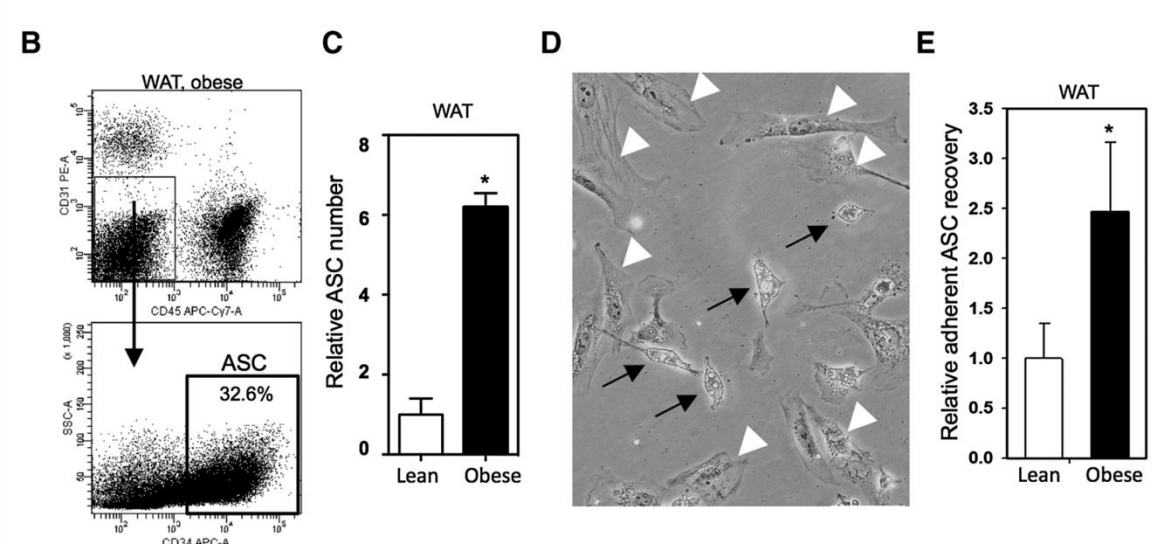

(B) Flow cytometric analysis of ASC in i.p. WAT (shown as percentage of viable cells). Viable SVF were gated for CD31-CD45- cells and subsequently on CD34+ cells. SSC-A, side scatter. (**C)** Relative ASC number in i.p.WAT of lean and obese mice. Quantification based on CD34+CD31-CD45- ASC frequency enumerated by flow cytometry and total i.p. WAT mass recovered from lean and obese mice. (**D)** Representative bright field

micrograph of Indian ink-stained i.p.WAT cells cultured for a day. ASC (white arrowheads) and monocytes (black arrows). (**E**) Relative adherent ASC number recovered from i.p.WAT of lean and obese. Scale bar, 50 mm. Error bars, SEM. *, $P < 0.05$.

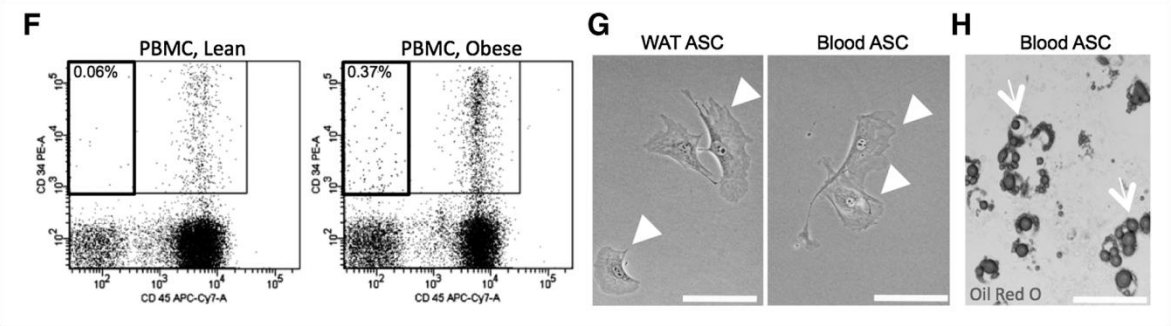

(**F**) Flow cytometry enumeration of CD34+CD31-CD45- cells from PBMC of lean and obese mice with tumor, shown as percentage of viable cells. (**G**) Representative phase contrast micrographs of FACS-sorted cells from WAT or PBMC (CD34+CD31-CD45-) of an obese mouse. (**H**) Micrographs of PBMC–derived CD34+CD31-CD45- stained with Oil red O, showing lipid droplets (white arrows).

Experiments in figure 4-1 were conducted by Yan Zhang, Felipe Amaya-Manzanares, Olga Sirin and Chieh Tseng.

Bone marrow transplantation model for tracking WAT-derived cells

Next, to test whether excessive WAT contributes to circulating ASC, we designed an *in vivo* model to enable us to distinguish ASC from cells of hematopoietic origin (Chantrain et al., 2008; Du et al., 2008; Kolonin et al., 2012). The chimeric GFP-RFP bone marrow transplant model was generated by replacing irradiated GFP-mouse bone marrow with RFP cells. Both GFP+ and RFP+ cells were found in all tissues evaluated and we have confirmed RFP+ cells to co-express CD45+ leukocyte markers.

Similar to the no color mice, chimeric GFP-RFP mice placed on HFD or LFD were normalized to the regular chow diet prior to EO771 tumor engraftment. Tumor growth and volume were significantly greater in obese chimeric GFP-RFP. Consistently, higher GFP+ infiltrating cell numbers with ASC phenotype were recovered from tumors of obese chimeric mice. Our result demonstrates a higher ASC trafficking from WAT to tumor in obesity.

4-2. Pericyte recruitment in obesity and tumor vascularization

To determine the functional roles of recruited ASC in tumor, we evaluated the difference in tumor structures between lean and obese mice. Haematoxylin eosin staining of tumor revealed increased malignant cells viability with reduced hemorrhagic and necrotic regions in obese mice. On the basis that angiogenesis is a key determinant in tumor growth that is crucial in providing oxygenation, nutrient delivery and waste removal (Du et al., 2008; Hanahan and Weinberg, 2011). We therefore assessed whether ASC infiltrating into tumor is associated with angiogenesis and blood vessel remodeling. Comparative immunofluorescence analysis of tumor sections demonstrated that a higher number of host-derived GFP+ cells reside in close proximity with CD31+ endothelial cells in tumors of obese mice (Fig. 4-2A and 4-2B). The co-localization of GFP+ cells with pericyte marker: desmin, revealed them to be involved in tumor vessels maturation. Notably, in obese mice, the tumor vasculature density was 2-fold higher than the lean mice. (Fig. 4-2C). Tumor blood vessels in lean mice were found sparsely distributed and structurally more compressed, whereas in obese mice, the tumor vasculature was larger and better perfused with blood cells (Fig. 4-2A and 4-2B). Quantification of blood vessels co-expressing desmin and GFP in tumors showed a higher frequency in the obese mice (Fig. 4-2D), suggesting increased vessel maturation associated with obesity (Fig. 4-2C). Combined, these results reinforce the notion that ASC expansion in obesity contributes to the perivascular cell pool, thereby promoting tumor progression.

4-2. Pericyte recruitment in obesity and tumor vascularization

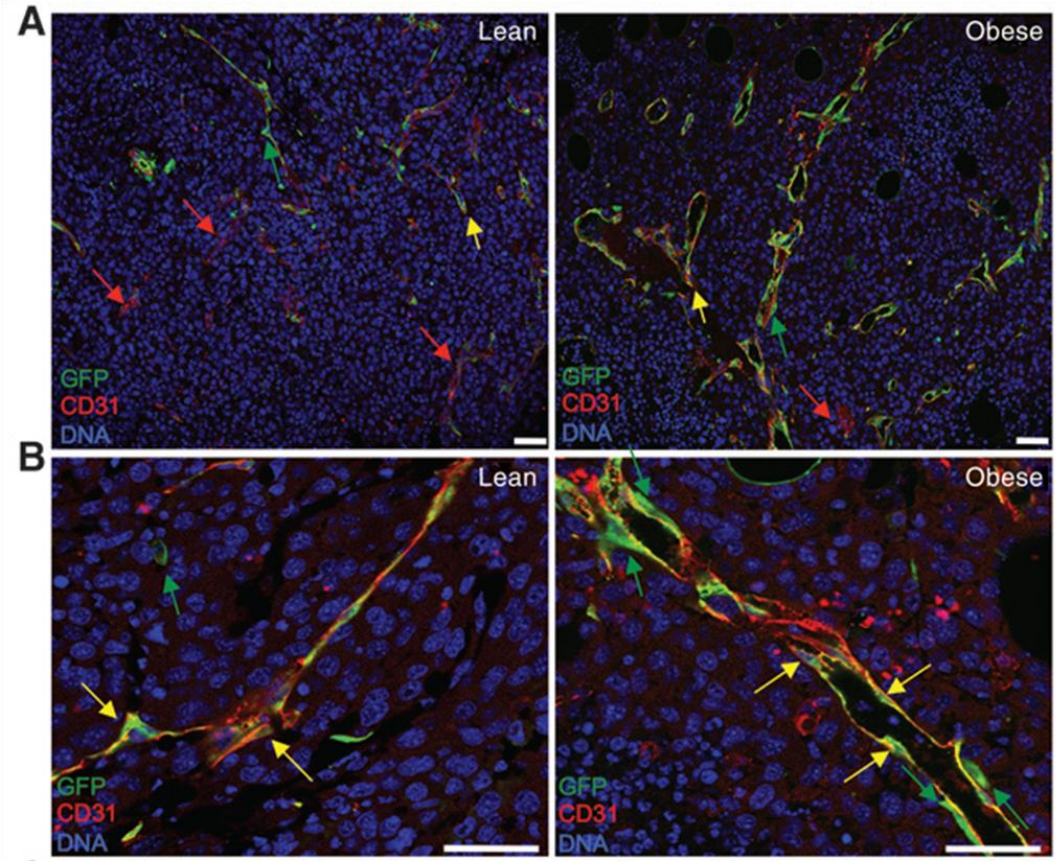

(A & B) Representative immunofluorescence images of tumor section from obese and lean mice stained with antibodies against CD31 (red) and GFP (green). Images shown were taken at high (B) and low (A) magnification of tumor internal viable regions. Tumor vessels contains GFP+CD31- perivascular/stromal cells indicated by green arrows and luminal GFP+CD31+ endothelial cells (yellow arrows) and. Note increased pericyte coverage and larger in size of the tumor vessels in obese mice.

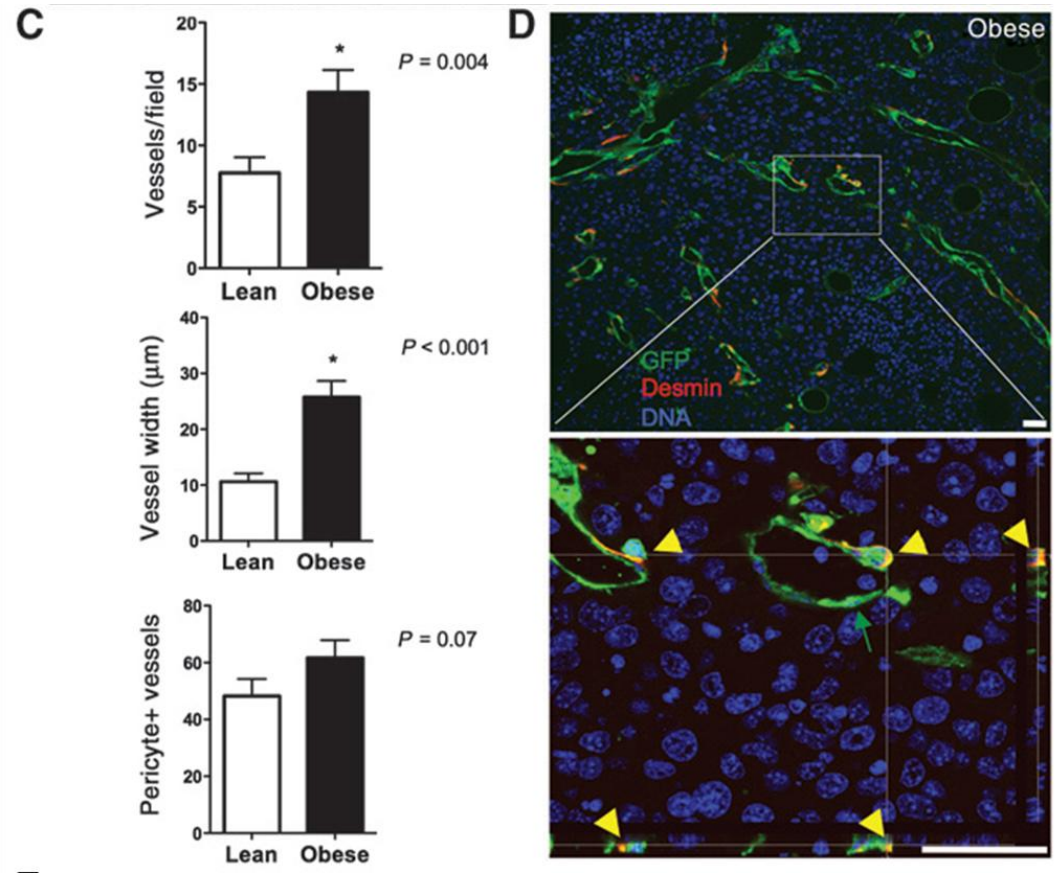

(**C**) Comparative analysis of tumor vessel density, width and pericytes coverage between obese and lean. Vessel density was quantified as mean number of vessels/100x view field. Vascular size was assessed as mean lumen width for all vessels scored. The maturity of vessel was assessed as mean percentage of vessels associated with desmin+ pericytes among all vessels scored. Error bar, SEM. D, confocal immunofluorescence tumor analysis with antibodies against GFP (green) and desmin (red). Yellow signal indicates GFP+ pericytes, which is confirmed by Z-stack projections of median series for individual cells in the indicated magnified area (bottom).

Experiments in figure 4-2 were conducted by Yan Zhang, Felipe Amaya-Manzanares and Chieh Tseng.

4-3. SPARC Promotes Mouse ASC Motility and Mobilization

Having shown that ASC are mobilized in cancer and obesity (Zhang et al., 2012) and our observations that SPARC induces ASC de-adhesion and motility (Nie et al., 2008), we hypothesized that SPARC promotes ASC mobilization. To test this *in vivo*, we compared ASC circulation in *SPARC*$^{-/-}$ mice (Bradshaw et al., 2003a; Norose et al., 1998) and *wild-type* (*WT) SPARC*$^{+/+}$ mice. Peripheral blood mononuclear cells (PBMC) were analyzed in lean mice (<30 g) raised on chow and in diet-induced obese (DIO) mice (>45 g) raised on high-fat diet for 5 months. Circulating ASC among PBMC were enumerated by flow cytometry based on the previously established $CD34^{+}CD31^{-}CD45^{-}$ cell surface signature and gating strategy (Daquinag et al., 2015; Daquinag et al., 2011; Zhang et al., 2012). Only background (0.01%) of PBMC had the ASC immunophenotype in lean mice, while upon DIO induction 0.12% of PBMC were registered as ASC (Fig. 4-3A). In contrast, only background (0.015% of PBMC) ASC circulation was observed in obese *SPARC*$^{-/-}$ mice, while the frequency of $CD45^{+}$ leukocytes was unaffected by SPARC deficiency.

We then explored the mechanism through which SPARC may induce cell mobilization. Our previous analysis of human SPARC effect on ASC motility was potentially confounded by secretion of endogenous SPARC by ASC (Nie et al., 2008). Here, based on a reported approach (Bradshaw et al., 1999), we used cells from *SPARC*$^{-/-}$ mice to avoid interference by autocrine secretion of SPARC. In a trans-well assay, recombinant mouse SPARC protein added to the cell culture medium promoted migration of suspended murine ASC in a dose-dependent manner (Fig. 4-3B). To assess the effect of SPARC on adherent ASC, we examined the response of ASC cultured on plates coated with fibronectin, an

adhesion ligand of α5β1 integrin. After 10 minutes of incubation with SPARC, the majority of ASC exhibited a rounded morphology and after 12 hours underwent partial detachment, while untreated ASC remained well spread (Fig. 4-3C). These results suggested that SPARC induces ASC mobilization by promoting their de-adhesion from the matrix.

4-3 SPARC promotes ASC mobilization and migration

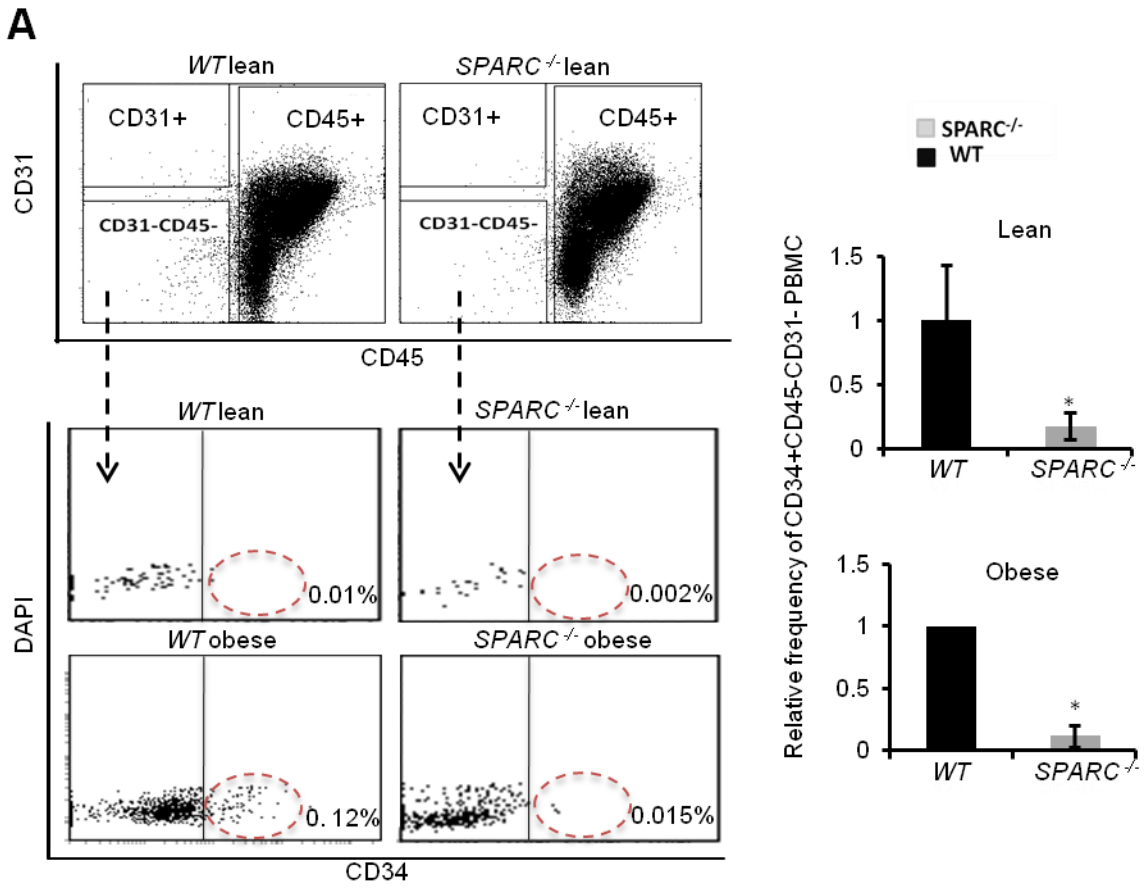

(**A**) SPARC is required for ASC mobilization. Viable PBMC stained with CD45-APC-cy7, CD31-PE and CD34-eFluor 660 were gated based on isotype controls to identify ASC as $CD34^{+}CD31^{-}CD45^{-}$ cells. The graphs show relative percentage of ASC in PBMC of lean and obese *WT* and *SPARC*$^{-/-}$ mice (n=3/group).

4-3. SPARC promotes ASC mobilization and migration

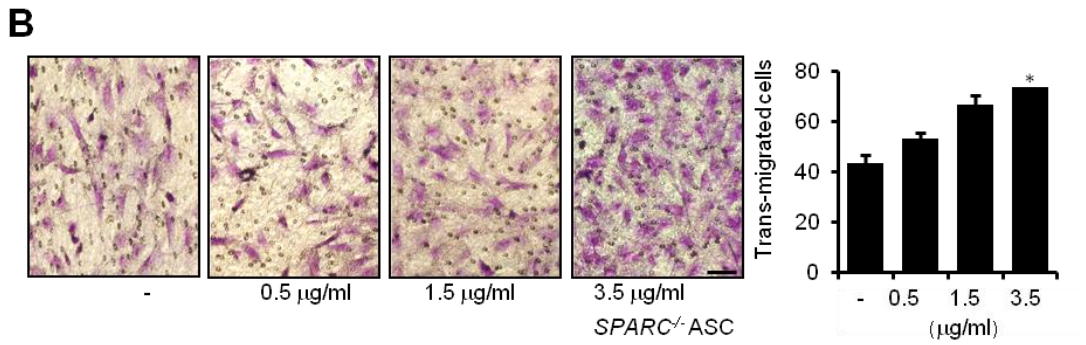

(**B**) SPARC promotes ASC motility. Primary ASC from *SPARC*$^{-/-}$ mice were incubated without (-) or with indicated concentrations of mouse recombinant SPARC and allowed to trans-migrate through 8 μm pores within 16 hrs and stained with crystal violet. Representative micrographs are shown. Mean numbers of trans-migrated cells / view field at indicated SPARC concentration are quantified in the graph.

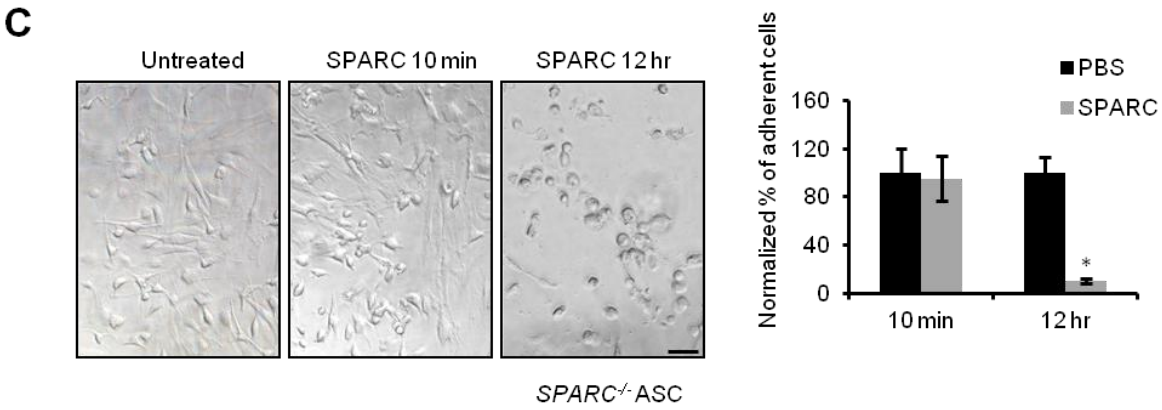

(**C**) SPARC induces ASC de-adhesion. Phase-contrast images of *SPARC*$^{-/-}$ ASC on fibronectin-coated plate were taken at 10 min and 12 hrs after exposure to 25 μg/ml (735 nM) SPARC. Normalized percentage of adherent cells at indicated time point is quantified in the graph. Experiments shown were repeated at least three times with similar result. Scale bar, 50 μm. Error bars, SEM from triplicate wells. * $P<0.05$.

4-4. SPARC-induced ASC deadhesion is linked with β1 integrin signaling

Based on previous studies suggesting that SPARC promotes cell motility by binding to β1 integrin at focal adhesions (Nie et al., 2008; Weaver et al., 2008), we further investigated the signaling events activated by this protein interaction. *SPARC*$^{-/-}$ ASC treated with mouse SPARC, which induced a time-dependent change in cell morphology evident by bright-field microscopy (Fig. 4-4A), were subjected to immunofluorescence analysis. An antibody against phosphorylated (Tyr118) paxillin demonstrated that focal adhesions observed in untreated cells became disassembled upon SPARC treatment (Fig. 4-4A). This was concomitant with active β1 integrin changing its localization from the cell surface to the peri-nuclear area, as revealed with an antibody specifically binding to active β1 integrin (Fig. 4-4A). This integrin redistribution, indicative of integrin internalization and recycling typically observed upon stimulation of cell migration (Gu et al., 2011), was associated with a marked cytoskeleton reorganization revealed by F-actin staining with phallodin (Fig. 4-4A).

Our previous work showed that 3T3-L1 preadipocytes serve as a convenient model to study SPARC / β1 integrin interaction (Nie et al., 2008). The response of 3T3-L1 cells to SPARC was similar to that of *SPARC*$^{-/-}$ ASC, albeit less striking (Fig. 4-4B). This indicated that endogenous SPARC, which is produced by 3T3-L1 cells (Chavey et al., 2006), does not preclude the effect of exogenous SPARC. To determine whether β1 integrin, ILK, or FAK are essential for SPARC signaling, we individually silenced each of these genes in 3T3-L1 cells using lentivirus expressing targeted short hairpin RNAs (shRNA); 3T3-L1 cells transduced with a non-targeted shRNA were used as control. For

each gene, we tested several clones and chose a representative clone displaying expression silencing of the respective protein, as verified by immunoblotting (Fig. 4-4C). We serum-starved the cells and examined the effect of SPARC on signaling after 5 and 15 min. FAK phosphorylation was substantial in control untreated cells, while treatment with SPARC reduced FAK phosphorylation at Tyr397 in a time-dependent manner (Fig. 4-4C). Tyr397 is a site of FAK autophosphorylation, reduction in which is observed upon a decrease in integrin signaling (Caswell and Norman, 2006; Eke et al., 2012; Lu et al., 2001; Zheng and Lu, 2009). Concomitantly, increased Thr202/Tyr204 phosphorylation of ERK1/2 was observed for SPARC-treated cells (Fig. 4-4C). Baseline FAK phosphorylation in the absence of SPARC was decreased for both β1 integrin knockdown and ILK knockdown cells (Fig. 4-4C). The changes in FAK and ERK1/2 phosphorylation upon SPARC treatment were not observed in cells with silenced β1 integrin, ILK, or FAK. These data indicate that MAPK activation by SPARC relies on β1 integrin signaling through both ILK and FAK (Fig. 4-4C). Because SPARC signaling is mediated by protein kinase B (Akt) in cancer cells (Alachkar et al., 2014; Shi et al., 2007), we also analyzed Akt activation. Akt phosphorylation (S473) was modestly induced by SPARC not only in control but also in β1 integrin, ILK, and FAK knockdown cells (Fig. 4-4C). This suggests that Akt activation in SPARC-treated cells is likely a non-specific response to cell de-adhesion rather than due to β1 integrin signaling.

Loss of either β1 integrin, FAK, or ILK resulted in abrogation of SPARC-induced induction of suspended cell motility (Fig. 4-4D). We also observed a reduction in SPARC-mediated cell de-adhesion in the absence of β1 integrin, FAK, or ILK (Fig. 4-4E).

Combined, these results indicate that SPARC-mediated cell de-adhesion and migration is associated with inhibition of β1 integrin signaling through ILK and FAK.

4-4. SPARC-induced ASC deadhesion is linked with β1 integrin signaling

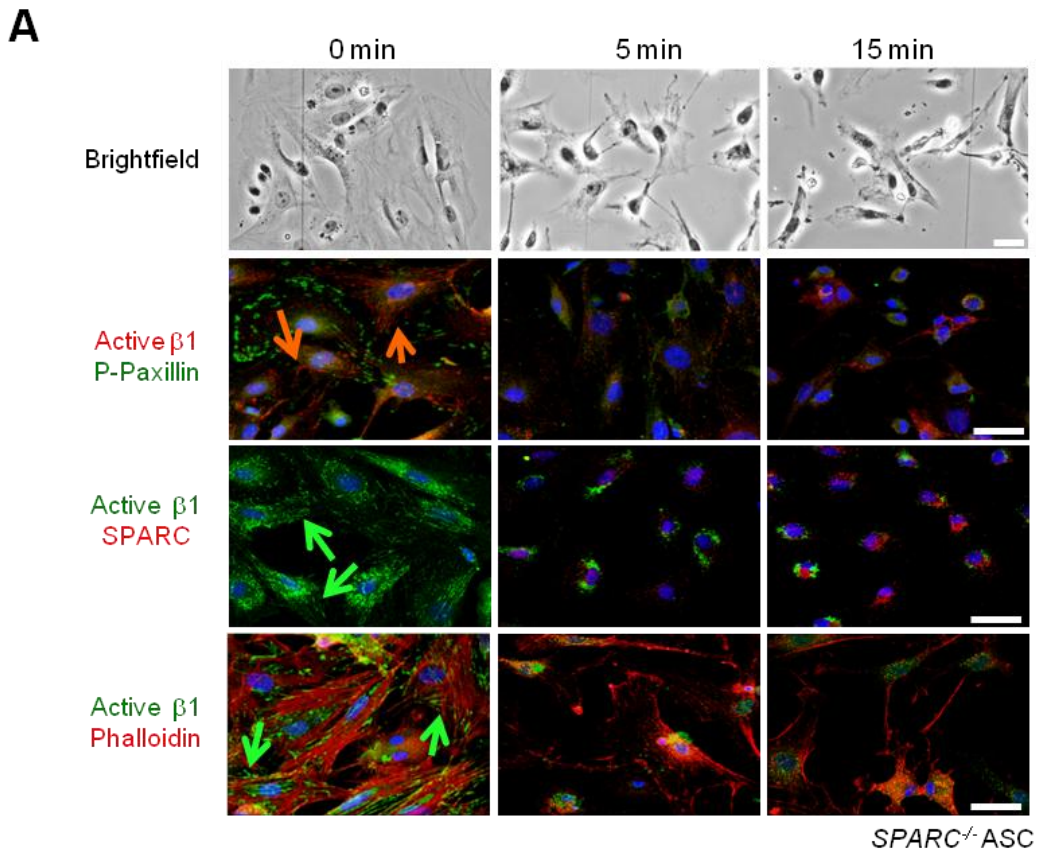

(**A**) Representative phase-contrast images of *SPARC-/-* ASC on fibronectin-coated plates incubated with 500 nM of FL-SPARC for indicated periods of time. Immunofluorescence with antibodies against activated β1 integrin (arrow) costained with p-paxillin (Tyr118) antibodies, SPARC antibodies, or phalloidin revealing cytoskeletal filaments is shown. Nuclei are blue.

4-4. SPARC-induced ASC deadhesion is linked with β1 integrin signaling

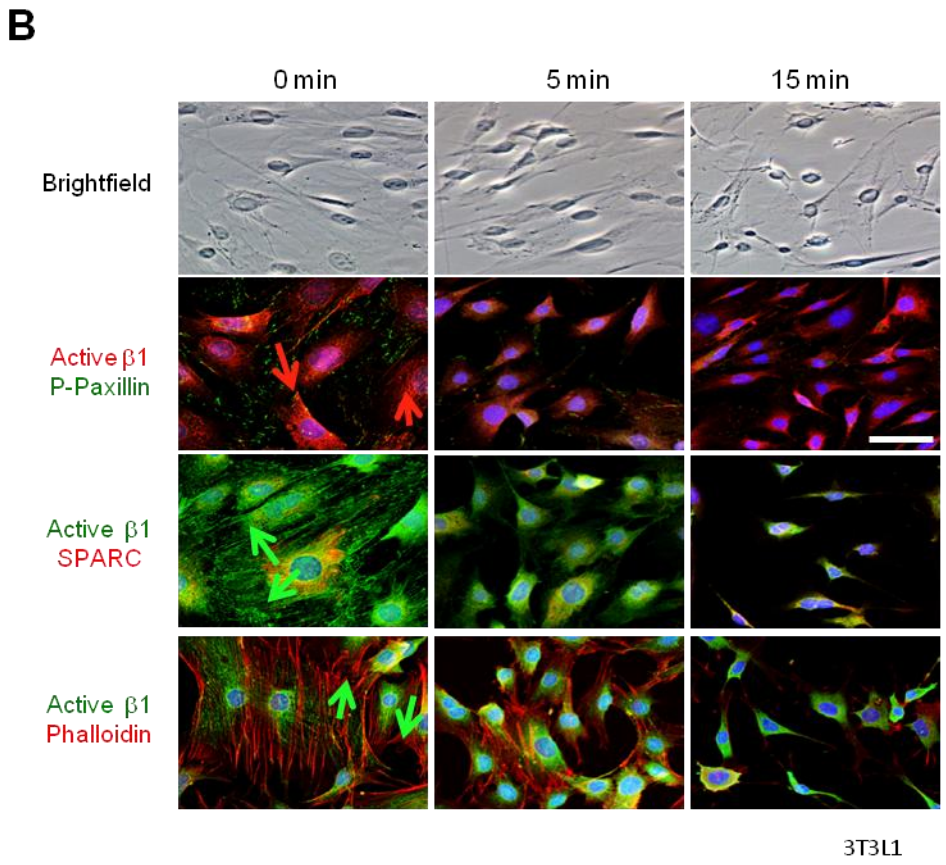

(**B**) SPARC-induced 3T3L1 de-adhesion is linked with β1 integrin signaling. Representative phase-contrast images of *3T3L1* on fibronectin-coated plates incubated with 500 nM of FL-SPARC for 0, 5 and 15 min time interval. Immunofluorescence with antibodies against activated β1 integrin (arrow) co stained with p-paxillin (Tyr118), SPARC and phalloidin revealing cytoskeletal filaments is presented. Nuclei are blue. Scale bar, 50 μm.

4-4. SPARC-induced ASC deadhesion is linked with β1 integrin signaling

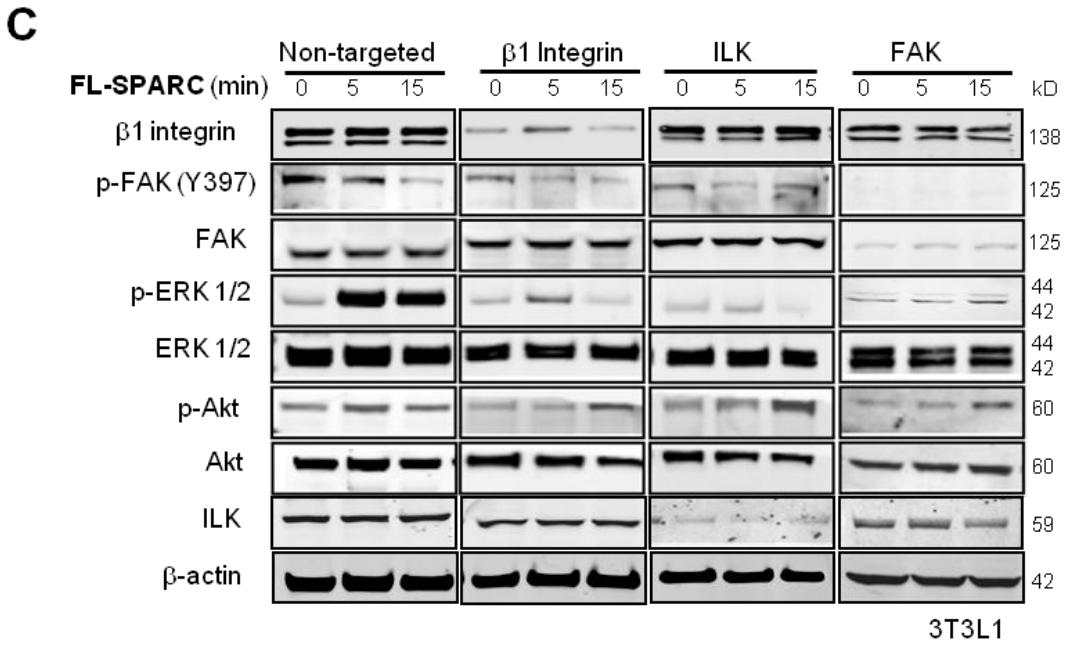

(**C**) 3T3-L1 cells were transduced with non-targeted shRNA (control) or shRNA silencing β1 integrin, ILK, or FAK. Serum-starved cells were incubated with mouse SPARC (500 nM) and cell lysates obtained at 0, 5, and 15 minutes post treatment were analyzed by Western blotting using antibodies against indicated antigens. Anti-β-actin immunoblotting demonstrates equal protein loading for different time points.

4-4. SPARC-induced ASC deadhesion is linked with β1 integrin signaling

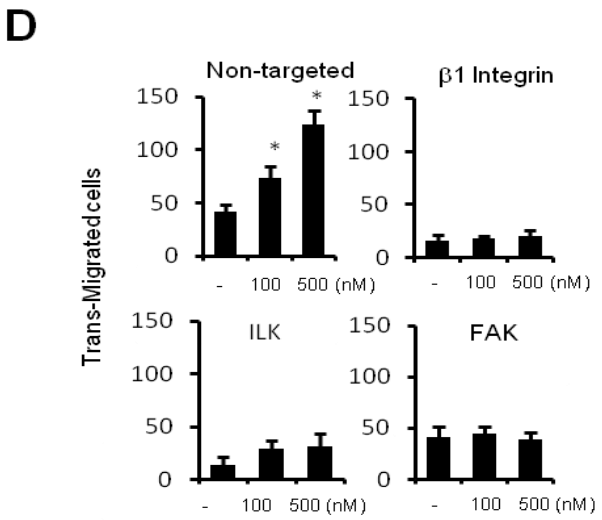

(**D**) Dose-dependent trans-well migration of 3T3-L1 cells transduced with non-targeted shRNA or shRNA silencing β1 integrin, ILK, or FAK. For the assay, cells were exposed to SPARC at indicated concentrations.

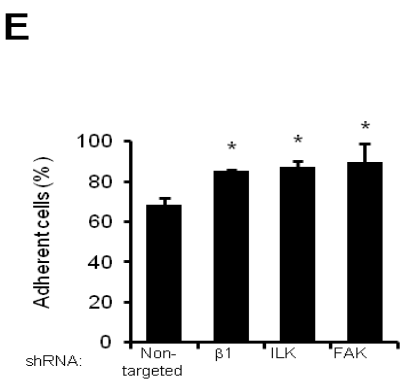

(**E**) Cell detachment assay with 3T3-L1 cells transduced with non-targeted shRNA or shRNA silencing b1 integrin, ILK, or FAK incubated with 500 nM SPARC for 30 minutes. Data shown are representative of two or three independent experiments. Error bars, SEM from triplicate wells. *, $p<0.05$.

4-5. Obesity-induced SPARC isoforms in MS WAT

To identify the source of ASC mobilized in obesity, we investigated the differences in SPARC expression in individual WAT depots of lean and DIO mice. Immunofluorescence analysis revealed high expression of SPARC protein in mesenteric (MS) WAT of DIO mice (Fig. 4-5A). Distribution is very different while in WAT of lean mice SPARC was observed mainly in stromal cells; in DIO mice SPARC was also abundant in adipocytes (Fig. 4-5A). To quantify this change, protein extracts from MS, subcutaneous (SC), and epididymal (EP) WAT from lean and obese mice were immunoblotted with SPARC antibodies. This confirmed the highest (5.5-fold) induction in SPARC levels for MS WAT in obesity, while less than a 2-fold obesity-associated elevation was observed for SC and EP WAT after normalization to β-actin expression (Fig. 4-5B).

We next investigated if obesity results in generation of SPARC isoforms. Immunoprecipitation from distinct WAT depots was performed using an antibody mab303 that recognizes an epitope R149-L198 within the EC domain of SPARC (Weaver et al., 2008). Immunoblotting with polyclonal anti-SPARC antibodies demonstrated the presence of a lower molecular weight obesity-specific SPARC isoform in MS WAT (Fig. 4-5C). Scaled-up immunoprecipitate separated on a protein gel revealed the presence of an additional SPARC isoform generated in MS WAT of obese mice (Fig. 4-5D). Densitometry quantification of protein bands revealed that the abundance of full length (FL)-SPARC: C-SPARC: N-SPARC was 2.3: 1.3: 1.0, respectively, in MS WAT. The two MS WAT obesity-specific SPARC isoforms were subjected to Edman degradation protein sequencing, which identified them as proteolytic fragments of SPARC. The longer

fragment (amino acids 14-285) missing the 13 N-terminal residues was termed C-SPARC; the shorter fragment (amino acids 1-196) missing amino acids (197-285) was termed N-SPARC (Fig. 4-5E). According to previous SPARC domain mapping (Hohenester et al., 2008; Kzhyshkowska et al., 2006; Nie et al., 2008; Sasaki et al., 1998; Weaver et al., 2008), C-SPARC is expected to bind to β1 integrin, while N-SPARC, lacking the C-terminal β1 integrin-binding domain, is expected to be deficient in integrin binding but still bind to stabilin-1.

To analyze the function of SPARC proteolytic isoforms, we constructed vectors for expression of FL-SPARC, C-SPARC, and N-SPARC as fusions with a His_6 tag. To ensure glycosylation and functionality of the secreted proteins, mammalian HEK293 cells were stably transfected with the expression vectors or insertless vector control. His_6-tagged FL-SPARC, C-SPARC, and N-SPARC were affinity-purified from conditioned media collected from transfection clones. Identity, purity, and concentration normalization of the soluble recombinant proteins was performed by immunoblotting with anti-SPARC antibodies (Fig. 4-5F). To test whether N-SPARC retains β integrin interaction, we precipitated protein complexes from cells co-transfected with β1 integrin and indicated SPARC variants with anti-His tag antibodies and immunoblotted the co-immunoprecipitates with anti-β1 integrin antibodies. As expected, β1 integrin co-immunoprecipitated with FL-SPARC and C-SPARC, while its co-immunoprecipitation with N-SPARC was markedly lower (Fig. 4-5F). We further validated our observation by assessing direct binding of biotinylated α5β1 integrin to SPARC variants. While FL-SPARC and C-SPARC displayed direct α5β1 integrin binding, N-SPARC binding was not significantly above nonspecific background (Fig. 4-5G). These data confirm that the

SPARC C-terminus mediates β1 integrin binding and suggest that the C-SPARC and N-SPARC isoforms may have distinct functions.

4-5. Obesity-induced SPARC isoforms in MS WAT

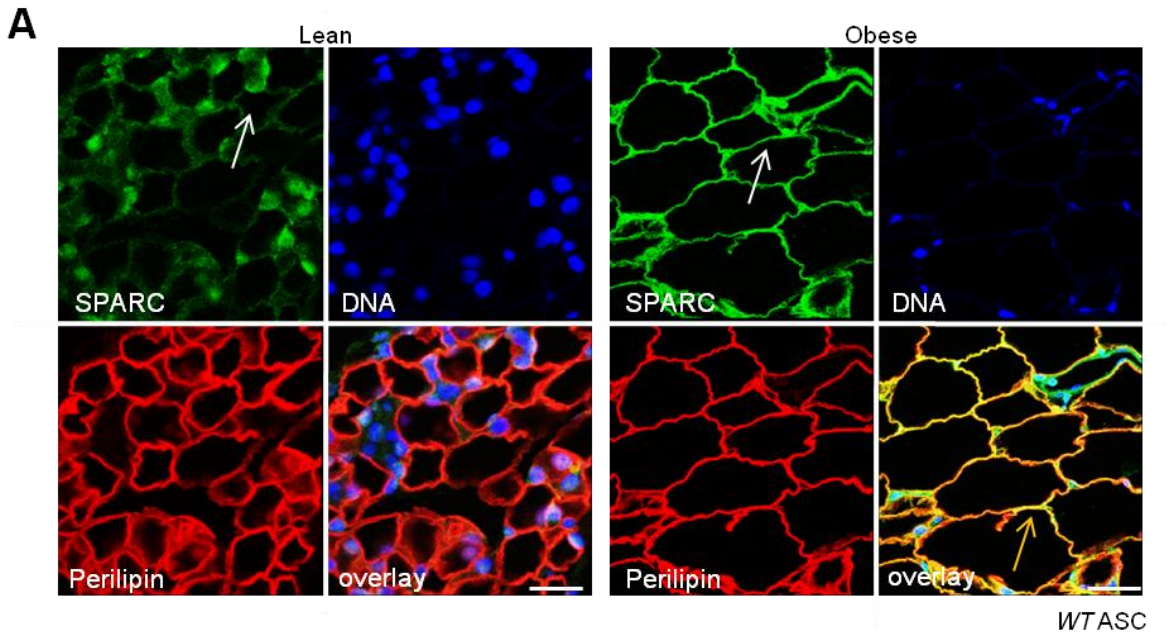

(**A**) Immunofluorescence analysis of MS WAT sections from lean and obese mice with anti-SPARC (green), anti-perilipin (red) antibodies. Nuclei are blue.

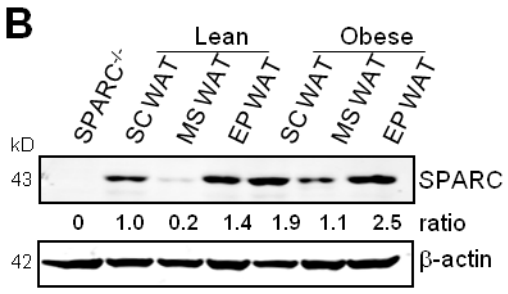

(**B**) Tissue lysates obtained from SC, MS, and EP WAT of *WT* lean and obese mice were analyzed for SPARC expression by Western blotting. Densitometry values were adjusted

to β-actin intensity and expression above level observed in SC WAT of lean mice was calculated (ratio) with AlphEaseFC software.

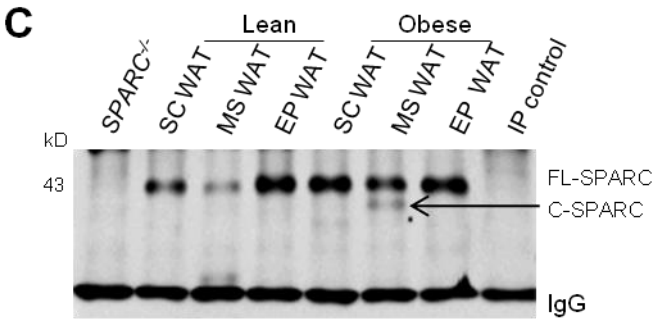

(**C**) Tissue lysates obtained from distinct WAT depots of lean and obese mice were IP with a SPARC monoclonal antibody Mab303. Non-immune IgG IP from obese MS WAT extracts served as a negative control. A single full-length (FL)-SPARC protein band at 43 kDa is present for SC, MS, and EP WAT of *WT* but not *SPARC-/-* mice. Arrow: additional 39 kDa C-SPARC band immunoprecipitated from obese MS WAT. Light chain IgG recognized by the secondary antibody demonstrates equal protein loading.

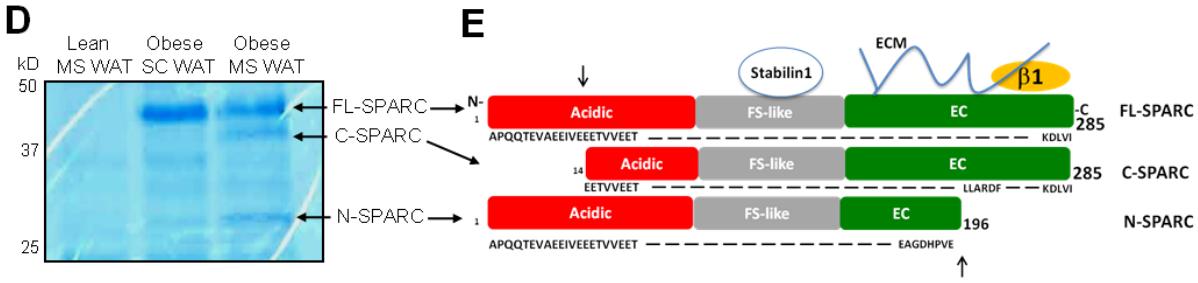

(**D**) For indicated WAT depots, scale-up Mab303 immunoprecipitation and immunoblotting was performed as in (C) Shown is Coomassie blue staining of the PVDF membrane prepared for Edman degradation sequencing that identified two indicated bands as C-SPARC and N-SPARC (arrows). (**E**) A schematic map of reported protein binding domains on FL-SPARC and sites of proteolytic cleave (arrows) giving rise to C-SPARC

and N-SPARC. Edman degradation sequence terminal are numbered in the SPARC sequence, most of which is abbreviated (–). Acidic, FS-like, and EC domains of SPARC are indicated. Abbreviations: ASC, adipose stromal cells; ECM, extracellular matrix; EP, epididymal; IP, immunoprecipitated; MS, mesenteric; SC, subcutaneous; SPARC, secreted protein acidic and rich in cysteine; WAT, white adipose tissue; WCE, whole cell extract; *WT, wild type*.

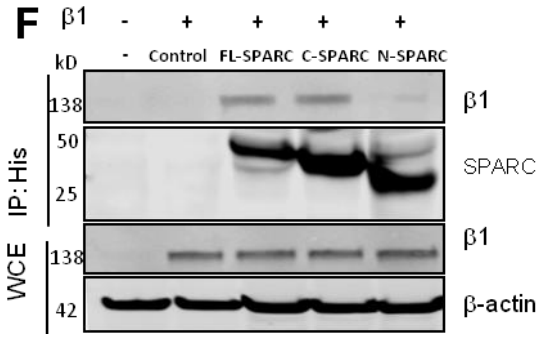

(**F**) Whole cell extracts from HEK293T of β1 integrin co-transfected with His6-tagged FL-SPARC, C-SPARC, N-SPARC, or control vector were immunoprecipitated with anti-His tag antibody, and immunoprecipitates were immunoblotted with β1 integrin and SPARC antibodies, which shows preferential FL-SPARC and C-SPARC integrin binding.

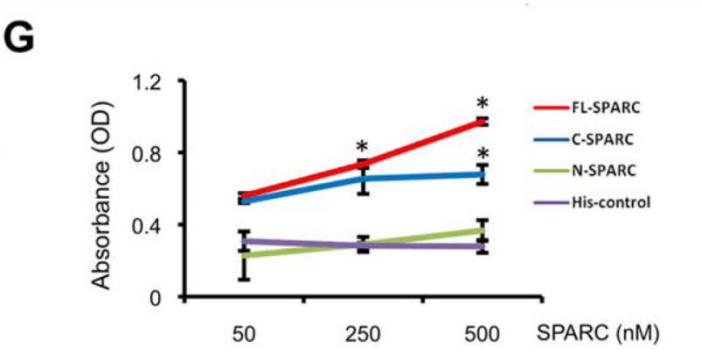

(**G**) Wells coated with FL-SPARC, C-SPARC, N-SPARC, or control protein were incubated with 1.25 mg/ml of biotinylated α5β1 integrin. Mean protein binding was measured with a secondary streptavidin-HRP conjugate and calorimetric spectroscopy (OD450), which shows preferential FL-SPARC and C-SPARC integrin binding. Representative data shown are from experiments repeated three (B–D, G) or two (F) times. Error bars, SEM from triplicate wells. *, $p<0.05$ versus His control. Scale bar 50 μm.

4-6. C-SPARC, but not N-SPARC, binds to ASC

Because SPARC binds to ASC as a ligand of β1 integrin, we predicted that N-SPARC lacking the integrin interaction domain might have reduced binding to ASC. To test this hypothesis, *SPARC*$^{-/-}$ ASC were incubated with FL-SPARC, C-SPARC, or N-SPARC in the medium, washed, and subjected to immunofluorescence analysis with polyclonal anti-SPARC antibodies that recognize all SPARC isoforms. Our data show that FL-SPARC and C-SPARC bind to ASC surface, while N-SPARC does not (Fig. 4-6A). To quantify binding differences, we immunoblotted protein extracts from ASC after SPARC isoform addition at several time points. This result indicated that the kinetics of FL-SPARC and C-SPARC to ASC is comparable, while N-SPARC completely lacks the capacity to bind ASC (Fig. 4-6B).

To further assess selectivity of FL-SPARC, C-SPARC, and N-SPARC for distinct cell types, we exposed partly enzymatically-digested fragments of WAT from *SPARC*$^{-/-}$ mice to the His-tagged SPARC fragments. Upon washing and fixation, whole mounts were subjected to immunofluorescence (Fig. 4-6C). Counterstaining with isolectin B4 (IB4), which specifically binds to the endothelium, demonstrated that all three recombinant proteins bound to stromal cells. FL-SPARC and C-SPARC binding was localized to ASC, identified as perivascular cells negative for IB4 and CD45 (data not shown) and positive for CD34, as well as to alternatively activated macrophages, identified as IB4- cells positive for F4/80 and stabilin-1 (Fig. 4-6C). In contrast, N-SPARC bound exclusively to IB4- / F4/80+ / stabilin-1+ macrophages but not to IB4- / CD34+ ASC (Fig. 4-6C). These results indicate that FL-SPARC and C-SPARC bind to both ASC and macrophages, while N-SPARC lacking the integrin-binding domain is only capable of binding to macrophages.

4-6 C-SPARC but not N-SPARC binds to ASC

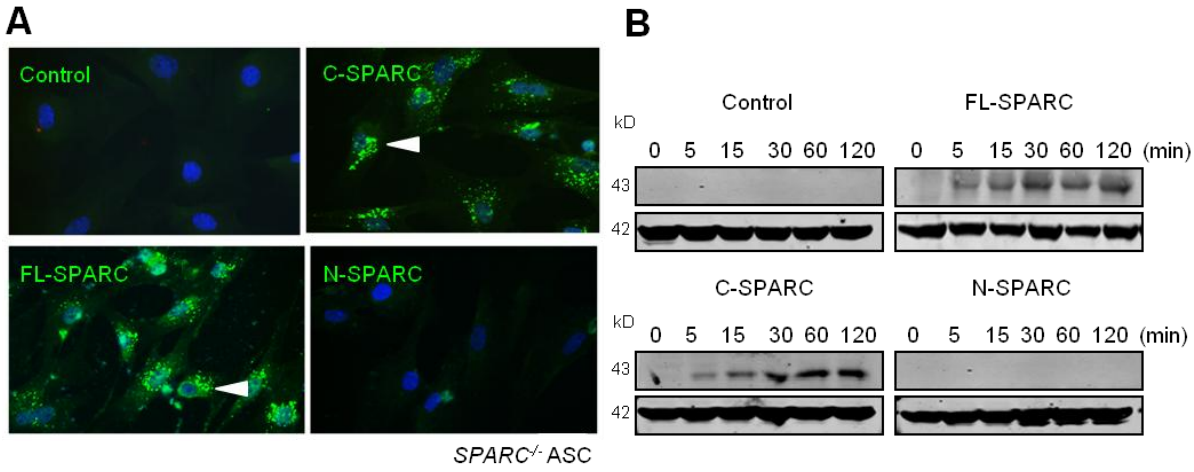

(A) Adherent *SPARC*$^{-/-}$ ASC were incubated with 100 nM of indicated recombinant His_6-tagged SPARC isoforms or control vector in serum-free medium for 10 min. Immunofluorescence with anti-SPARC antibody (green) reveals that FL-SPARC and C-SPARC, but not N-SPARC, bind to ASC. **(B):** Anti-SPARC immunoblotting of protein extracts from ASC treated as in (**A**) for indicated time intervals. Anti-β-actin immunoblotting demonstrates equal protein loading.

4-6 C-SPARC but not N-SPARC binds to ASC

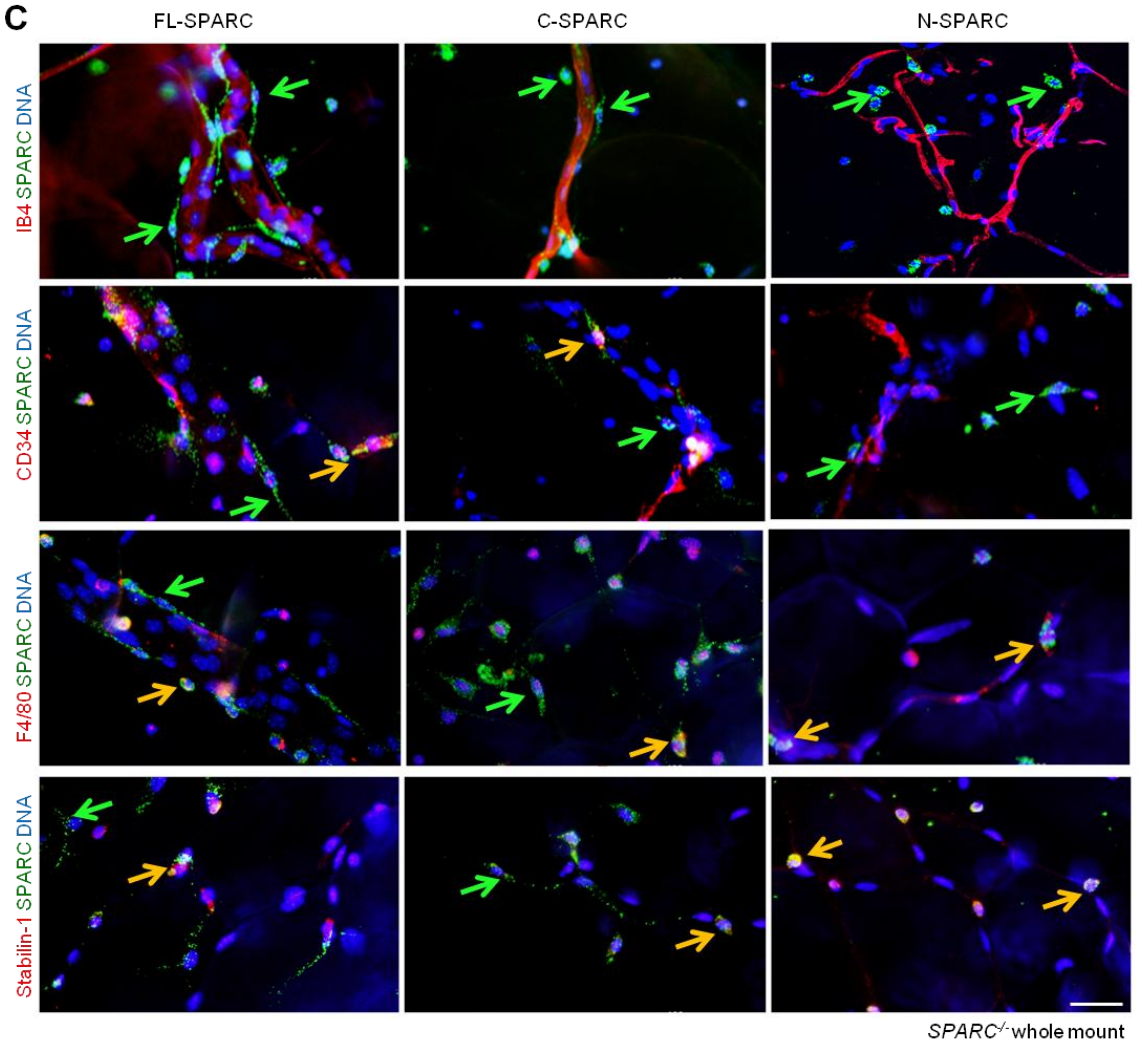

(C) Partly enzymatically digested fragments of MS WAT from *SPARC*$^{-/-}$ mice were treated with 100 nM of FL-SPARC, C-SPARC, or N-SPARC for 30 min, washed, and then fixed whole mounts were subjected to immunofluorescence with antibodies against the indicated antigens. Endothelium is stained with isolectin B4 (IB4). Green arrows point to SPARC isoform on antigen-negative cells; yellow co-localization signal reveals that C-SPARC binds to CD34+ ASC and to F4/80+ and stabilin-1+ macrophages, while N-SPARC binds only to F4/80+ / stabilin-1+ macrophages. Representative data shown are from experiments repeated three times. Nuclei are blue. Scale bar, 50 µm.

4-7 N-SPARC is a potent extracellular matrix (ECM) binder and integrin/ECM blocker

Because N-SPARC retains its ECM-binding domain, we investigated the effect of this isoform on integrin / ECM interaction. First, we compared the binding of biotinylated recombinant SPARC variants to fibronectin and collagen I. N-SPARC displayed a slightly higher binding to these ECM molecules than FL-SPARC at higher concentrations, while C-SPARC binding was decreased (Fig. 4-7A). Binding of FL-SPARC to collagen was competed by N-SPARC (data not shown), confirming the retention of ECM-binding site in this isoform. Because N-SPARC binds ECM but does not bind to β1 integrin, we predicted that it may have the capacity to block integrin / ECM interaction. To assess that, we compared the effects of the SPARC isoforms in a competitive ELISA assay. Biotinylated α5β1 integrin was pre-incubated with the recombinant SPARC proteins and its binding to fibronectin was quantified. Compared to FL-SPARC and C-SPARC, N-SPARC demonstrated a higher capacity to block α5β1 integrin binding to fibronectin (Fig. 4-7B). N-SPARC also blocked α1β1 integrin / collagen I binding more efficiently than FL-SPARC and C-SPARC (Fig. 4-7B). These results suggest that N-SPARC has an increased capacity to inhibit ASC adhesion to the ECM.

4-.7 N-SPARC is a potent extracellular matrix (ECM) binder and integrin interaction blocker

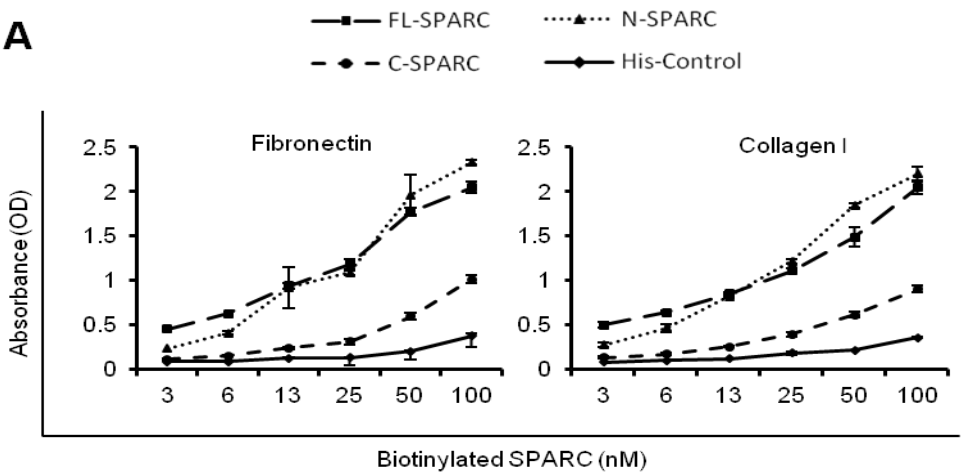

(A) ECM molecule-coated wells were incubated with biotinylated recombinant His_6-tagged FL-SPARC, C-SPARC, N-SPARC or control protein at indicated concentrations. Mean protein binding was measured with a secondary streptavidin-HRP conjugate and calorimetric spectroscopy (OD450).

4-7. N-SPARC is a potent extracellular matrix (ECM) binder and integrin interaction blocker

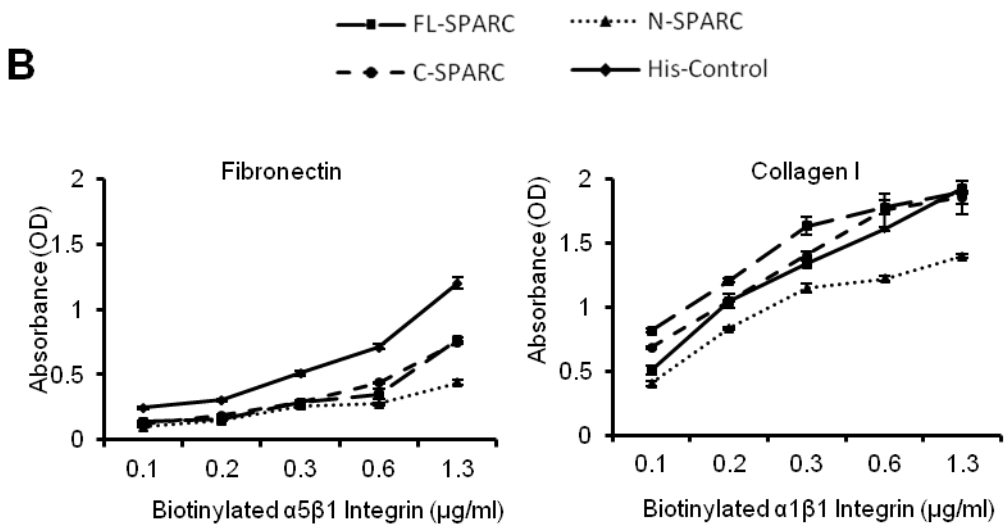

(B) Biotinylated α5β1 or α1β1 integrin were pre-incubated with 100 nM recombinant His_6-tagged FL-SPARC, C-SPARC, N-SPARC or control protein. Wells, which were ECM molecule-coated as in (**A**), were incubated with the pretreated biotinylated α5β1 or α1β1 integrin at indicated concentrations. Mean biotinylated protein binding was measured with secondary streptavidin-HRP conjugates and calorimetric spectroscopy (OD450). Representative data shown are from experiments repeated twice with triplicate wells. Error bars, SEM from triplicate wells.

4-8. Both C-SPARC and N-SPARC modulate β1 integrin signaling

The differences in ASC and ECM binding observed for N-SPARC and C-SPARC suggested that these isoforms might differ in their capacity to activate β1 integrin signaling. To test this hypothesis, we performed an experiment analogous to Figure 4-4C: 3T3-L1 cells expressing either a non-targeted shRNA (control cells) or shRNA silencing β1 integrin, ILK, or FAK were treated with N-SPARC and C-SPARC. Surprisingly, time course immunoblotting analysis demonstrated that treatment with both C-SPARC and N-SPARC still reduced Y397 FAK phosphorylation in a time-dependent manner in control cells (Fig. 4-8A, B). Treatment with both C-SPARC and N-SPARC also transiently increased Thr202/Tyr204 phosphorylation of ERK1/2 in control cells (Fig. 4-8A, B). As seen with FL-SPARC, FAK autophosphorylation and ERK1/2 phosphorylation were not affected in β1 integrin knockdown and ILK knockdown cells by either C-SPARC or N-SPARC treatment (Fig. 4-8A, B).

We also compared the effect of proteolytic SPARC isoforms on ILK activity. Serum-starved 3T3L1 cells expressing either non-targeted shRNA or β1 integrin, ILK or FAK silencing shRNA were incubated with FL-SPARC, C-SPARC or N-SPARC. After incubation, proteins were immunoprecipitated with ILK antibodies and then incubated with glycogen synthase kinase 3 (GSK-3β), a model ILK substrate (Yokoyama et al., 2011). By immunoblotting the kinase reactions with an anti-phospho-GSK-3β antibody, we found that GSK-3β phosphorylation by ILK was promoted upon cell treatment with FL-SPARC, C-SPARC, and N-SPARC in control cells (Fig. 4-8C). Residual ILK kinase activity was also detectable in treated cells transduced with ILK shRNA, which can be explained by the

observed ILK immunoprecipitation even despite its substantial silencing (Fig. 4-8C). Interestingly, ILK kinase activity was still induced by FL-SPARC, C-SPARC and N-SPARC upon β1 integrin or FAK silencing (Fig. 4-8C). These data from the 3T3-L1 model were reproduced with immortalized mouse ASC (Zhang et al., 2009). Our results suggest that SPARC-induced activation of ILK, as well as of Akt (Fig. 4-4C), is regulated by signaling independent of β1 integrin and FAK.

4-8. Both C-SPARC and N-SPARC modulate β1 integrin signaling

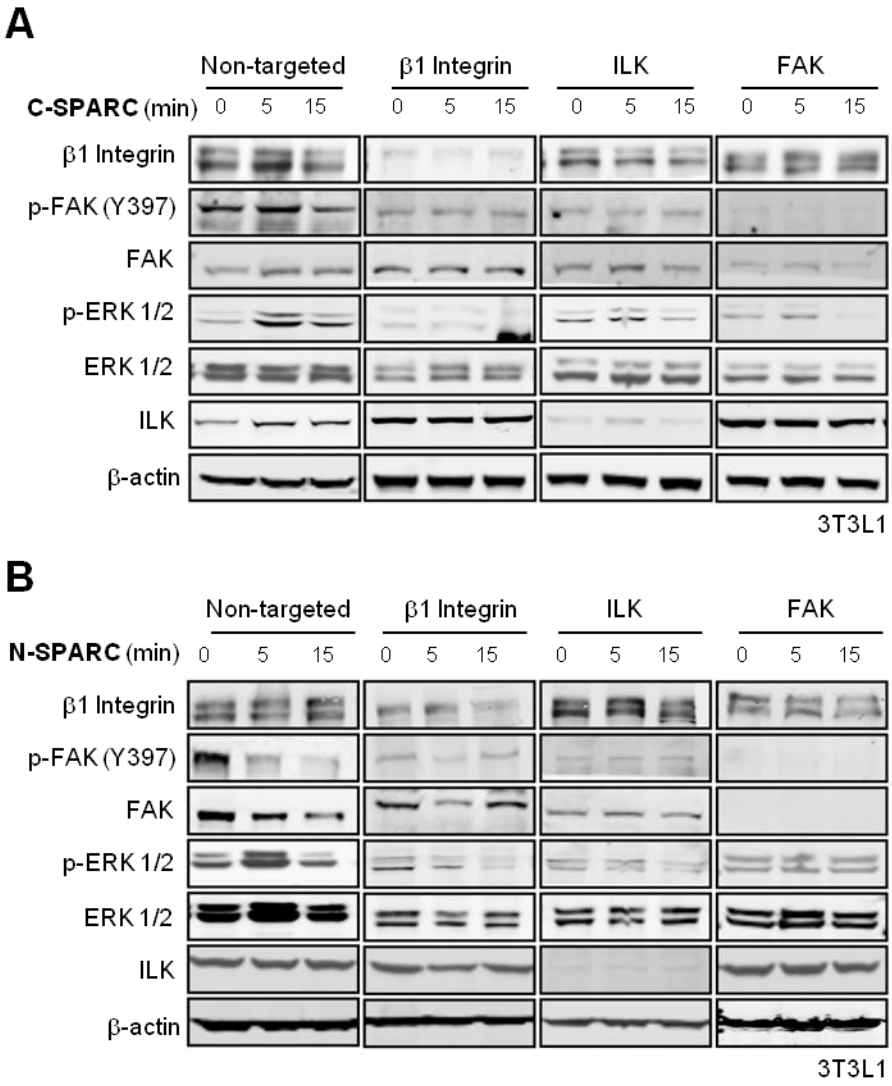

Both C-SPARC and N-SPARC modulate β1 integrin signaling. 3T3-L1 cells were transduced with non-targeted shRNA (control) or shRNA silencing β1 integrin, ILK or FAK. **(A, B):** Serum-starved cells were incubated with 500 nM His_6-tagged C-SPARC **(A)** or N-SPARC **(B)** and cell lysates obtained at 0, 5 and 15 min post-treatment were analyzed by Western blotting using antibodies against indicated antigens. Anti-β-actin immunoblotting demonstrates equal protein loading for different time points.

4-8 Both C-SPARC and N-SPARC modulate β1 integrin signaling

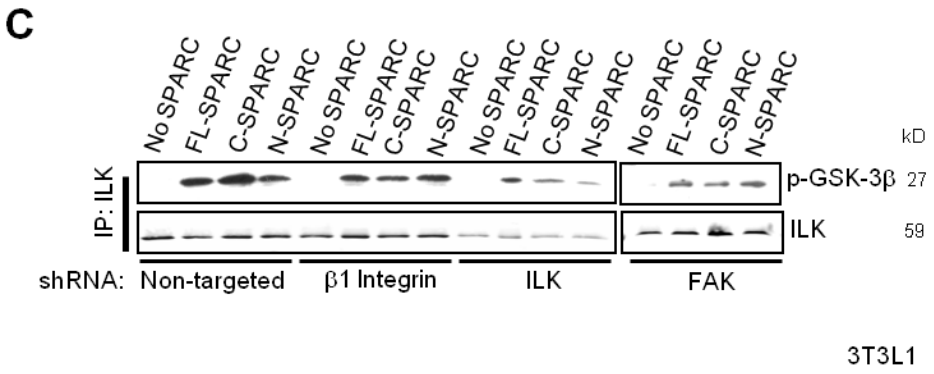

(**C**) Serum-starved cells were untreated (No SPARC) or incubated with 500 nM His_6-tagged FL-SPARC, C-SPARC or N-SPARC for 10 min. Then cells were subjected to the ILK kinase assay using GSK-3β as a substrate. Anti-p-GSK-3β immunoblotting signal reflects the amount of active ILK immunoprecipitated. Anti-ILK immunoblotting demonstrates reduced, yet measurable, ILK immunoprecipitation from cells transduced with ILK shRNA. Representative data shown are from experiments repeated three times.

4-9. Both C-SPARC and N-SPARC Induce ASC De-adhesion and cooperate in triggering ASC migration

Because N-SPARC and C-SPARC have different binding target preferences but have similar effect on cell signaling, we sought to compare their effects on cell attachment to the ECM. To assess their effect on adherence, ASC in suspension were treated with recombinant SPARC proteins and their ability to attach to fibronectin-coated plates was evaluated. After 15 minutes, the majority of untreated ASC displayed spreading morphology, whereas FL-SPARC, C-SPARC, and N-SPARC prevented fibronectin-induced ASC attachment (Fig. 4-9A). We verified this result upon longer (1 hour) cell observation (Fig. 4-9B). Compared to untreated control, treatment with FL-SPARC, C-SPARC, and N-SPARC led to a comparable increase in the frequency of ASC with loosely adherent morphology (Fig. 4-9B graph). We also compared the effect of recombinant SPARC proteins on attached ASC grown on fibronectin-coated plates. Consistent with the attachment data, the rounded cell phenotype indicating de-adhesion was induced not only by FL-SPARC and C-SPARC, but also by N-SPARC treatment (Fig. 4-9C).

Finally, we compared the effects of recombinant SPARC isoforms on motility of suspended serum-deprived ASC in a transwell assay. ASC trans-well migration was induced not only by FL-SPARC but also by individual cleavage isoforms (Fig. 4-9D). Because our data show that C-SPARC and N-SPARC are both generated in MS WAT and induce ASC de-adhesion through distinct mechanisms, we hypothesized that they might have additive effects. To test this hypothesis, we treated ASC from *SPARC*$^{-/-}$ mice with combinations of recombinant SPARC isoforms at equimolar concentrations and quantified the capacity of cells to migrate in the trans-well assay. The effect of FL-SPARC and C-

SPARC treatment alone on cell migration was comparable and more robust than that of N-SPARC. Adding C-SPARC along with FL-SPARC did not further increase cell migration, consistent with them acting through the same mechanism. Interestingly, combination of N-SPARC and FL-SPARC had a reduced capacity in activating cell migration compared to FL-SPARC alone. Importantly, while N-SPARC alone had a relatively modest effect on cell motility, when it was added in combination with C-SPARC cell migration was increased by 2-fold, compared to N-SPARC alone (Fig. 4-9D). The combination of C-SPARC and N-SPARC was the only setting where cell migration induction was significantly higher than by FL-SPARC alone. Combined, our data indicate that N-SPARC and C-SPARC cooperate in detaching ASC from the ECM, which leads to their motility.

4-9. Both C-SPARC and N-SPARC induce ASC deadhesion and cooperate in triggering ASC migration

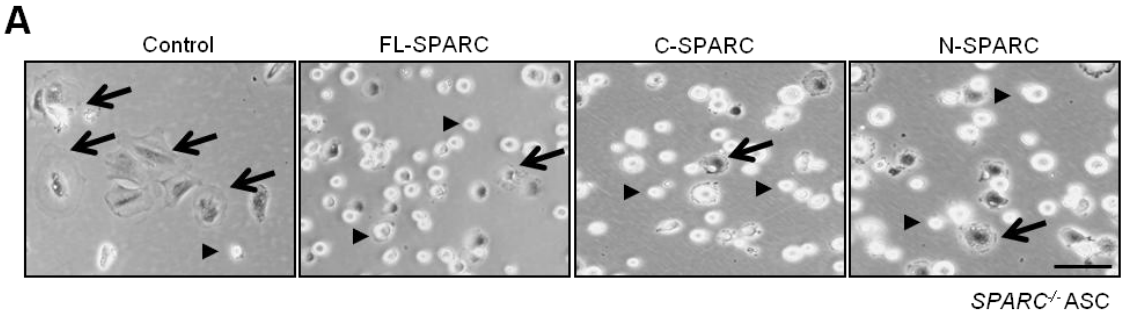

(**A**) Phase contrast images of *SPARC*$^{-/-}$ ASC 15 min after plating on fibronectin-coated plates in serum-free medium containing control (eluate from control vector), His_6-tagged FL-SPARC, C-SPARC, or N-SPARC (500 nM).

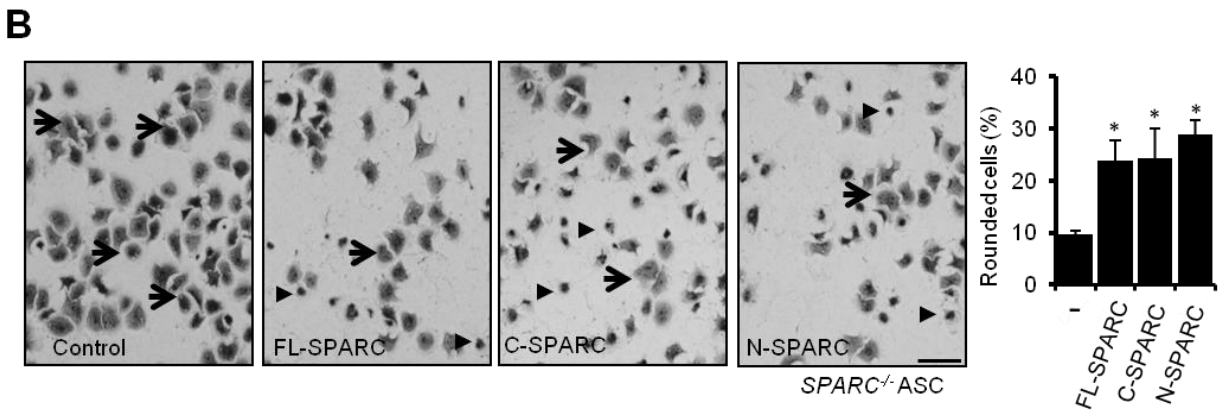

(**B**) Crystal violet staining of *SPARC*$^{-/-}$ ASC 1 hr after plating on fibronectin-coated plates in serum-free medium containing control, His_6-tagged FL-SPARC, C-SPARC, or N-SPARC (500 nM).

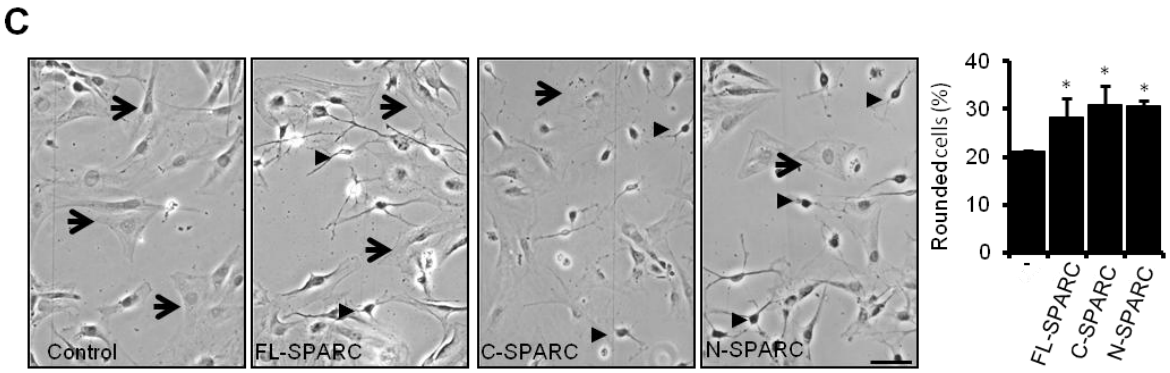

*(***C***) SPARC*$^{-/-}$ ASC pre-grown on fibronectin-coated plated were incubated with control, His_6-tagged FL-SPARC, C-SPARC, or N-SPARC (500 nM) for 1hr. Arrows: well adherent cells, arrowheads: weekly adherent rounded cells. Graph shows the mean percentage of rounded cells.

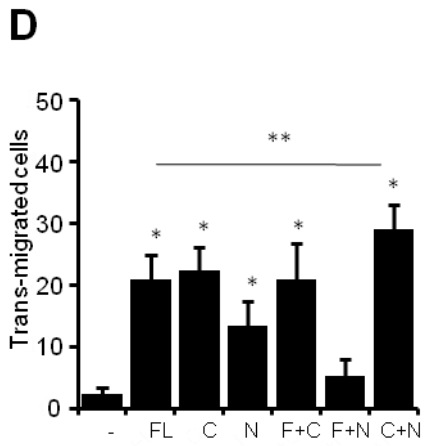

(**D**) *SPARC*$^{-/-}$ ASC incubated with His_6-tagged FL-SPARC, C-SPARC, or N-SPARC (500 nM) or their indicated equimolar admixes (combined concentration 500 nM) were subjected to the trans-well assay. The graph shows the mean numbers of trans-migrated cells/view field. Error bars, SEM from triplicate wells. $P<0.05$ (* compared to untreated; ** compared to FL-SPARC).

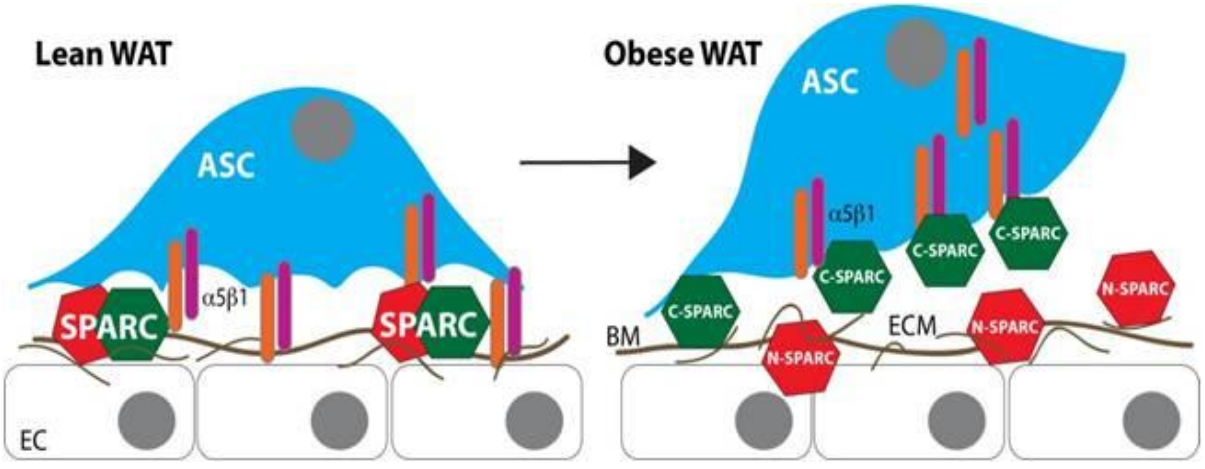

A proposed model for the function of C-SPARC and N-SPARC in WAT. In lean mice, adipocytes (not shown) express a basal level of FL-SPARC (RED: N-terminal domain; GREEN: C-terminal domain). FL-SPARC binding to α5β1 integrin on ASC, as well as to

the ECM and the basement membrane (BM) separating ASC and endothelial cells (EC), maintains the dynamic equilibrium of ASC intermediate adhesion. In MS WAT of obese mice, adipocytes express increased levels of FL-SPARC that undergoes proteolytic processing resulting in N-SPARC and C-SPARC. N-SPARC blocks α5β1 integrin binding to the ECM and the BM, while C-SPARC directly modulates β1 integrin signaling favoring cell motility and survival. The additive effects of N-SPARC and C-SPARC induce ASC de-adhesion and mobilization. Grey circles: nuclei. Representative data shown are from experiments repeated at least twice with similar result.

Chapter 5

Discussion & Conclusion

5-1. Significance

Adipose stromal cells (ASC) are mesenchymal adipocyte progenitors abundant in fat tissue. The increasing application of ASC in regenerative medicines has been reported in multiple randomized clinical trials worldwide (Kolle et al., 2013; Lendeckel et al., 2004), examining their efficacy across different areas including cardiovascular diseases, autoimmune diseases, and plastic/reconstructive surgery. With ASCs' vast potential for clinical use, it is crucial to better understand their safety and mechanism involved in regulating their mobilization.

Here, along with accumulating preclinical data (Park et al., 2011; Rowan et al., 2015; Strong et al., 2015), we show that the ASC pool expands with obesity and contributes to tumor growth by supporting tumor vasculature. We further evaluate the mechanism involved in regulating ASC mobility. Extending our previous finding that the matricellular protein SPARC binding to β1 integrin on ASC promoted its migration, we demonstrate the physiological significance of SPARC in mobilizing ASC into the peripheral circulation. We further identify novel proteolytic SPARC isoforms and demonstrate their involvement in ASC migration. My thesis study contributes to unraveling the molecular mechanisms involved in stem cell trafficking.

DISCUSSION

It has been long believed that the systemic circulating adipokines are the main pathophysiological connection between obesity and cancer (Calle and Kaaks, 2004). Recently, the tumor-stimulating effect of cells recruited by tumors has been recognized. Tumor growth/survival-promoting effects based on direct cellular contact and locally secreted paracrine factors have been identified (Nieman et al., 2011; Zhang et al., 2009). In our study, we tested the hypothesis of expanded adiposity in obesity, serving as a cell source for tumor recruitment to support the tumor microenvironment. Here, we provide evidence of ASC pool expansion in obesity and show an increased ASC in circulation. Consistent with our model, a similar phenomenon is reported in patients with cancer (Bellows et al., 2011; Mancuso et al., 2011). Concomitantly, higher frequency of ASC recruitment in tumor engrafted in obese mice associates with increased pericytes coverage and tumor growth. These findings are in accordance with pro-angiogenic effects of trophic factors secreted by ASC (Gimble et al., 2007; Rehman et al., 2004). In sum, our data on expanded ASC pool contributing to increased ASC recruitment to tumor caution against the use of cell therapy in patients with cancer (Bertolini et al., 2012). Importantly, ASC mobilization in cancer may be the functional determinant of their capacity to promote cancer. This has prompted us to understand the mechanisms involved.

Chemotatic stimuli direct cell migration by inducing cell contraction and changes in integrin clustering and attachment to the ECM. Integrin β1 is selectively overexpressed on ASC is likely to control their migration. Previously, we reported that binding of matricellular protein SPARC to integrin β1 on ASC induces migration. However, it remains largely unknown what role SPARC plays in integrin signal transduction and to

what extent its capacity to elicit cell detachment from ECM is due to modulating α5β1 signaling contributes to ASC mobilization (Legate et al., 2009). In our study, we demonstrate that SPARC treatment induces focal adhesion disassembly in ASC, hallmarked by decreased paxillin phosphorylation and rapid dephosphorylation of FAK at Tyr^{397} which accompanied by integrin endocytosis (Nagano et al., 2012). Integrin β1–ECM binding leads to integrin activation characterized by FAK autophosphorylation at Tyr^{397}, therefore, reduced FAK autophosphorylation at Tyr^{397} integrin is consistent with integrin disengagement from ECM. Previously, SPARC signaling involving β1 integrin, FAK, ILK, ERK and Akt had been evaluated in cancer cells (Shi et al., 2007; Shin et al., 2013). From gene knockout experiments, we demonstrated that SPARC-mediated dephosphorylation of FAK signaling is β1 integrin-dependent and is required for increased ERK1/2 phosphorylation on Thr^{202}/Tyr^{204}. This signaling cascade has been formerly demonstrated as key in detachment and migration of epithelial cells (Lu et al., 2001; Teranishi et al., 2009). Our data suggest that in stromal cells, this signaling pathway is also triggered by SPARC. In addition, we show that SPARC induces ILK/Akt activation independent of the β1 integrin activity; we propose that it is non-specifically turned on in response to cell detachment. In sum, our data show that SPARC disruption of integrin-engagement to ECM and regulation of growth factor signaling.

Building on the earlier evidence of SPARC promoting ASC migration (Nie et al., 2008), we show that SPARC activity is required for ASC mobilization. SPARC-deficient mice exhibit impairment in ASC mobilization (Fig. 4-3A) and tumor engrafted onto SPARC-deficient mice present with increased permeability, reduced pericytes and lower microvessel density (Arnold et al., 2010; Brekken et al., 2003), consistent with ASC's role

in protecting vessel patency.

Matricellular protein SPARC is a substrate for numerous extracellular proteases. Cleavage of SPARC produces bioactive fragments with distinct functions that are context-dependent. For instance, SPARC proteolytic derivatives from exogenous MMP3 cleavage modulate cell proliferation, migration and angiogenesis (Sage et al., 2003) while cleavage of SPARC in chicken chorioallantoic membrane is associated with pro-angiogenic properties (Iruela-Arispe et al., 1995). SPARC cleaved by Cathepsin K promotes bone metastasis (Podgorski et al., 2009) and limited proteolysis in the SPARC EC domain increases collagens binding (Sasaki et al., 1997; Sasaki et al., 1998; Sasaki et al., 1999). Interestingly, most of the proteolytic SPARC functions are associated with tissue remodeling. In mesenteric adipose tissue of obese mice, we discovered two novel proteolytic SPARC isoforms. Truncation of SPARC within the extracellular calcium-binding domain III in helix αC (PVE–LLA) (Sasaki et al., 1999), generates N-SPARC fragment (Fig 4-5E). This truncation leads to loss of putative β1 integrin binding site but retains some collagen-binding residues (R149, N156). Consistent with previous reports of proteolytic cleavage revealing masked epitopes for collagen on SPARC (Sasaki et al., 1997; Sasaki et al., 1999), N-SPARC displays increased collagen binding affinity and ability to block integrin interacting with collagen I and fibronectin, but fails to bind ASC. Proteolytic cleavage of C-SPARC occurs within domain I of SPARC (IVE-EET) and does not affect its binding to ASC, however, results in decreased interaction of C-SPARC to collagens and fibronectin. As no known ECM-interacting sites have been reported in the N-terminus of SPARC, this unanticipated reduction with ECM proteins is likely due to structural changes of SPARC induced by proteolytic cleavage.

Our data demonstrate that FL-SPARC and both proteolytic isoforms induce cell de-adhesion by acting through distinct mechanisms. Interestingly, despite the loss of its capacity to bind ASC through β1 integrin, N-SPARC elicits alterations in integrin-mediated signaling pathway comparable to those induced by FL-SPARC and C-SPARC. These data suggest that integrin-FAK-MAPK signaling is modulated by integrin-disengagement in cell de-adhesion rather than only by SPARC acting as a ligand. Similarly, ILK-Akt signaling well known for a role in regulating cell survival is also activated by all SPARC isoforms. This could be a compensatory mechanism trigger by cell de-adhesion to avoid anoikis in mobilized cells.

Our study shows that N-SPARC and C-SPARC are generated in the MS WAT of obese mice and display an additive effect in promoting ASC migration. Building upon our experimental results and the previously recognized function of SPARC in tissue remodeling, we propose a model converging functions of SPARC isoforms in tissue expansion. In WAT of lean mice, basal level of SPARC is expressed by adipocyte, allowing firm binding of ASC to the perivascular matrix and basement membrane via integrin α5β1, therefore, retaining ASC in their niche. In obesity, adipose tissue undergoes expansion. The increased of SPARC expression and its targeting protease in MS WAT leads to C-SPARC and N-SPARC accumulation. FL-SPARC, N-SPARC and C-SPARC promote ASC detachment, by exerting coordinated effect to disrupt α5β1 integrin engagement with the ECM. FL-SPARC and C-SPARC bind directly to integrin α5β1, while N-SPARC interacts with ECM to block integrin/ ECM interaction. Detached ASC migrate and integrate into expanding neovasculature, facilitating WAT expansion. We

propose that a similar mechanism is accountable for ASC mobilization and underlies the pathophysiological connection between obesity and cancer.

CONCLUSION

Our study demonstrates that the increased adiposity expands ASC pool which results in higher frequency of ASC in circulation and tumors. The pro-angiogenic functions of ASC in stimulating tumor vascularization and growth upon ASC recruitment to tumors explain the function of WAT in obesity and cancer pathophysiology.

Next, we identified SPARC and its obesity -induced proteolytic derivatives as modulators of ASC mobilization and migration. The fundamental mechanism of ASC mobilization is believed to be essential in modulating obesity and applies to activation of ASC in tumor progression. Protease(s) responsible for SPARC proteolytic derivatives in MS WAT remain to be identified. Our work highlights the importance of proteolytic processing in regulation of cellular functions.

Chapter 6

Future Direction

In this thesis study, we demonstrate that SPARC is required for ASC mobilization. And for the first time, obesity-induced proteolytic derivatives of SPARC are identified in the mesenteric WAT. SPARC proteolytic derivative C-SPARC has cleavage occurring within domain I, while N-SPARC is proteolytically cleaved at the (PVE–LLA) extracellular calcium-binding domain III in helix αC. Our result shows that C-SPARC binds to β1 integrin on ASC, while N-SPARC shows a preferential binding to the ECM and blocks ECM / integrin interaction. Interestingly, both C-SPARC and N-SPARC induce ASC de-adhesion from the ECM and cooperate in promoting cell migration. Although we have shown that SPARC and its proteolytic derivatives regulate ASC mobilization, the proteases cleaving it remains to be identified.

In attempt to identify putative proteases for generating N-SPARC and C-SPARC in MS WAT, we evaluated the potential protease cleavage site(s) close to the cleavage region of N-SPARC and C-SPARC. We identify MMP8 and MMP13 recognition sites to correspond to N-SPARC cleavage region. Consistently, previous studies reported comparable molecular weight proteolytic fragments generated by MMP13 proteolysis *in vitro (Sasaki et al., 1997; Sasaki et al., 1998; Sasaki et al., 1999)*. Lastly, upregulation of MMP8, MMP13 (Chavey et al., 2003) (Belo et al., 2009; Maquoi et al., 2002) and cathepsins B, D, K and S (Nadler et al., 2000) are reported in obesity. Therefore, we hypothesize that MMP8 and MMP13 to be potential protease cleaving SPARC in MS WAT. Additional studies are required to validate our prediction.

The multifactorial functions of SPARC are controversial and have shown to be highly contextual. SPARC functions as a tumor suppressor or pro-tumorgenic factor depending on the stage and cancer types. Our result showing that SPARC proteolytic isoforms

accumulate in mesenteric WAT is particularly intriguing as visceral adiposity is associated with numerous pathologies including cancer. Therefore, it would be interesting to evaluate SPARC and its proteolytic derivative roles in modulating cancer progression.

Our pilot study of EO771 breast adenocarcinoma grafted into SPARC-deficient mice shows reduced tumor growth (Fig. 6-1A,B) in particular obesity. Haematoxylin eosin staining of tumor grafts reveals increased viable region in obese *WT* tumor compared to *SPARC*$^{-/-}$ and lean *WT* counterparts (Fig. 6-1C). These data are consistent with our previous result showing obesity-associated ASC recruitment support tumor cell survival and growth. Importantly, tumor grafted onto obese *SPARC*$^{-/-}$ mice fails to confer growth and survival advantage, consistent with predicted reduced ASC recruitment in the absence of SPARC. Immunofluorescence analysis of tumor sections revealed a decrease in ASC-associated progenitor and endothelium markers in *SPARC*$^{-/-}$ tumors compared to *WT* (Fig. 6-2). This tumor study reinforces the role of SPARC in modulating ASC mobilization and tumor trafficking. In the future, we aim to delineate the functional role of SPARC isoforms in ASC trafficking in the context of tumor progression.

Figure 6-1. Absence of host SPARC is associated with tumor growth deficiency

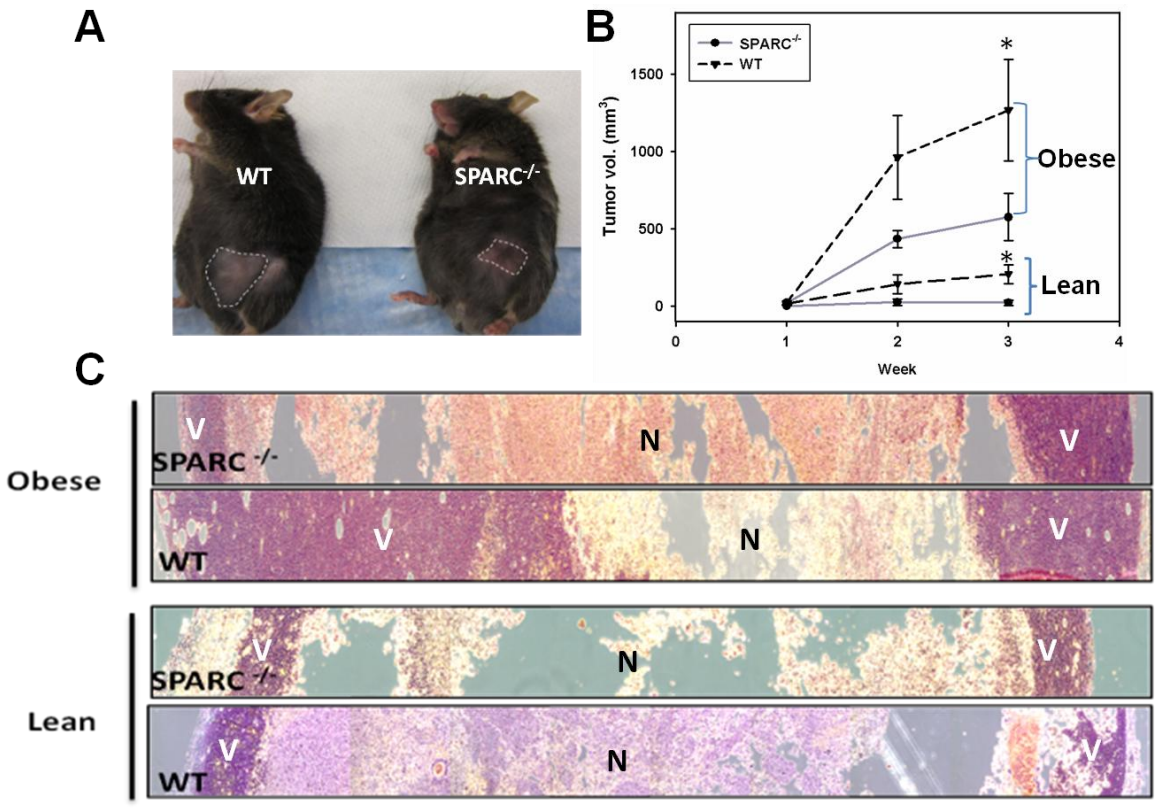

(**A**) Representative breast adenocarcinoma E0771 grafts grown in lean wild type or *SPARC*$^{-/-}$ mice (n=5/group). (**B**) Graph shows volume of tumor grafts from lean and obese wild type or *SPARC*$^{-/-}$ mice. (**C**) Haematoxylin eosin staining of tumor grafts from (B) shows increased viable region in tumor grafted onto obese wild type mice. N: necrotic, V: viable. Error bars, SEM from 5 mice. $P<0.05$

Figure 6-2. Decreased vasculature in tumor grown in SPARC$^{-/-}$ mice.

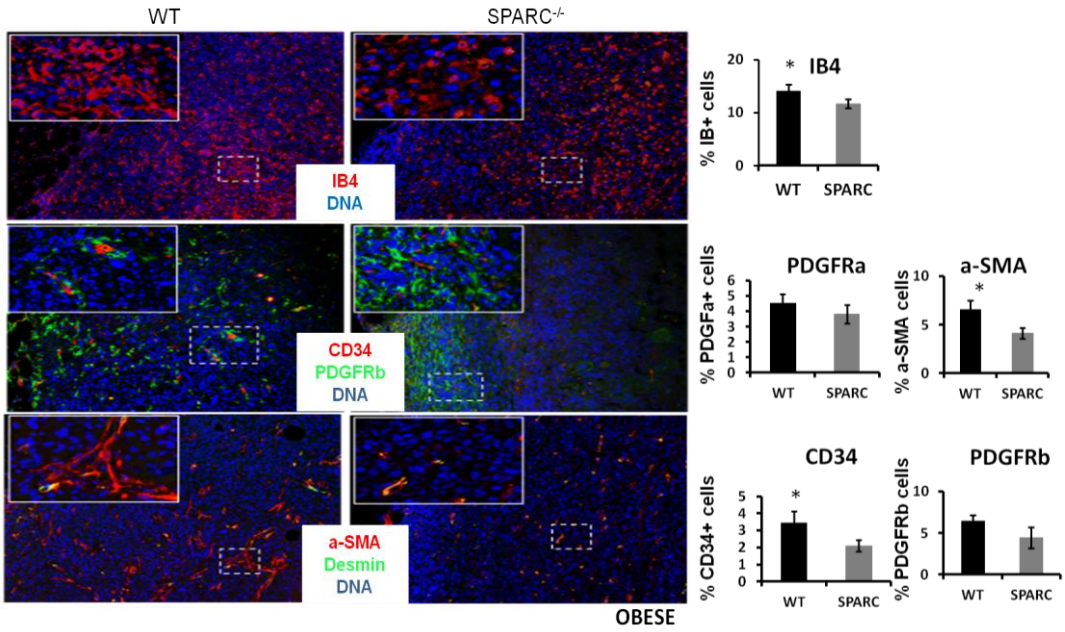

Immunofluorescence analysis of EO771 tumor sections comparing ASC-associated endothelium (IB+) and progenitor markers (CD34+, α-SMA, PDGFRα, PDGFRβ) expression in tumor viable regions.

BIBLIOGRAPHY

Abbott, J.D., Huang, Y., Liu, D., Hickey, R., Krause, D.S., and Giordano, F.J. (2004). Stromal cell-derived factor-1alpha plays a critical role in stem cell recruitment to the heart after myocardial infarction but is not sufficient to induce homing in the absence of injury. Circulation *110*, 3300-3305.

Alachkar, H., Santhanam, R., Maharry, K., Metzeler, K.H., Huang, X., Kohlschmidt, J., Mendler, J.H., Benito, J.M., Hickey, C., Neviani, P., *et al.* (2014). SPARC promotes leukemic cell growth and predicts acute myeloid leukemia outcome. J Clin Invest *124*, 1512-1524.

Alexander, N.R., Branch, K.M., Parekh, A., Clark, E.S., Iwueke, I.C., Guelcher, S.A., and Weaver, A.M. (2008). Extracellular matrix rigidity promotes invadopodia activity. Curr Biol *18*, 1295-1299.

Allott, E.H., and Hursting, S.D. (2015). Obesity and cancer: mechanistic insights from transdisciplinary studies. Endocr Relat Cancer *22*, R365-386.

Arnold, S.A., Rivera, L.B., Miller, A.F., Carbon, J.G., Dineen, S.P., Xie, Y., Castrillon, D.H., Sage, E.H., Puolakkainen, P., Bradshaw, A.D., *et al.* (2010). Lack of host SPARC enhances vascular function and tumor spread in an orthotopic murine model of pancreatic carcinoma. Dis Model Mech *3*, 57-72.

Bagno, L.L., Werneck-de-Castro, J.P., Oliveira, P.F., Cunha-Abreu, M.S., Rocha, N.N., Kasai-Brunswick, T.H., Lago, V.M., Goldenberg, R.C., and Campos-de-Carvalho, A.C. (2012). Adipose-derived stromal cell therapy improves cardiac function after coronary occlusion in rats. Cell Transplant *21*, 1985-1996.

Barsh, G.S., Farooqi, I.S., and O'Rahilly, S. (2000). Genetics of body-weight regulation. Nature *404*, 644-651.

Basen-Engquist, K., and Chang, M. (2011). Obesity and cancer risk: recent review and evidence. Curr Oncol Rep *13*, 71-76.

Bellows, C.F., Zhang, Y., Chen, J., Frazier, M.L., and Kolonin, M.G. (2011). Circulation of progenitor cells in obese and lean colorectal cancer patients. Cancer Epidemiol Biomarkers Prev *20*, 2461-2468.

Belo, V.A., Souza-Costa, D.C., Lana, C.M., Caputo, F.L., Marcaccini, A.M., Gerlach, R.F., Bastos, M.G., and Tanus-Santos, J.E. (2009). Assessment of matrix metalloproteinase (MMP)-2, MMP-8, MMP-9, and their inhibitors, the tissue inhibitors of metalloproteinase (TIMP)-1 and TIMP-2 in obese children and adolescents. Clin Biochem *42*, 984-990.

Bertolini, F., Lohsiriwat, V., Petit, J.Y., and Kolonin, M.G. (2012). Adipose tissue cells, lipotransfer and cancer: a challenge for scientists, oncologists and surgeons. Biochim Biophys Acta *1826*, 209-214.

Bertolini, F., Petit, J.Y., and Kolonin, M.G. (2015). Stem cells from adipose tissue and breast cancer: hype, risks and hope. Br J Cancer *112*, 419-423.

Bjorndal, B., Burri, L., Staalesen, V., Skorve, J., and Berge, R.K. (2011). Different adipose depots: their role in the development of metabolic syndrome and mitochondrial response to hypolipidemic agents. J Obes *2011*, 490650.

Bolander, M.E., Young, M.F., Fisher, L.W., Yamada, Y., and Termine, J.D. (1988). Osteonectin cDNA sequence reveals potential binding regions for calcium and hydroxyapatite and shows homologies with both a basement membrane protein (SPARC) and a serine proteinase inhibitor (ovomucoid). Proc Natl Acad Sci U S A *85*, 2919-2923.

Bourin, P., Bunnell, B.A., Casteilla, L., Dominici, M., Katz, A.J., March, K.L., Redl, H., Rubin, J.P., Yoshimura, K., and Gimble, J.M. (2013). Stromal cells from the adipose tissue-derived stromal vascular fraction and culture expanded adipose tissue-derived stromal/stem cells: a joint statement of the International Federation for Adipose Therapeutics and Science (IFATS) and the International Society for Cellular Therapy (ISCT). Cytotherapy *15*, 641-648.

Bradshaw, A.D., Francki, A., Motamed, K., Howe, C., and Sage, E.H. (1999). Primary mesenchymal cells isolated from SPARC-null mice exhibit altered morphology and rates of proliferation. Mol Biol Cell *10*, 1569-1579.

Bradshaw, A.D., Graves, D.C., Motamed, K., and Sage, E.H. (2003a). SPARC-null mice exhibit increased adiposity without significant differences in overall body weight. Proc Natl Acad Sci U S A *100*, 6045-6050.

Bradshaw, A.D., Puolakkainen, P., Dasgupta, J., Davidson, J.M., Wight, T.N., and Helene Sage, E. (2003b). SPARC-null mice display abnormalities in the dermis characterized by decreased collagen fibril diameter and reduced tensile strength. J Invest Dermatol *120*, 949-955.

Bradshaw, A.D., and Sage, E.H. (2001). SPARC, a matricellular protein that functions in cellular differentiation and tissue response to injury. J Clin Invest *107*, 1049-1054.

Brekken, R.A., Puolakkainen, P., Graves, D.C., Workman, G., Lubkin, S.R., and Sage, E.H. (2003). Enhanced growth of tumors in SPARC null mice is associated with changes in the ECM. J Clin Invest *111*, 487-495.

Brekken, R.A., and Sage, E.H. (2001). SPARC, a matricellular protein: at the crossroads of cell-matrix communication. Matrix Biol *19*, 816-827.

Cai, L., Johnstone, B.H., Cook, T.G., Tan, J., Fishbein, M.C., Chen, P.S., and March, K.L. (2009). IFATS collection: Human adipose tissue-derived stem cells induce angiogenesis and nerve sprouting following myocardial infarction, in conjunction with potent preservation of cardiac function. Stem Cells *27*, 230-237.

Calle, E.E., and Kaaks, R. (2004). Overweight, obesity and cancer: epidemiological evidence and proposed mechanisms. Nat Rev Cancer *4*, 579-591.

Calle, E.E., Rodriguez, C., Walker-Thurmond, K., and Thun, M.J. (2003). Overweight, obesity, and mortality from cancer in a prospectively studied cohort of U.S. adults. N Engl J Med *348*, 1625-1638.

Cao, Y. (2010). Adipose tissue angiogenesis as a therapeutic target for obesity and metabolic diseases. Nat Rev Drug Discov *9*, 107-115.

Caswell, P.T., and Norman, J.C. (2006). Integrin trafficking and the control of cell migration. Traffic *7*, 14-21.

Chandler, E.M., Seo, B.R., Califano, J.P., Andresen Eguiluz, R.C., Lee, J.S., Yoon, C.J., Tims, D.T., Wang, J.X., Cheng, L., Mohanan, S., *et al.* (2012). Implanted adipose progenitor cells as physicochemical regulators of breast cancer. Proc Natl Acad Sci U S A *109*, 9786-9791.

Chantrain, C.F., Feron, O., Marbaix, E., and DeClerck, Y.A. (2008). Bone marrow microenvironment and tumor progression. Cancer Microenviron *1*, 23-35.

Chavey, C., Boucher, J., Monthouel-Kartmann, M.N., Sage, E.H., Castan-Laurell, I., Valet, P., Tartare-Deckert, S., and Van Obberghen, E. (2006). Regulation of secreted protein acidic and rich in cysteine during adipose conversion and adipose tissue hyperplasia. Obesity (Silver Spring) *14*, 1890-1897.

Chavey, C., Mari, B., Monthouel, M.N., Bonnafous, S., Anglard, P., Van Obberghen, E., and Tartare-Deckert, S. (2003). Matrix metalloproteinases are differentially expressed in adipose tissue during obesity and modulate adipocyte differentiation. J Biol Chem *278*, 11888-11896.

Chlenski, A., and Cohn, S.L. (2010). Modulation of matrix remodeling by SPARC in neoplastic progression. Semin Cell Dev Biol *21*, 55-65.

Chlenski, A., Liu, S., Baker, L.J., Yang, Q., Tian, Y., Salwen, H.R., and Cohn, S.L. (2004). Neuroblastoma angiogenesis is inhibited with a folded synthetic molecule corresponding to the epidermal growth factor-like module of the follistatin domain of SPARC. Cancer Res *64*, 7420-7425.

Cinti, S. (2005). The adipose organ. Prostaglandins Leukot Essent Fatty Acids *73*, 9-15.

Cinti, S. (2011). Between brown and white: novel aspects of adipocyte differentiation. Ann Med *43*, 104-115.

Cinti, S. (2012). The adipose organ at a glance. Dis Model Mech *5*, 588-594.

Cooke, V.G., LeBleu, V.S., Keskin, D., Khan, Z., O'Connell, J.T., Teng, Y., Duncan, M.B., Xie, L., Maeda, G., Vong, S., *et al.* (2012). Pericyte depletion results in hypoxia-associated epithelial-to-mesenchymal transition and metastasis mediated by met signaling pathway. Cancer Cell *21*, 66-81.

Daley, W.P., Peters, S.B., and Larsen, M. (2008). Extracellular matrix dynamics in development and regenerative medicine. J Cell Sci *121*, 255-264.

Daquinag, A.C., Tseng, C., Salameh, A., Zhang, Y., Amaya-Manzanares, F., Dadbin, A., Florez, F., Xu, Y., Tong, Q., and Kolonin, M.G. (2015). Depletion of white adipocyte

progenitors induces beige adipocyte differentiation and suppresses obesity development. Cell Death Differ *22*, 351-363.

Daquinag, A.C., Zhang, Y., Amaya-Manzanares, F., Simmons, P.J., and Kolonin, M.G. (2011). An isoform of decorin is a resistin receptor on the surface of adipose progenitor cells. Cell Stem Cell *9*, 74-86.

de Luca, C., and Olefsky, J.M. (2008). Inflammation and insulin resistance. FEBS Lett *582*, 97-105.

Delany, A.M., Amling, M., Priemel, M., Howe, C., Baron, R., and Canalis, E. (2000). Osteopenia and decreased bone formation in osteonectin-deficient mice. J Clin Invest *105*, 1325.

Delany, A.M., Kalajzic, I., Bradshaw, A.D., Sage, E.H., and Canalis, E. (2003). Osteonectin-null mutation compromises osteoblast formation, maturation, and survival. Endocrinology *144*, 2588-2596.

Du, R., Lu, K.V., Petritsch, C., Liu, P., Ganss, R., Passegue, E., Song, H., Vandenberg, S., Johnson, R.S., Werb, Z., *et al.* (2008). HIF1alpha induces the recruitment of bone marrow-derived vascular modulatory cells to regulate tumor angiogenesis and invasion. Cancer Cell *13*, 206-220.

Dziadek, M., Paulsson, M., Aumailley, M., and Timpl, R. (1986). Purification and tissue distribution of a small protein (BM-40) extracted from a basement membrane tumor. Eur J Biochem *161*, 455-464.

Eke, I., Deuse, Y., Hehlgans, S., Gurtner, K., Krause, M., Baumann, M., Shevchenko, A., Sandfort, V., and Cordes, N. (2012). beta(1)Integrin/FAK/cortactin signaling is essential for human head and neck cancer resistance to radiotherapy. J Clin Invest *122*, 1529-1540.

Frantz, C., Stewart, K.M., and Weaver, V.M. (2010). The extracellular matrix at a glance. J Cell Sci *123*, 4195-4200.

Gerhardt, H., and Semb, H. (2008). Pericytes: gatekeepers in tumour cell metastasis? J Mol Med (Berl) *86*, 135-144.

Gibbons, L.M. (2008). Nature + nurture > 100%: genetic and environmental influences on child obesity. Am J Clin Nutr *87*, 1968.

Gil-Ortega, M., Garidou, L., Barreau, C., Maumus, M., Breasson, L., Tavernier, G., Garcia-Prieto, C.F., Bouloumie, A., Casteilla, L., and Sengenes, C. (2013). Native adipose stromal cells egress from adipose tissue in vivo: evidence during lymph node activation. Stem Cells *31*, 1309-1320.

Gilles, C., Bassuk, J.A., Pulyaeva, H., Sage, E.H., Foidart, J.M., and Thompson, E.W. (1998). SPARC/osteonectin induces matrix metalloproteinase 2 activation in human breast cancer cell lines. Cancer Res *58*, 5529-5536.

Gilmour, D.T., Lyon, G.J., Carlton, M.B., Sanes, J.R., Cunningham, J.M., Anderson, J.R., Hogan, B.L., Evans, M.J., and Colledge, W.H. (1998). Mice deficient for the secreted glycoprotein SPARC/osteonectin/BM40 develop normally but show severe age-onset cataract formation and disruption of the lens. EMBO J *17*, 1860-1870.

Gimble, J.M., Bunnell, B.A., Chiu, E.S., and Guilak, F. (2011). Concise review: Adipose-derived stromal vascular fraction cells and stem cells: let's not get lost in translation. Stem Cells *29*, 749-754.

Gimble, J.M., Katz, A.J., and Bunnell, B.A. (2007). Adipose-derived stem cells for regenerative medicine. Circ Res *100*, 1249-1260.

Giudici, C., Raynal, N., Wiedemann, H., Cabral, W.A., Marini, J.C., Timpl, R., Bachinger, H.P., Farndale, R.W., Sasaki, T., and Tenni, R. (2008). Mapping of SPARC/BM-40/osteonectin-binding sites on fibrillar collagens. J Biol Chem *283*, 19551-19560.

Goldblum, S.E., Ding, X., Funk, S.E., and Sage, E.H. (1994). SPARC (secreted protein acidic and rich in cysteine) regulates endothelial cell shape and barrier function. Proc Natl Acad Sci U S A *91*, 3448-3452.

Gu, Z., Noss, E.H., Hsu, V.W., and Brenner, M.B. (2011). Integrins traffic rapidly via circular dorsal ruffles and macropinocytosis during stimulated cell migration. J Cell Biol *193*, 61-70.

Hanahan, D., and Weinberg, R.A. (2011). Hallmarks of cancer: the next generation. Cell *144*, 646-674.

Haslam, D.W., and James, W.P. (2005). Obesity. Lancet *366*, 1197-1209.

Hassan, M., Latif, N., and Yacoub, M. (2012). Adipose tissue: friend or foe? Nat Rev Cardiol *9*, 689-702.

Henegar, C., Tordjman, J., Achard, V., Lacasa, D., Cremer, I., Guerre-Millo, M., Poitou, C., Basdevant, A., Stich, V., Viguerie, N., *et al.* (2008). Adipose tissue transcriptomic signature highlights the pathological relevance of extracellular matrix in human obesity. Genome Biol *9*, R14.

Hohenester, E., Sasaki, T., Giudici, C., Farndale, R.W., and Bachinger, H.P. (2008). Structural basis of sequence-specific collagen recognition by SPARC. Proc Natl Acad Sci U S A *105*, 18273-18277.

Hotamisligil, G.S., Murray, D.L., Choy, L.N., and Spiegelman, B.M. (1994). Tumor necrosis factor alpha inhibits signaling from the insulin receptor. Proc Natl Acad Sci U S A *91*, 4854-4858.

Huang, J.I., Kazmi, N., Durbhakula, M.M., Hering, T.M., Yoo, J.U., and Johnstone, B. (2005). Chondrogenic potential of progenitor cells derived from human bone marrow and adipose tissue: a patient-matched comparison. J Orthop Res *23*, 1383-1389.

Huber, J., Kiefer, F.W., Zeyda, M., Ludvik, B., Silberhumer, G.R., Prager, G., Zlabinger, G.J., and Stulnig, T.M. (2008). CC chemokine and CC chemokine receptor profiles in visceral and subcutaneous adipose tissue are altered in human obesity. J Clin Endocrinol Metab *93*, 3215-3221.

Humphries, M.J. (2009). Cell adhesion assays. Methods Mol Biol *522*, 203-210.

Hynes, R.O. (2002). Integrins: bidirectional, allosteric signaling machines. Cell *110*, 673-687.

Ikuta, Y., Nakatsura, T., Kageshita, T., Fukushima, S., Ito, S., Wakamatsu, K., Baba, H., and Nishimura, Y. (2005). Highly sensitive detection of melanoma at an early stage based on the increased serum secreted protein acidic and rich in cysteine and glypican-3 levels. Clin Cancer Res *11*, 8079-8088.

Im, G.I., Shin, Y.W., and Lee, K.B. (2005). Do adipose tissue-derived mesenchymal stem cells have the same osteogenic and chondrogenic potential as bone marrow-derived cells? Osteoarthritis Cartilage *13*, 845-853.

Imtiyaz, H.Z., Williams, E.P., Hickey, M.M., Patel, S.A., Durham, A.C., Yuan, L.J., Hammond, R., Gimotty, P.A., Keith, B., and Simon, M.C. (2010). Hypoxia-inducible

factor 2alpha regulates macrophage function in mouse models of acute and tumor inflammation. J Clin Invest *120*, 2699-2714.

Iruela-Arispe, M.L., Lane, T.F., Redmond, D., Reilly, M., Bolender, R.P., Kavanagh, T.J., and Sage, E.H. (1995). Expression of SPARC during development of the chicken chorioallantoic membrane: evidence for regulated proteolysis in vivo. Mol Biol Cell *6*, 327-343.

Ivaska, J. (2012). Unanchoring integrins in focal adhesions. Nat Cell Biol *14*, 981-983.

Iwamoto, D.V., and Calderwood, D.A. (2015). Regulation of integrin-mediated adhesions. Curr Opin Cell Biol *36*, 41-47.

Karnoub, A.E., Dash, A.B., Vo, A.P., Sullivan, A., Brooks, M.W., Bell, G.W., Richardson, A.L., Polyak, K., Tubo, R., and Weinberg, R.A. (2007). Mesenchymal stem cells within tumour stroma promote breast cancer metastasis. Nature *449*, 557-563.

Kidd, S., Spaeth, E., Watson, K., Burks, J., Lu, H., Klopp, A., Andreeff, M., and Marini, F.C. (2012). Origins of the tumor microenvironment: quantitative assessment of adipose-derived and bone marrow-derived stroma. PLoS One *7*, e30563.

Klopp, A.H., Zhang, Y., Solley, T., Amaya-Manzanares, F., Marini, F., Andreeff, M., Debeb, B., Woodward, W., Schmandt, R., Broaddus, R., *et al.* (2012). Omental adipose tissue-derived stromal cells promote vascularization and growth of endometrial tumors. Clin Cancer Res *18*, 771-782.

Kolle, S.F., Fischer-Nielsen, A., Mathiasen, A.B., Elberg, J.J., Oliveri, R.S., Glovinski, P.V., Kastrup, J., Kirchhoff, M., Rasmussen, B.S., Talman, M.L., *et al.* (2013). Enrichment of autologous fat grafts with ex-vivo expanded adipose tissue-derived stem cells for graft survival: a randomised placebo-controlled trial. Lancet *382*, 1113-1120.

Kolonin, M.G., Evans, K.W., Mani, S.A., and Gomer, R.H. (2012). Alternative origins of stroma in normal organs and disease. Stem Cell Res *8*, 312-323.

Kopelman, P.G. (2000). Obesity as a medical problem. Nature *404*, 635-643.

Kos, K., and Wilding, J.P. (2010). SPARC: a key player in the pathologies associated with obesity and diabetes. Nat Rev Endocrinol *6*, 225-235.

Kzhyshkowska, J., Workman, G., Cardo-Vila, M., Arap, W., Pasqualini, R., Gratchev, A., Krusell, L., Goerdt, S., and Sage, E.H. (2006). Novel function of alternatively activated macrophages: stabilin-1-mediated clearance of SPARC. J Immunol *176*, 5825-5832.

Lane, T.F., and Sage, E.H. (1990). Functional mapping of SPARC: peptides from two distinct Ca+(+)-binding sites modulate cell shape. J Cell Biol *111*, 3065-3076.

Leask, A., and Abraham, D.J. (2004). TGF-beta signaling and the fibrotic response. FASEB J *18*, 816-827.

Lee, M.J., Wu, Y., and Fried, S.K. (2013). Adipose tissue heterogeneity: implication of depot differences in adipose tissue for obesity complications. Mol Aspects Med *34*, 1-11.

Legate, K.R., Wickstrom, S.A., and Fassler, R. (2009). Genetic and cell biological analysis of integrin outside-in signaling. Genes Dev *23*, 397-418.

Lendeckel, S., Jodicke, A., Christophis, P., Heidinger, K., Wolff, J., Fraser, J.K., Hedrick, M.H., Berthold, L., and Howaldt, H.P. (2004). Autologous stem cells (adipose) and fibrin glue used to treat widespread traumatic calvarial defects: case report. J Craniomaxillofac Surg *32*, 370-373.

Lin, K.J., Loi, M.X., Lien, G.S., Cheng, C.F., Pao, H.Y., Chang, Y.C., Ji, A.T., and Ho, J.H. (2013). Topical administration of orbital fat-derived stem cells promotes corneal tissue regeneration. Stem Cell Res Ther *4*, 72.

Liu, Z.J., and Velazquez, O.C. (2008). Hyperoxia, endothelial progenitor cell mobilization, and diabetic wound healing. Antioxid Redox Signal *10*, 1869-1882.

Lo, S.H. (2006). Focal adhesions: what's new inside. Dev Biol *294*, 280-291.

Loeffler, M., Kruger, J.A., Niethammer, A.G., and Reisfeld, R.A. (2006). Targeting tumor-associated fibroblasts improves cancer chemotherapy by increasing intratumoral drug uptake. J Clin Invest *116*, 1955-1962.

Long, M.W. (2001). Osteogenesis and bone-marrow-derived cells. Blood Cells Mol Dis *27*, 677-690.

Lu, Z., Jiang, G., Blume-Jensen, P., and Hunter, T. (2001). Epidermal growth factor-induced tumor cell invasion and metastasis initiated by dephosphorylation and downregulation of focal adhesion kinase. Mol Cell Biol *21*, 4016-4031.

Lumeng, C.N., Deyoung, S.M., and Saltiel, A.R. (2007). Macrophages block insulin action in adipocytes by altering expression of signaling and glucose transport proteins. Am J Physiol Endocrinol Metab *292*, E166-174.

Makki, K., Froguel, P., and Wolowczuk, I. (2013). Adipose tissue in obesity-related inflammation and insulin resistance: cells, cytokines, and chemokines. ISRN Inflamm *2013*, 139239.

Mancuso, P., Martin-Padura, I., Calleri, A., Marighetti, P., Quarna, J., Rabascio, C., Braidotti, P., and Bertolini, F. (2011). Circulating perivascular progenitors: a target of PDGFR inhibition. Int J Cancer *129*, 1344-1350.

Mansergh, F.C., Wells, T., Elford, C., Evans, S.L., Perry, M.J., Evans, M.J., and Evans, B.A. (2007). Osteopenia in Sparc (osteonectin)-deficient mice: characterization of

phenotypic determinants of femoral strength and changes in gene expression. Physiol Genomics *32*, 64-73.

Maquoi, E., Munaut, C., Colige, A., Collen, D., and Lijnen, H.R. (2002). Modulation of adipose tissue expression of murine matrix metalloproteinases and their tissue inhibitors with obesity. Diabetes *51*, 1093-1101.

Mariman, E.C., and Wang, P. (2010). Adipocyte extracellular matrix composition, dynamics and role in obesity. Cell Mol Life Sci *67*, 1277-1292.

Martinek, N., Shahab, J., Sodek, J., and Ringuette, M. (2007). Is SPARC an evolutionarily conserved collagen chaperone? J Dent Res *86*, 296-305.

Maumus, M., Peyrafitte, J.A., D'Angelo, R., Fournier-Wirth, C., Bouloumie, A., Casteilla, L., Sengenes, C., and Bourin, P. (2011). Native human adipose stromal cells: localization, morphology and phenotype. Int J Obes (Lond) *35*, 1141-1153.

McDonald, P.C., Fielding, A.B., and Dedhar, S. (2008). Integrin-linked kinase--essential roles in physiology and cancer biology. J Cell Sci *121*, 3121-3132.

Medzhitov, R. (2008). Origin and physiological roles of inflammation. Nature *454*, 428-435.

Mitra, S.K., Hanson, D.A., and Schlaepfer, D.D. (2005). Focal adhesion kinase: in command and control of cell motility. Nat Rev Mol Cell Biol *6*, 56-68.

Muoio, D.M., and Newgard, C.B. (2008). Mechanisms of disease:Molecular and metabolic mechanisms of insulin resistance and beta-cell failure in type 2 diabetes. Nat Rev Mol Cell Biol *9*, 193-205.

Murdoch, C., Giannoudis, A., and Lewis, C.E. (2004). Mechanisms regulating the recruitment of macrophages into hypoxic areas of tumors and other ischemic tissues. Blood *104*, 2224-2234.

Murphy-Ullrich, J.E., Lane, T.F., Pallero, M.A., and Sage, E.H. (1995). SPARC mediates focal adhesion disassembly in endothelial cells through a follistatin-like region and the Ca(2+)-binding EF-hand. J Cell Biochem *57*, 341-350.

Nadler, S.T., Stoehr, J.P., Schueler, K.L., Tanimoto, G., Yandell, B.S., and Attie, A.D. (2000). The expression of adipogenic genes is decreased in obesity and diabetes mellitus. Proc Natl Acad Sci U S A *97*, 11371-11376.

Nagano, M., Hoshino, D., Koshikawa, N., Akizawa, T., and Seiki, M. (2012). Turnover of focal adhesions and cancer cell migration. Int J Cell Biol *2012*, 310616.

Nagy, J.A., and Dvorak, H.F. (2012). Heterogeneity of the tumor vasculature: the need for new tumor blood vessel type-specific targets. Clin Exp Metastasis *29*, 657-662.

Naimi, M., and Van Obberghen, E. (2009). Inflammation: where is the SPARC in adipose-tissue inflammation? Nat Rev Endocrinol *5*, 648-649.

Nie, J., Chang, B., Traktuev, D.O., Sun, J., March, K., Chan, L., Sage, E.H., Pasqualini, R., Arap, W., and Kolonin, M.G. (2008). IFATS collection: Combinatorial peptides identify alpha5beta1 integrin as a receptor for the matricellular protein SPARC on adipose stromal cells. Stem Cells *26*, 2735-2745.

Nie, J., and Sage, E.H. (2009). SPARC functions as an inhibitor of adipogenesis. J Cell Commun Signal *3*, 247-254.

Nieman, K.M., Kenny, H.A., Penicka, C.V., Ladanyi, A., Buell-Gutbrod, R., Zillhardt, M.R., Romero, I.L., Carey, M.S., Mills, G.B., Hotamisligil, G.S., *et al.* (2011). Adipocytes

promote ovarian cancer metastasis and provide energy for rapid tumor growth. Nat Med *17*, 1498-1503.

Norose, K., Clark, J.I., Syed, N.A., Basu, A., Heber-Katz, E., Sage, E.H., and Howe, C.C. (1998). SPARC deficiency leads to early-onset cataractogenesis. Invest Ophthalmol Vis Sci *39*, 2674-2680.

Norose, K., Lo, W.K., Clark, J.I., Sage, E.H., and Howe, C.C. (2000). Lenses of SPARC-null mice exhibit an abnormal cell surface-basement membrane interface. Exp Eye Res *71*, 295-307.

Olumi, A.F., Grossfeld, G.D., Hayward, S.W., Carroll, P.R., Tlsty, T.D., and Cunha, G.R. (1999). Carcinoma-associated fibroblasts direct tumor progression of initiated human prostatic epithelium. Cancer Res *59*, 5002-5011.

Ota, T. (2013). Chemokine systems link obesity to insulin resistance. Diabetes Metab J *37*, 165-172.

Ouchi, N., Parker, J.L., Lugus, J.J., and Walsh, K. (2011). Adipokines in inflammation and metabolic disease. Nat Rev Immunol *11*, 85-97.

Ouellet, V., Labbe, S.M., Blondin, D.P., Phoenix, S., Guerin, B., Haman, F., Turcotte, E.E., Richard, D., and Carpentier, A.C. (2012). Brown adipose tissue oxidative metabolism contributes to energy expenditure during acute cold exposure in humans. J Clin Invest *122*, 545-552.

Pachon-Pena, G., Yu, G., Tucker, A., Wu, X., Vendrell, J., Bunnell, B.A., and Gimble, J.M. (2011). Stromal stem cells from adipose tissue and bone marrow of age-matched female donors display distinct immunophenotypic profiles. J Cell Physiol *226*, 843-851.

Park, J., Euhus, D.M., and Scherer, P.E. (2011). Paracrine and endocrine effects of adipose tissue on cancer development and progression. Endocr Rev *32*, 550-570.

Parsons, J.T. (2003). Focal adhesion kinase: the first ten years. J Cell Sci *116*, 1409-1416.

Petit, I., Szyper-Kravitz, M., Nagler, A., Lahav, M., Peled, A., Habler, L., Ponomaryov, T., Taichman, R.S., Arenzana-Seisdedos, F., Fujii, N., *et al.* (2002). G-CSF induces stem cell mobilization by decreasing bone marrow SDF-1 and up-regulating CXCR4. Nat Immunol *3*, 687-694.

Podgorski, I., Linebaugh, B.E., Koblinski, J.E., Rudy, D.L., Herroon, M.K., Olive, M.B., and Sloane, B.F. (2009). Bone marrow-derived cathepsin K cleaves SPARC in bone metastasis. Am J Pathol *175*, 1255-1269.

Ponte, A.L., Marais, E., Gallay, N., Langonne, A., Delorme, B., Herault, O., Charbord, P., and Domenech, J. (2007). The in vitro migration capacity of human bone marrow mesenchymal stem cells: comparison of chemokine and growth factor chemotactic activities. Stem Cells *25*, 1737-1745.

Puissant, B., Barreau, C., Bourin, P., Clavel, C., Corre, J., Bousquet, C., Taureau, C., Cousin, B., Abbal, M., Laharrague, P., *et al.* (2005). Immunomodulatory effect of human adipose tissue-derived adult stem cells: comparison with bone marrow mesenchymal stem cells. Br J Haematol *129*, 118-129.

Rahman, M., Chan, A.P., and Tai, I.T. (2011). A peptide of SPARC interferes with the interaction between caspase8 and Bcl2 to resensitize chemoresistant tumors and enhance their regression in vivo. PLoS One *6*, e26390.

Rehman, J., Traktuev, D., Li, J., Merfeld-Clauss, S., Temm-Grove, C.J., Bovenkerk, J.E., Pell, C.L., Johnstone, B.H., Considine, R.V., and March, K.L. (2004). Secretion of

angiogenic and antiapoptotic factors by human adipose stromal cells. Circulation *109*, 1292-1298.

Renehan, A.G., Tyson, M., Egger, M., Heller, R.F., and Zwahlen, M. (2008). Body-mass index and incidence of cancer: a systematic review and meta-analysis of prospective observational studies. Lancet *371*, 569-578.

Renehan, A.G., Zwahlen, M., and Egger, M. (2015). Adiposity and cancer risk: new mechanistic insights from epidemiology. Nat Rev Cancer *15*, 484-498.

Rentz, T.J., Poobalarahi, F., Bornstein, P., Sage, E.H., and Bradshaw, A.D. (2007). SPARC regulates processing of procollagen I and collagen fibrillogenesis in dermal fibroblasts. J Biol Chem *282*, 22062-22071.

Rivera, L.B., and Brekken, R.A. (2011). SPARC promotes pericyte recruitment via inhibition of endoglin-dependent TGF-beta1 activity. J Cell Biol *193*, 1305-1319.

Rowan, B.G., Lacayo, E.A., Sheng, M., Anbalagan, M., Gimble, J.M., Jones, R.K., Joseph, W.J., Friedlander, P.L., and Chiu, E.S. (2015). Human Adipose Tissue-Derived Stromal/Stem Cells Promote Migration and Early Metastasis of Head and Neck Cancer Xenografts. Aesthet Surg J.

Sage, E.H., Reed, M., Funk, S.E., Truong, T., Steadele, M., Puolakkainen, P., Maurice, D.H., and Bassuk, J.A. (2003). Cleavage of the matricellular protein SPARC by matrix metalloproteinase 3 produces polypeptides that influence angiogenesis. J Biol Chem *278*, 37849-37857.

Sage, H., Vernon, R.B., Funk, S.E., Everitt, E.A., and Angello, J. (1989). SPARC, a secreted protein associated with cellular proliferation, inhibits cell spreading in vitro and exhibits Ca+2-dependent binding to the extracellular matrix. J Cell Biol *109*, 341-356.

Sasaki, T., Gohring, W., Mann, K., Maurer, P., Hohenester, E., Knauper, V., Murphy, G., and Timpl, R. (1997). Limited cleavage of extracellular matrix protein BM-40 by matrix metalloproteinases increases its affinity for collagens. J Biol Chem *272*, 9237-9243.

Sasaki, T., Hohenester, E., Gohring, W., and Timpl, R. (1998). Crystal structure and mapping by site-directed mutagenesis of the collagen-binding epitope of an activated form of BM-40/SPARC/osteonectin. EMBO J *17*, 1625-1634.

Sasaki, T., Miosge, N., and Timpl, R. (1999). Immunochemical and tissue analysis of protease generated neoepitopes of BM-40 (osteonectin, SPARC) which are correlated to a higher affinity binding to collagens. Matrix Biol *18*, 499-508.

Schipper, H.S., Prakken, B., Kalkhoven, E., and Boes, M. (2012). Adipose tissue-resident immune cells: key players in immunometabolism. Trends Endocrinol Metab *23*, 407-415.

Sengenes, C., Lolmede, K., Zakaroff-Girard, A., Busse, R., and Bouloumie, A. (2005). Preadipocytes in the human subcutaneous adipose tissue display distinct features from the adult mesenchymal and hematopoietic stem cells. J Cell Physiol *205*, 114-122.

Shi, Q., Bao, S., Song, L., Wu, Q., Bigner, D.D., Hjelmeland, A.B., and Rich, J.N. (2007). Targeting SPARC expression decreases glioma cellular survival and invasion associated with reduced activities of FAK and ILK kinases. Oncogene *26*, 4084-4094.

Shin, M., Mizokami, A., Kim, J., Ofude, M., Konaka, H., Kadono, Y., Kitagawa, Y., Miwa, S., Kumaki, M., Keller, E.T., *et al.* (2013). Exogenous SPARC suppresses proliferation and migration of prostate cancer by interacting with integrin beta1. Prostate *73*, 1159-1170.

Silventoinen, K., Rokholm, B., Kaprio, J., and Sorensen, T.I. (2010). The genetic and environmental influences on childhood obesity: a systematic review of twin and adoption studies. Int J Obes (Lond) *34*, 29-40.

Song, S., Ewald, A.J., Stallcup, W., Werb, Z., and Bergers, G. (2005). PDGFRbeta+ perivascular progenitor cells in tumours regulate pericyte differentiation and vascular survival. Nat Cell Biol *7*, 870-879.

Strong, A.L., Ohlstein, J.F., Biagas, B.A., Rhodes, L.V., Pei, D.T., Tucker, H.A., Llamas, C., Bowles, A.C., Dutreil, M.F., Zhang, S., *et al.* (2015). Leptin produced by obese adipose stromal/stem cells enhances proliferation and metastasis of estrogen receptor positive breast cancers. Breast Cancer Res *17*, 112.

Stunkard, A.J., Foch, T.T., and Hrubec, Z. (1986). A twin study of human obesity. JAMA *256*, 51-54.

Sun, K., Kusminski, C.M., and Scherer, P.E. (2011). Adipose tissue remodeling and obesity. J Clin Invest *121*, 2094-2101.

Surmi, B.K., and Hasty, A.H. (2008). Macrophage infiltration into adipose tissue: initiation, propagation and remodeling. Future Lipidol *3*, 545-556.

Taicher, G.Z., Tinsley, F.C., Reiderman, A., and Heiman, M.L. (2003). Quantitative magnetic resonance (QMR) method for bone and whole-body-composition analysis. Anal Bioanal Chem *377*, 990-1002.

Takahashi, M., Nagaretani, H., Funahashi, T., Nishizawa, H., Maeda, N., Kishida, K., Kuriyama, H., Shimomura, I., Maeda, K., Hotta, K., *et al.* (2001). The expression of SPARC in adipose tissue and its increased plasma concentration in patients with coronary artery disease. Obes Res *9*, 388-393.

Taneda, S., Pippin, J.W., Sage, E.H., Hudkins, K.L., Takeuchi, Y., Couser, W.G., and Alpers, C.E. (2003). Amelioration of diabetic nephropathy in SPARC-null mice. J Am Soc Nephrol *14*, 968-980.

Tang, W., Zeve, D., Suh, J.M., Bosnakovski, D., Kyba, M., Hammer, R.E., Tallquist, M.D., and Graff, J.M. (2008). White fat progenitor cells reside in the adipose vasculature. Science *322*, 583-586.

Tartare-Deckert, S., Chavey, C., Monthouel, M.N., Gautier, N., and Van Obberghen, E. (2001). The matricellular protein SPARC/osteonectin as a newly identified factor up-regulated in obesity. J Biol Chem *276*, 22231-22237.

Teranishi, S., Kimura, K., and Nishida, T. (2009). Role of formation of an ERK-FAK-paxillin complex in migration of human corneal epithelial cells during wound closure in vitro. Invest Ophthalmol Vis Sci *50*, 5646-5652.

Thangarajah, H., Vial, I.N., Chang, E., El-Ftesi, S., Januszyk, M., Chang, E.I., Paterno, J., Neofytou, E., Longaker, M.T., and Gurtner, G.C. (2009). IFATS collection: Adipose stromal cells adopt a proangiogenic phenotype under the influence of hypoxia. Stem Cells *27*, 266-274.

Traktuev, D.O., Merfeld-Clauss, S., Li, J., Kolonin, M., Arap, W., Pasqualini, R., Johnstone, B.H., and March, K.L. (2008). A population of multipotent CD34-positive adipose stromal cells share pericyte and mesenchymal surface markers, reside in a periendothelial location, and stabilize endothelial networks. Circ Res *102*, 77-85.

Trayhurn, P., and Wood, I.S. (2005). Signalling role of adipose tissue: adipokines and inflammation in obesity. Biochem Soc Trans *33*, 1078-1081.

Tse, W.T., Pendleton, J.D., Beyer, W.M., Egalka, M.C., and Guinan, E.C. (2003). Suppression of allogeneic T-cell proliferation by human marrow stromal cells: implications in transplantation. Transplantation *75*, 389-397.

Tsuji, W., Rubin, J.P., and Marra, K.G. (2014). Adipose-derived stem cells: Implications in tissue regeneration. World J Stem Cells *6*, 312-321.

Ulrich, T.A., de Juan Pardo, E.M., and Kumar, S. (2009). The mechanical rigidity of the extracellular matrix regulates the structure, motility, and proliferation of glioma cells. Cancer Res *69*, 4167-4174.

Veevers-Lowe, J., Ball, S.G., Shuttleworth, A., and Kielty, C.M. (2011). Mesenchymal stem cell migration is regulated by fibronectin through alpha5beta1-integrin-mediated activation of PDGFR-beta and potentiation of growth factor signals. J Cell Sci *124*, 1288-1300.

Vicente-Manzanares, M., Webb, D.J., and Horwitz, A.R. (2005). Cell migration at a glance. J Cell Sci *118*, 4917-4919.

Virtanen, K.A., Lidell, M.E., Orava, J., Heglind, M., Westergren, R., Niemi, T., Taittonen, M., Laine, J., Savisto, N.J., Enerback, S., *et al.* (2009). Functional brown adipose tissue in healthy adults. N Engl J Med *360*, 1518-1525.

Von Luttichau, I., Notohamiprodjo, M., Wechselberger, A., Peters, C., Henger, A., Seliger, C., Djafarzadeh, R., Huss, R., and Nelson, P.J. (2005). Human adult CD34- progenitor cells functionally express the chemokine receptors CCR1, CCR4, CCR7, CXCR5, and CCR10 but not CXCR4. Stem Cells Dev *14*, 329-336.

von Tell, D., Armulik, A., and Betsholtz, C. (2006). Pericytes and vascular stability. Exp Cell Res *312*, 623-629.

Weaver, M.S., Workman, G., and Sage, E.H. (2008). The copper binding domain of SPARC mediates cell survival in vitro via interaction with integrin beta1 and activation of integrin-linked kinase. J Biol Chem *283*, 22826-22837.

Wellen, K.E., and Hotamisligil, G.S. (2003). Obesity-induced inflammatory changes in adipose tissue. J Clin Invest *112*, 1785-1788.

Wernstedt Asterholm, I., Tao, C., Morley, T.S., Wang, Q.A., Delgado-Lopez, F., Wang, Z.V., and Scherer, P.E. (2014). Adipocyte inflammation is essential for healthy adipose tissue expansion and remodeling. Cell Metab *20*, 103-118.

Widmaier, M., Rognoni, E., Radovanac, K., Azimifar, S.B., and Fassler, R. (2012). Integrin-linked kinase at a glance. J Cell Sci *125*, 1839-1843.

Wu, R.X., Laser, M., Han, H., Varadarajulu, J., Schuh, K., Hallhuber, M., Hu, K., Ertl, G., Hauck, C.R., and Ritter, O. (2006). Fibroblast migration after myocardial infarction is regulated by transient SPARC expression. J Mol Med (Berl) *84*, 241-252.

Xie, R.L., and Long, G.L. (1995). Role of N-linked glycosylation in human osteonectin. Effect of carbohydrate removal by N-glycanase and site-directed mutagenesis on structure and binding of type V collagen. J Biol Chem *270*, 23212-23217.

Yokoyama, H., Saito, S., Daitoku, K., Fukuda, I., Higuma, T., Hanada, H., Osanai, T., and Okumura, K. (2011). Effects of pravastatin and rosuvastatin on the generation of adiponectin in the visceral adipose tissue in patients with coronary artery disease. Fundam Clin Pharmacol *25*, 378-387.

Zhang, Y., Daquinag, A., Traktuev, D.O., Amaya-Manzanares, F., Simmons, P.J., March, K.L., Pasqualini, R., Arap, W., and Kolonin, M.G. (2009). White adipose tissue cells are recruited by experimental tumors and promote cancer progression in mouse models. Cancer Res *69*, 5259-5266.

Zhang, Y., Daquinag, A.C., Amaya-Manzanares, F., Sirin, O., Tseng, C., and Kolonin, M.G. (2012). Stromal progenitor cells from endogenous adipose tissue contribute to

pericytes and adipocytes that populate the tumor microenvironment. Cancer Res *72*, 5198-5208.

Zhao, X., and Guan, J.L. (2011). Focal adhesion kinase and its signaling pathways in cell migration and angiogenesis. Adv Drug Deliv Rev *63*, 610-615.

Zheng, Y., and Lu, Z. (2009). Paradoxical roles of FAK in tumor cell migration and metastasis. Cell Cycle *8*, 3474-3479.

Zhou, H., Yang, J., Xin, T., Zhang, T., Hu, S., Zhou, S., Chen, G., and Chen, Y. (2015). Exendin-4 enhances the migration of adipose-derived stem cells to neonatal rat ventricular cardiomyocyte-derived conditioned medium via the phosphoinositide 3-kinase/Akt-stromal cell-derived factor-1alpha/CXC chemokine receptor 4 pathway. Mol Med Rep *11*, 4063-4072.

Zimmerlin, L., Donnenberg, V.S., Pfeifer, M.E., Meyer, E.M., Peault, B., Rubin, J.P., and Donnenberg, A.D. (2010). Stromal vascular progenitors in adult human adipose tissue. Cytometry A *77*, 22-30.

VITA

Chieh Tseng was born in Taipei city, Taiwan on September 11th, 1982, the daughter of Wen-Chih Tseng and Chin-Chih Chiang. Before entering the UT-GSBS graduate program, she received her Bachelor degree of Science majoring Biomedical Sciences from Central Queensland University in 2007 while working in Mount Alvernia Hospital, Singapore. In August 2009, she entered the University of Texas Health Science Center at Houston Graduate School of Biomedical Sciences.

Permanent address:

2601 S Braeswood
Houston,Texas 77025